

UC San Diego

UC San Diego Electronic Theses and Dissertations

Title

Protein Kinase C Gene Fusions and Other Mechanisms for Loss of PKC Function in Cancer

Permalink

<https://escholarship.org/uc/item/72t421vp>

Author

Van, An-Angela Ngoc

Publication Date

2020

Peer reviewed|Thesis/dissertation

UNIVERSITY OF CALIFORNIA SAN DIEGO

**Protein Kinase C Gene Fusions and Other Mechanisms for Loss of PKC Function
in Cancer**

A dissertation submitted in partial satisfaction of the
requirements for the degree Doctor of Philosophy

in

Biomedical Sciences

by

An-Angela Ngoc Van

Committee in charge:

Professor Alexandra C. Newton, Chair
Professor Gen-Sheng Feng
Professor Frank B. Furnari
Professor Susan S. Taylor
Professor Jin Zhang

2020

Copyright

An-Angela Ngoc Van, 2020

All rights reserved.

The dissertation of An-Angela Ngoc Van is approved, and it is acceptable in quality and form for publication on microfilm and electronically:

Chair

University of California San Diego

2020

DEDICATION

To the strongest person I have ever known,

Mom

TABLE OF CONTENTS

Signature Page.....	iii
Dedication.....	iv
Table of Contents.....	v
List of Figures.....	vii
List of Tables.....	viii
Acknowledgments.....	ix
Vita.....	xii
Abstract of the Dissertation.....	xiii
Chapter 1 An Introduction to Protein Kinase C.....	1
1.1 The Prelude to Protein Kinase C (PKC).....	2
1.2 The PKC Family: Structure and Regulation.....	3
1.3 The Life and Death of PKC.....	6
1.4 Substrates of PKC.....	9
1.5 Dysregulation of PKC in Disease.....	10
Metabolic Disease.....	11
Cardiovascular Disease.....	12
Neurodegeneration.....	13
1.6 PKC in Cancer.....	13
1.7 Research Goals.....	17
1.8 Figures.....	19
Chapter 2 Protein Kinase C Fusions Reveal Mechanism for Loss of Protein Kinase C Function in Cancer.....	22
2.1 Abstract.....	23
2.2 Introduction.....	24
2.3 Results.....	26
A multitude of PKC fusions have been identified in cancer.....	26

	PKC catalytic domain fusions are unphosphorylated yet constitutively active.....	28
	Fusions of the PKC catalytic domain are unstable..	31
	CRISPR-edited cells exhibit detectable PKC fusion mRNA but not protein.....	33
	CRISPR-edited fusion cells exhibit reduced apoptosis.....	35
	PKC regulatory domain fusions are LOF and potentially dominant negative.....	36
	2.4 Discussion.....	39
	2.5 Materials and Methods.....	45
	2.6 Acknowledgments.....	55
	2.7 Table and Figures.....	57
Chapter 3	Mechanisms of Protein Kinase C Dysregulation in Cancer.....	75
	3.1 Abstract.....	76
	3.2 Introduction.....	77
	3.3 Results.....	80
	Activating PKC mutants in ATLL are phosphorylated yet loss-of-function.....	80
	Catalytic domain fusions are stabilized by chaperones and the pseudosubstrate.....	83
	Catalytically-dead PKC mutants are dominant negative.....	85
	PKC fusions demonstrate potential loss of PKC function via mislocalization.....	88
	PKC is negatively regulated by PHLPP1.....	91
	3.4 Discussion.....	93
	3.5 Materials and Methods.....	98
	3.6 Acknowledgments.....	104
	3.7 Figures.....	105
Chapter 4	Conclusions.....	114
	4.1 Conclusions.....	115
	4.2 Figures.....	121
References.....		123

LIST OF FIGURES

Figure 1.1	PKC in signal transduction.....	19
Figure 1.2	Domain composition of PKC family members and crystal structures.....	20
Figure 1.3	The life cycle of PKC.....	21
Figure 2.1	Fusions of the protein kinase C regulatory and catalytic moieties are detected in a multitude of cancers.....	59
Figure 2.2	3' PKC fusions yield proteins that are unphosphorylated at the PKC priming sites yet constitutively active.....	60
Figure 2.3	PKC fusion proteins require phosphorylatable residues at priming sites for activity.....	62
Figure 2.4	The open conformation that renders fusions of the PKC catalytic domain to be constitutively active also cause them to be markedly unstable.....	63
Figure 2.5	Purified GGA2-PKC β II fusion protein is in complex with other proteins, notably molecular chaperones.....	64
Figure 2.6	The <i>TANC2-PRKCA</i> fusion is detected at the mRNA level but not the protein level in CRISPR-edited cells	65
Figure 2.7	Less TANC2-PKC α protein is detected compared to wild-type PKC α in a titration of DNA transfected into cells.....	67
Figure 2.8	Inhibition of proteasomal or endosomal/lysosomal degradative pathways does not prevent degradation of TANC2-PKC α fusion protein upon cycloheximide treatment	68
Figure 2.9	Knockdown of E3 ligases does not allow for accumulation of the TANC2-PKC α fusion protein in CRISPR-edited cells	70
Figure 2.10	<i>TANC2-PRKCA</i> -expressing cells display a reduction in apoptosis as indicated by reduced cleaved caspase 3 levels	71
Figure 2.11	5' PKC fusions may act in a dominant-negative manner, suppressing the activity of wild-type PKC.....	72
Figure 2.12	Model of PKC fusions as mechanism for loss of PKC activity in cancer.....	74
Figure 3.1	ATLL mutants are activating, phosphorylated, and sensitive to dephosphorylation.....	105
Figure 3.2	Cancer-associated PKC fusions maintain an open conformation that attracts potential chaperones and can be inhibited in trans by the pseudosubstrate.....	106
Figure 3.3	Inactivating mutants of PKC act in a dominant-negative manner by sequestering common titratable components... ..	108
Figure 3.4	Cancer-associated PKC fusions are mislocalized upon stimulation.....	110
Figure 3.5	PHLPP negatively regulates steady-state levels of PKC....	112
Figure 4.1	Mechanisms of PKC dysregulation in cancer.....	121

LIST OF TABLES

Table 2.1	PKC gene fusions identified in cancer.....	57
-----------	--	----

ACKNOWLEDGEMENTS

They say that it takes a village to raise a child, and in some ways, a fresh graduate student is a sort of child. That being said, I would like to acknowledge my village.

First, I would like to thank my thesis advisor, Dr. Alexandra Newton. In addition to her scientific guidance over the course of my graduate studies, I cannot emphasize how appreciative I was of not only her willingness but genuine encouragement to pursue opportunities for my professional development outside of her lab. Furthermore, as anyone who has seen Alexandra speak can attest to her effectiveness as an orator, I have greatly benefitted from her fantastic science storytelling skills. I would also like to thank the members of my thesis committee, Drs. Gen-Sheng Feng, Frank Furnari, Susan Taylor, and Jin Zhang, for their insight and support. Additionally, I would like to thank the members of the Dixon laboratory as many members have been of great assistance to my thesis work over the years. I would especially like to acknowledge Dr. Sourav Banerjee, who exerted great efforts both stateside and abroad to advance my project and share his expertise, as well as Dr. Joshua Mayfield, who played a crucial role in the Great Pre-Quarantine Sac of 2020.

One of the pivotal factors in my decision to join the Newton laboratory was the supportive environment fostered by its members, so I would be remiss not to acknowledge them here. I would like to thank the past and present members of the laboratory for their input and support. In particular, I would like to thank Gema Lordén, Agnieszka Kawashima, and Alexander Jones for their enthusiastic feedback, constant encouragement, and most importantly, lasting friendship. Finally, I would like to specially acknowledge Dr. Maya Kunkel, who not only taught me invaluable skills to advance my

project and my research career but also served as a great pillar of strength. I have had the privilege of being able to learn so much from her, and for all that and more, I could not be more grateful.

I would also like to acknowledge a few other individuals that have played key roles in my professional and personal development. I am greatly appreciative of the support and encouragement that I have received from Drs. Kim Barrett and Ronald Marchelletta. Their kind words and guidance came during times when I needed it most. I also want to acknowledge Dr. Courtney Anderson, my mentor during my undergraduate years. If it were not for the positive experience I had with her, I might not have pursued my PhD. I would also like to thank my wonderful mentors and colleagues at GNF. I could not have asked to be placed with a better group of people. I am especially grateful towards Dr. Ramón Whitson, who not only served as an excellent mentor during my internship but continues to mentor me now.

I would like to thank all of my friends, both those that were with me before I began graduate school and those that I gained in the thick of it. Thank you to Chelsea Pretz for being an important source of support over the years and an excellent travel buddy. Thank you to my classmates with whom I shared many fond memories. An additional thank you to Gemo, Gemi, Gemu, and even Geme for being a constant source of laughter and undying encouragement. And thank you to my graduate school friends who have now turned into my lifelong friends: Jordan Campbell, Marcelis Muriel, Khari Rockward, Kwesi Rutledge, and Nailah Seale. One of the best things to come out of graduate school was meeting you all.

Finally, thank you to my family. Thank you to my Dad for all the good luck that he has sent my way. Thank you to my brother, Alan Huynh, for serving as a sounding board over these past six years and many years before that. Most of all, thank you to my Mom, the strongest woman I know. If it were not for everything that she has done over the entirety of my life, I would not be where I am nor who I am. I owe everything to her, and as much as this accomplishment is mine, it is also hers.

Chapter 2, in full, is currently being prepared for submission under the title “Protein Kinase C Fusions Reveal Mechanism for Loss of Protein Kinase C Function in Cancer.” The authors include An-Angela N. Van, Maya T. Kunkel, Corina E. Antal, and Alexandra C. Newton. The dissertation author was the primary investigator and author of this material.

Chapter 3, in part, contains material that appears in the publication “Protein kinase C quality control by phosphatase PHLPP1 unveils loss-of-function mechanism in cancer,” as published by Timothy R. Baffi, An-Angela N. Van, Wei Zhao, Gordon B. Mills, and Alexandra C. Newton in *Molecular Cell* 2019 Apr 18, 74(2):378-392. The dissertation author was a co-author of the publication and the primary investigator and author of the material included in this chapter of the dissertation (Figure 3.5A, B, C, D, E, F, J, and K). The remainder of Chapter 3 is unpublished material for which the dissertation author is the primary investigator and author of the work.

VITA

- 2020 Doctor of Philosophy, Biomedical Sciences
 University of California San Diego
- 2013 Bachelor of Science, Molecular Toxicology and Molecular Environmental
 Biology (Dual)
 University of California Berkeley

PUBLICATIONS

Baffi TR, **Van AN**, Zhao W, Mills GB, and Newton AC. (2019) Protein Kinase C Quality Control by Phosphatase PHLPP1 Unveils Loss-of-Function Mechanism in Cancer. *Molecular Cell* **74**(2):378-392.

Kajimoto T, Caliman AD, Tobias IS, Okada T, Pilo CA, **Van AN**, McCammon AJ, Nakamura S, and Newton AC. (2019) Activation of Atypical Protein Kinase C by Sphingosine 1-Phosphate Revealed by Atypical Protein Kinase C-Specific Activity Reporter. *Science Signaling* **12**(562): eaat6662.

Anderson CM, Kazantzis M, Wang J, Venkatraman S, Goncalves RLS, Quinlan CL, Ng R, Jastroch M, Benjamin DI, Nie B, Herber C, **Van AN**, Park MJ, Yun D, Chan K, Yu A, Vuong P, Febbraio M, Nomura D, Napoli J, Brand MD, and Stahl A. (2015) Dependence of Brown Adipose Tissue Function on CD36-Mediated Coenzyme Q Uptake. *Cell Reports* **10**(4): 505-515.

MANUSCRIPTS IN PROGRESS

Van AN, Kunkel MT, Antal CE, and Newton AC. Protein Kinase C Fusions Reveal Mechanism for Loss of Protein Kinase C Function in Cancer. In preparation.

ABSTRACT OF THE DISSERTATION

Protein Kinase C Gene Fusions and Other Mechanisms for Loss of PKC Function in
Cancer

by

An-Angela Ngoc Van

Doctor of Philosophy in Biomedical Sciences

University of California San Diego, 2020

Professor Alexandra C. Newton, Chair

Protein kinase C (PKC) plays a critical role in cell signaling and homeostasis, regulating biological processes such as proliferation, differentiation, and apoptosis. Its dysregulation is associated with a multitude of pathophysiological states, with recent analyses of disease-associated mutations indicating that loss of PKC function is generally associated with cancer and gain of function with degenerative diseases. This dissertation expands on the mechanisms of PKC dysregulation in cancer, focusing on how gene fusions or mutations that disrupt autoinhibition cause loss of PKC. In the first part of the

dissertation, newly identified PKC gene fusions in cancer encoding proteins that retain either the PKC catalytic or regulatory domain were characterized. Overexpression of catalytic domain fusions in cells revealed that they are constitutively active, as assessed using biosensors and other cellular assays. However, their inability to adopt an autoinhibited conformation resulted in their marked stability compared to full-length PKC. To assess whether these fusions were too unstable to accumulate at endogenous levels, CRISPR/Cas9-mediated gene editing was used to engineer a fusion of *TANC2* with *PRKCA*. While the fusion mRNA was detected in the engineered cells, no detectable protein was expressed. Thus, the catalytic domain fusions are paradoxically loss-of-function. Characterization of a regulatory domain fusion revealed a dominant-negative role for the protein, suppressing the activity of wild-type PKC. The second part of the dissertation focused on additional mechanisms by which PKC is dysregulated in cancer. This work showed that [1] PKC that cannot be autoinhibited is subject to dephosphorylation by the phosphatase PHLPP and unphosphorylated PKC is sensitive to degradation; [2] inactivating mutants of PKC can be dominant-negative by sequestering common titratable components; and [3] impairment of the regulatory domains causes mislocalization of PKC. Taken together, these studies illustrate the diverse ways in which PKC function is lost in cancer, allowing cancer cells to overcome this cellular brake to tumor growth.

Chapter 1

An Introduction to Protein Kinase C

1.1 The Prelude to Protein Kinase C (PKC)

In the late 1970s, Yasutomi Nishizuka and his team of researchers at Kobe University in Japan toiled away, seeking to understand the regulatory mechanisms of cGMP-dependent protein kinase (PKG) (1). However, during their study of PKG, they detected another active protein kinase whose requirement for activity was Mg^{2+} rather than cyclic nucleotides. As such, they tentatively named this new kinase protein kinase M (PKM). They were puzzled to find that their frozen stocks of rat brains yielded higher activities than their freshly prepared samples and that this was even more prominent when they reduced the amount of protease inhibitor used in their sample preparation. Recalling their previous lessons with PKG, namely that proteolysis of PKG yielded a constitutively active fragment, the astute researchers began their search for the parent enzyme of PKM (2). They encountered issues with loss of activity during the purification process but discovered that the pro-enzyme was stimulated by phospholipids from brain extracts, specifically phosphatidylserine, and a “trace impurity” that was subsequently identified as diacylglycerol (3, 4). The researchers named the pro-enzyme Ca^{2+} phospholipid-dependent protein kinase, which would later come to be known as protein kinase C (PKC).

The discovery of PKC provided resolution for a 25-year hunt initiated by Hokin and Hokin for the effector responsible for facilitating the cellular effects downstream of phospholipid hydrolysis upon cholinergic stimulation (5). However, the ramifications of this contribution would extend far beyond solving a decades long mystery. Through their identification of PKC, Nishizuka and colleagues unwittingly revealed a novel target for scientific inquiry that would be extensively studied for decades to come, resulting in

transformative findings that have allowed scientists to better understand the nuances of signal transduction, gain insight into kinase structure and function, and elucidate underlying mechanisms of disease.

1.2 The PKC Family: Structure and Regulation

Phosphorylation and, in turn, dephosphorylation serve as central mechanisms by which environmental cues are relayed throughout the cell (6). As the most prevalent type of post-translational modification, phosphorylation regulates the structure and function of many intracellular substrates involved in a diverse array of processes, from proliferation to hormone secretion. Kinases and phosphatases are kept in a precisely-regulated balance, and disturbance of this balance results in pathophysiologies (6–8). The PKC family, part of the AGC kinase super family, is among the most complex enzyme families, involved in the transduction of signals initiated by receptor-mediated hydrolysis of phospholipids (Figure 1.1) (7, 9, 10). With its activity tightly regulated, dysregulation of PKC has been implicated in the pathogenesis of a variety of diseases, including metabolic disorders, neurodegeneration, and most notably, cancer (11–17).

The PKC family of Ser/Thr kinases consists of nine isozymes which are categorized into three subclasses, conventional, novel, and atypical (Figure 1.2A) (9, 18–21). The general domain structure shared by the members of the PKC family includes an amino-terminal regulatory moiety with a hinge region linking to a carboxy-terminal catalytic domain. The isozymes are separated into their respective classes based on the composition of their regulatory domains, with the nature of the regulatory moiety revealing the distinct co-factor dependency of each PKC subclass (19, 20). Conventional isozymes,

consisting of α , the alternatively spliced β I and β II, and γ , contain adjacent C1A and C1B domains that bind to diacylglycerol (DAG) in membranes, followed by a C2 domain that binds membranes in the presence of the second messenger Ca^{2+} (18–21). Novel isozyms, consisting of δ , ϵ , η , and θ , also contain tandem C1A and C1B domains but possess a novel C2 domain that lacks key residues required for coordinating Ca^{2+} . Thus, while novel isozyms are sensitive to DAG, they are not responsive to Ca^{2+} . However, although they are regulated by only one membrane-targeting module, the C1B domain of novel isozyms has a 100-fold higher affinity for DAG compared to that of conventional isozyms (22). This affinity for DAG is tuned by a single amino acid, present as a Tyr in conventional isozyms and a Trp in novel isozyms (23). The Trp residue restricts movement of the ligand-binding loops within the C1B domain to create a closed pocket that is more favorable for DAG binding (24). In contrast, the Tyr residue permits increased movement which disfavors binding to DAG. Atypical isozyms, consisting of ζ and ι/λ , respond to neither DAG nor Ca^{2+} , instead containing an atypical, non-ligand binding C1 domain and a protein-binding PB1 domain that serves to mediate protein-protein interactions (25). Finally, the regulatory domains of all three PKC subclasses contain a short autoinhibitory pseudosubstrate sequence that maintains PKC in an inactivate state by occupying the substrate-binding site of the kinase domain. The pseudosubstrate is comprised of basic amino acids that resemble the consensus substrate sequence but contains an Ala at the phosphoacceptor site (26).

While the regulatory domains vary significantly based on the subclass, the catalytic domain is conserved across the PKC family members, consisting of a kinase domain followed by a C-terminal tail. The C-terminal tail plays an important role among all AGC

kinases as it is necessary for catalytic activity and also serves as a docking surface for various regulatory proteins. For instance, it contains a conserved PXXP motif that mediates binding to heat shock protein 90 (Hsp90) and Hsp90 co-chaperone Cdc37 (Cdc37), an interaction which is required for PKC maturation (27). Through this manner, the domain composition for each PKC isozyme has important implications with respect to its activation and regulation.

Full-length rat PKC β II was successfully crystallized in 2011 by Hurley and colleagues, who were able to resolve the C1B, C2, and kinase domains (28). Prior to this, only individual domains of PKC had been resolved. These include the kinase domains of PKC α , β II, θ , and ι ; the C1 domains of PKC α , γ , and δ ; and the C2 domains of PKC α , β , δ , ϵ , and η (Figure 1.2B) (29–38). Antal and colleagues utilized the crystal packing data from Hurley and colleagues to propose a model in which the C2 domain clamps against the kinase domain (Figure 1.2C) (39). This serves to tether the pseudosubstrate in the active site and autoinhibit the enzyme, providing a means to inhibit PKC signaling output in the absence of the appropriate second messengers. This finding further corroborates that while the pseudosubstrate is an important contributor in the autoinhibition of PKC, it is not the sole contributor (40).

The closed and inactive conformation of PKC facilitated by intramolecular contacts between its C2 and kinase domains highlight a previously undefined mechanism of structural autoinhibition. The structural basis of this autoinhibition is likely shared among the conventional isozymes of PKC given that they possess a high degree of homology. In fact, a study by Igumenova and colleagues supports a similar model for PKC α (41). The authors utilized molecular modeling and NMR spectroscopy to propose a model in

which the C2 domain of PKC α interfaces with the C-terminal tail in the autoinhibited conformation of the enzyme. Thus, investigating PKC structure has shed insight into the basis for autoinhibition of the enzyme, allowing for a better understanding of how PKC activity is exquisitely tuned and alternatively, how it may be disrupted in pathophysiological conditions.

1.3 The Life and Death of PKC

When translated, unprimed PKC is localized to the plasma membrane (Figure 1.2, *(i)*). According to studies with PKC β II, enzyme that is newly-synthesized adopts an open conformation wherein the pseudosubstrate is not occupying the active site and the membrane-targeting modules are exposed. In order to become catalytically competent and subject to the allosteric regulation of second messengers, PKC must first undergo a series of tightly coupled, constitutive phosphorylations (Figure 1.2, *(ii)*) (8, 42). PKC phosphorylation requires binding to the molecular chaperones Hsp90 and Cdc37, which occurs via the PXXP motif in the C-terminal tail. The priming phosphorylations, lending stability to the PKC isozymes, occur at three sites: the activation loop in the kinase domain and the turn motif and hydrophobic motif in the C-terminal tail (18, 21). Phosphorylation at the activation loop is mediated by the phosphoinositide-dependent kinase PDK1 for conventional, novel, and atypical isozymes (19, 43, 44). In the case of conventional isozymes, subsequent phosphorylation at the turn motif and hydrophobic motif is dependent on the mammalian target of Rapamycin complex 2 (mTORC2) (45). Phosphorylation of the hydrophobic motif has been shown *in vitro* to occur via an intramolecular autophosphorylation mechanism and is thus dependent on the intrinsic

catalytic activity of PKC (20, 46). With the exception of PKC ϵ , mTORC2 is not required for phosphorylation of novel isozymes (45, 47). Atypical isozymes are phosphorylated co-translationally at the turn motif by ribosome-associated mTORC2 and are not phosphorylated at the hydrophobic motif as that site is occupied by a Glu residue at that position. Conventional and novel PKC isozymes, in their mature but inactive form, are retained within the cytosol. At this stage, PKC is in a closed conformation, autoinhibited by the pseudosubstrate which then occupies the substrate-binding cavity. In this conformation, the formerly exposed C1 and C2 domains are also masked (12). Thus, while PKC is primed and poised to signal, its autoinhibition minimizes signaling in the absence of agonists.

Activation of PKC occurs via the agonist-induced generation of second messengers, resulting from the hydrolysis of phosphatidylinositol-4,5-bisphosphate (PIP₂) (Figure 1.2, *(iii)*). Specifically, activation of G α_q -coupled receptors results in phospholipase C (PLC)-mediated hydrolysis of PIP₂ into its constituents inositol 1,4,5-triphosphate (IP₃) and DAG. IP₃ stimulates release of Ca²⁺ from intracellular stores in the endoplasmic reticulum. Conventional PKCs are targeted to the membrane upon binding of Ca²⁺ to the C2 domain, which results in displacement of the C2 domain from the kinase domain and exposure of a basic face. Retention of the C2 domain at the membrane is facilitated by interaction of this basic face with PIP₂. At the membrane, the C1 domain, predominantly the C1B domain, binds membrane-embedded DAG. This causes a conformational change that expels the pseudosubstrate from the active site, effectively activating PKC and allowing it to engage in downstream signaling (48). In contrast, novel PKC isozymes are activated by DAG alone. Thus, they can be activated by PLC-

catalyzed hydrolysis of other phospholipids. Upon agonist stimulation, novel isozymes of PKC can also translocate to intracellular sites other than the plasma membrane, including the Golgi and mitochondria (6). Activation of atypical PKC isozymes is dependent upon protein-protein interactions. While they also require relief of autoinhibition for activation, this occurs through binding of their PB1 domains to protein scaffolds such as p62 and Par6 (25, 49–51). In addition to activation, scaffold binding also serves to compensate for the low catalytic rate of the atypical isozymes, bringing the enzymes in close proximity with their substrates to ensure efficient phosphorylation. It was also recently revealed that sphingosine 1-phosphate (S1P), a lipid mediator, may function as a second messenger for the atypical isozymes (52). S1P was shown to be capable of activating atypical PKC isozymes by directly binding to the kinase domain and relieving autoinhibitory constraints. Activation of PKC is reversible, with the kinetics of inactivation associated with the decay of its second messengers. For conventional and novel isozymes, PKC returns to the inactive state as DAG is metabolized (6).

In its active form, PKC is in an open conformation and sensitive to dephosphorylation by phosphatases, such as the phosphatase PH domain leucine-rich repeat protein phosphatase (PHLPP) and protein phosphatase 2A (PP2A) (Figure 1.2, *(iv)*) (53). Thus, prolonged activation of PKC leads to dephosphorylation. PHLPP catalyzes the first dephosphorylation event by targeting the hydrophobic motif site while PP2A mediates dephosphorylation of the other sites. Dephosphorylation effectively destabilizes the kinase and targets it for ubiquitination and subsequent degradation via the proteasome, a process referred to as PKC downregulation (54). Pin1 catalyzes isomerization of the turn motif site in conventional PKC isozymes which is required for

their dephosphorylation, ubiquitination, and degradation (55). Ubiquitination of PKC has been shown to be facilitated by the E3 ligase Ring-finger protein that interacts with C kinase (RINCK), which binds PKC through its C1A domain (56). Rephosphorylation of PKC can occur through binding of the molecular chaperone heat shock protein 70 (Hsp70) to the dephosphorylated turn motif. This event stabilizes PKC, promoting its rephosphorylation and allowing it to return to a signaling-competent state.

Given the number of proteins involved in the life cycle of PKC, there are many ways in which the steady-state levels of PKC in the cell can be altered. Hsp90, PDK1, and mTORC2 play critical roles in the maturation of PKC and thus function to increase levels of PKC in the cell. Inhibition of these proteins prevents appropriate processing of PKC by phosphorylation, which results in the dephosphorylated enzyme being targeted for degradation. Alternatively, Pin1, PHLPP, PP2A and RINCK negatively regulate PKC levels in the cell. Inhibition of these proteins result in increases in the steady-state levels of PKC. Dysregulation of PKC signaling, particularly in disease states, can therefore occur through perturbation of these proteins that function to regulate the phosphorylation, dephosphorylation, and degradation of PKC.

1.4 Substrates of PKC

PKC plays a crucial role in cell signaling and homeostasis, and as such, phosphorylates a variety of substrates. With the activation of conventional and novel PKC isozymes occurring in association with cellular membranes, these substrates include membrane proteins. For example, PKC has been shown to phosphorylate epidermal growth factor receptor (EGFR), which results in a reduction of activity and ligand-binding

affinity as well as an increase in receptor internalization (57). PKC-mediated phosphorylation of human epidermal growth factor receptor 2 (HER2) also causes receptor internalization, decreasing its signaling duration (58). PKC also phosphorylates a variety of G-protein coupled receptors, such as muscarinic, dopamine, and histamine receptors (59–61). In addition to receptors, PKC regulates various transporters by phosphorylation, including solute carrier (SLC) and ATP-binding cassette (ABC) drug transporters (62). Phosphorylation of these transporters is often isoform-specific and results in changes in transporter activity, membrane localization, and/or expression. Additionally, PKC phosphorylates cytoskeleton proteins, like α 6-tubulin and vinculin, and nuclear proteins, like histones, lamins, and DNA topoisomerases (63–66). The substrates for PKC extend far beyond those listed here, and through regulation of these substrates, PKC exerts an important influence over a multitude of biological processes, including, but not limited to, cell adhesion, cell motility, proliferation, and inflammation.

1.5 Dysregulation of PKC in Disease

Because PKC regulates such diverse cellular processes by phosphorylating diverse substrates, PKC activity is frequently dysregulated in disease. The many roles that PKC plays in different disease states is often dependent upon factors such as the specific PKC isozyme, the tissue type, and the cell type in question. Consequently, the same isozyme may exert very different effects in different biological contexts. To add further complexity, different PKC isozymes in the same disease state may have opposing roles. Studies of PKC in pathophysiologies thus must investigate potential roles of the enzyme in an isozyme-specific manner (65). Along those lines, it is crucial that therapies

designed to target PKC consider specificity for the desired isozyme and the potential off-target effects on other isoforms. Discussion of some of the diseases in which PKC has been implicated follows.

Metabolic Disease

PKC may have an important role in type 2 diabetes and other metabolic disorders. Atypical isoforms of PKC have been shown to regulate glucose transport upon insulin stimulation. Deletion of PKC λ in mice caused diminished glucose transport and translocation of glucose transporter 4 (GLUT4) to the plasma membrane in muscle, resulting in systemic insulin resistance, impaired glucose tolerance, and islet β cell hyperplasia (67). In preadipocyte-derived human adipocytes, insulin-stimulated glucose transport was inhibited by expression of catalytically dead PKC ζ and treatment of cells with the cell-permeable myristoylated PKC ζ pseudosubstrate (68). Expression of wild-type PKC ζ or a constitutively active, in contrast, increased glucose transport. Additionally, a breadth of studies has implicated PKC in complications associated with diabetes, including a number of vascular pathologies (69, 70). A common feature of a hyperglycemic or diabetic environment is chronically elevated DAG levels, which has been detected in both vascular tissues, such as the heart, and nonvascular tissues, such as the liver. Consequently, it serves as an environment conducive to PKC activation. Activation of different PKC isoforms in various cell types has been shown to result in dysregulation of cellular processes such as endothelial function, vascular permeability, angiogenesis, cell growth, and apoptosis, among others. For instance, uptake of oxidized low density lipoprotein (oxLDL) by monocyte-derived macrophages facilitates lipid

accumulation in the arterial wall, one of the earliest events in the development of atherosclerosis (69, 71). In hyperglycemic conditions, these macrophages have enhanced expression of PKC β and enhanced PKC β activity (71–73).

Cardiovascular Disease

Given that PKC has been shown to affect physiological processes in the heart, such as heart rate, contraction, and relaxation, it is not surprising that PKC plays a role in cardiovascular disease. The roles of PKC in the heart appear to be isozyme-specific (74). Studies have shown that PKC δ and PKC ϵ have opposing roles, with PKC δ facilitating cardiac dysfunction and PKC ϵ playing a protective role (74–76). Prolonged ischemia and reperfusion results in activation of PKC δ and its translocation into mitochondria, leading to inhibition of ATP regeneration, accumulation of reactive oxygen species (ROS) and toxic aldehydes, and ultimately, apoptosis and necrosis. PKC δ inhibition has been shown to reduce reperfusion injury by inhibiting apoptosis and necrosis (77). PKC ϵ also translocates into mitochondria upon activation, but its activity is cardioprotective (78, 79). PKC ϵ activation results in activation of aldehyde dehydrogenase 2 (ALDH2) which removes toxic aldehydes and peroxidation byproducts (80). ALDH2 activation lowers concentration of ROS, promotes recovery of ATP, and diminishes apoptosis and necrosis (81). PKC ϵ also mediates cardioprotection through several other mechanisms, including stabilization of mitochondria in cardiac tissue through inhibition of the mitochondria permeability transition pore, increased activity of cytochrome c activity, and down-regulation of activated PKC δ (82–84).

Neurodegeneration

PKC has been implicated in neurodegenerative disorders, with germline mutations in PKC α identified in Alzheimer's disease and germline mutations in PKC γ identified in spinocerebellar ataxia type 14 (SCA14). PKC mutations associated with neurodegeneration have been found to enhance activity of the kinase. One mutation in PKC α , M489V, was identified in four unrelated families among the members affected by Alzheimer's Disease but was absent among unaffected members (85, 86). The mutation caused an approximate 30% increase in the catalytic rate of PKC α , enhancing PKC activity while evading down-regulation. In support of this, elevated PKC signaling was found to be one of the earliest events in Alzheimer's disease as reported in a phosphoproteomics analysis of post-mortem brains (87). Moreover, there are many PKC substrates in the brain that may be involved in these pathophysiologies, notably MARCKS, GAP43, and tau (65, 88). More than 30 germline mutations in PKC γ have been identified in SCA14 (89). As with the PKC α mutations associated with Alzheimer's disease, some of these PKC γ mutations also appear to loosen autoinhibitory constraints to modestly activate the enzyme without targeting it for down-regulation (90).

1.6 PKC in Cancer

While PKC is indeed implicated in a variety of diseases, its most notable pathophysiological role is arguably in cancer. The history of PKC's role in cancer can be traced back to its association with the compounds known as phorbol esters. Phorbol esters, derived from the seed oil of *Croton tiglium*, have been a topic of interest in cancer research since the establishment of the mouse skin carcinogenesis model in the mid-20th

century. This model demonstrated that repeated application of phorbol esters following treatment with a sub-threshold amount of a mutagenic agent, namely 7,12-dimethylbenz(a)anthracene (DMBA), promoted the formation of papillomas on the skin of mice (16). It was then discovered that PKC served as a high-affinity receptor for these tumor-promoting compounds, binding its C1 domains, and thereafter became subject to intense study (91–93). The dogma for PKC in cancer was thus established: PKC functions as an oncogene, with its activation promoting tumor progression. However, PKC has remained an elusive target as cancer therapeutics designed to inhibit its activity have consistently failed in clinical trials (17). Furthermore, not only have therapies targeting PKC been unsuccessful, PKC inhibitors have at times worsened patient outcome (94). Conflicting evidence in the literature concerning the role of PKC in tumorigenesis as well as the failure of PKC inhibitors in clinical trials has brought its oncogenic function into question.

To this end, reexamination of the effect of phorbol ester treatment on PKC biology reveals a paradoxical role for the compounds. While phorbol esters indeed activate PKC, they are not metabolized like PKC's physiological second messengers. Thus, phorbol ester-mediated activation of PKC is constitutive rather than transient, and as a result, PKC is maintained in an open conformation. This open conformation renders PKC sensitive to dephosphorylation and consequently targets it for degradation. Acute activation of PKC mediated by phorbol esters is therefore followed by PKC down-regulation (95, 96). Ultimately, this suggests that the capacity for phorbol esters to promote tumor growth stems from the loss of PKC.

An analysis of 46 cancer-associated mutations in PKC revealed that the vast majority of them were loss-of-function while none were gain-of-function (11). These mutations occurred in isozymes from all three subclasses of PKC and were identified in a wide variety of cancer types. The mutations also occurred all along the domain structure of PKC. Biochemical characterization of the mutations revealed that inactivation of PKC can be mediated through several ways, namely preventing PKC processing by phosphorylation, impeding second messenger binding, and impairing catalysis. Because there are several avenues for PKC inactivation, no mutational hotspots were identified. Additionally, some mutations were observed to dominant-negative, with the mutant PKC suppressing the global signaling output its wild-type counterpart. Importantly, correction of a loss-of-function PKC β mutation (A509T) in the DLD1 colon cancer cell line by CRISPR/Cas9-mediated gene editing suppressed anchorage-independent growth in soft agar. Deletion of the mutant allele to generate a cell line with a single wild-type allele of PKC β revealed that PKC is haploinsufficient, suggesting that loss of a single copy of functional PKC will result in increased tumor growth. Moreover, reduced tumor growth was observed for the CRISPR-corrected line compared to the parental in a mouse xenograft model. Ultimately, this study demonstrated that inactivation of PKC confers a survival advantage while restoration of PKC function suppresses tumor growth. Thus, a new role was established for PKC as a tumor suppressor rather than an oncogene, with PKC inactivation contributing to tumorigenesis.

Other evidence in the literature supports a tumor suppressive role for PKC (97). Decades prior to the establishment of PKC's tumor suppressive function, a loss-of-function mutation in PKC α was identified in pituitary tumors and a separate study

demonstrated that PKC α facilitated suppression of cell growth (98, 99). Additionally, levels of PKC have been shown to predict outcome for various cancers, with low levels predicting poor outcome and high levels correlated with increased survival. Low levels of PKC β II in colorectal cancer, PKC δ in bladder cancer, and PKC η in liver cancer have all been associated with poor patient outcome (100–102). High levels of PKC ϵ in lung and renal cancer and PKC η in head and neck cancers have, in contrast, found to be favorable (103). Lastly, in addition to somatic mutations, loss-of-function germline mutations have also been identified in PKC. Specifically, four mutations in PKC δ have shown to be causal in juvenile systemic lupus erythematosus (JSLE), resulting in increased proliferation and resistance to apoptosis in immune cells (104–106). In fact, individuals with JSLE are predisposed to developing B-cell lymphomas. With mounting evidence serving to validate its tumor suppressive function, the paradigm for PKC as an oncogene has been effectively reversed. Consequently, this novel role for PKC has profound implications in regards to the design of targeted therapeutics in cancer, which should seek to restore rather than inhibit PKC function.

While a general role for PKC as a tumor suppressor has been established, PKC may function as an oncogene in specific contexts. There is evidence that the atypical isozymes of PKC, in particular, have oncogenic roles. A bona fide role for PKC ι has been well-established, with its gene residing on one of the most frequently amplified regions in human cancers (3q26) (107). Studies have shown that the protein promotes tumorigenesis by regulating transformed cell growth, survival, and chemoresistance in cancers such as prostate cancer, glioma, and non-small cell lung cancer (NSCLC). Elevated PKC ι expression has also been associated with decreased survival in NSCLC,

ovarian cancer, and prostate cancer and increased relapse in gastric cancer. Moreover, sphingosine 1-phosphate (S1P) has been recently shown to activate atypical PKC isoforms (52). S1P is recognized as a mediator of survival signaling, and the enzyme responsible for its generation, sphingosine kinase, has been identified as an oncogene. However, studies also show that these isoforms may have a tumor suppressive function in other cancers. Loss of PKC δ in the intestinal epithelium has been observed in patients with Crohn's disease who are predisposed for small bowel, colon, and extraintestinal cancer (108). In mice, loss of PKC δ in the intestinal epithelium exhibited increased inflammation and tumor growth (109). PKC ζ may also have a protective role in the intestine as loss of PKC ζ in intestinal cells promoted metabolic reprogramming necessary for facilitating cancer cell survival under nutrient stress (110). Given the contrasting roles observed for PKC in different cancers, it is thus crucial to consider the particular isoform and specific biological context in question when evaluating the contribution of PKC to tumorigenesis.

1.7 Research Goals

The overarching objective of the work presented in this thesis is to elucidate the mechanisms by which PKC is perturbed in cancer. This is accomplished through 1) characterization of cancer-associated PKC gene fusions and 2) investigation of PKC regulatory mechanisms that may be exploited in cancer. Chapter 2 explores the prevalence and relevance of newly identified PKC gene fusions in cancer. A series of biochemical and cellular experiments, including live-cell imaging and CRISPR/Cas9-mediated gene editing reveal that these gene fusions are loss-of-function. Chapter 3

focuses on various aspects of PKC regulation and how they present vulnerabilities that may be targeted in a cancer context. These biochemical and cellular data underscore the crucial role autoinhibition plays in PKC biology. Taken together, these studies expand upon the underlying molecular mechanisms that facilitate loss of PKC function in cancer, allowing for further appreciation of PKC's role as a tumor suppressor.

1.8 Figures

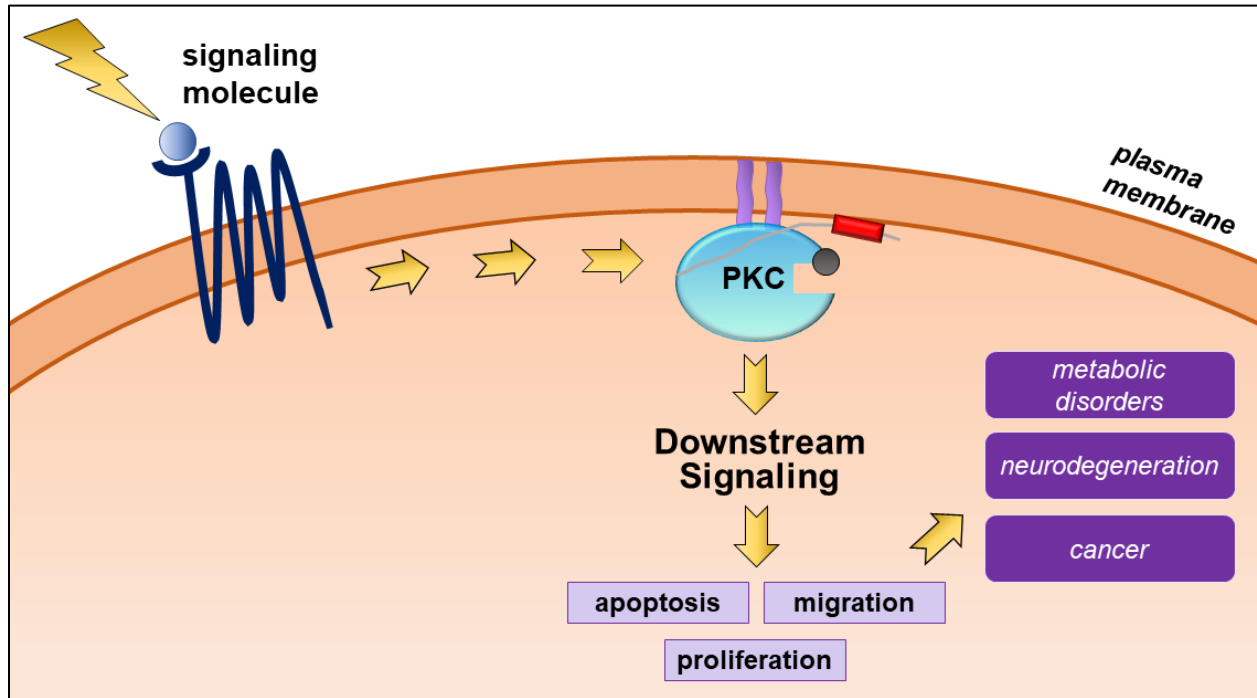


Figure 1.1: PKC in signal transduction. PKC transduces signals downstream of receptor-mediated hydrolysis of phospholipids. Activation of PKC results in downstream signaling associated with a myriad of cellular processes, including apoptosis, migration, and proliferation. As such, PKC activity is frequently dysregulated in disease and has been implicated in metabolic disorders, neurodegeneration, and cancer, among others.

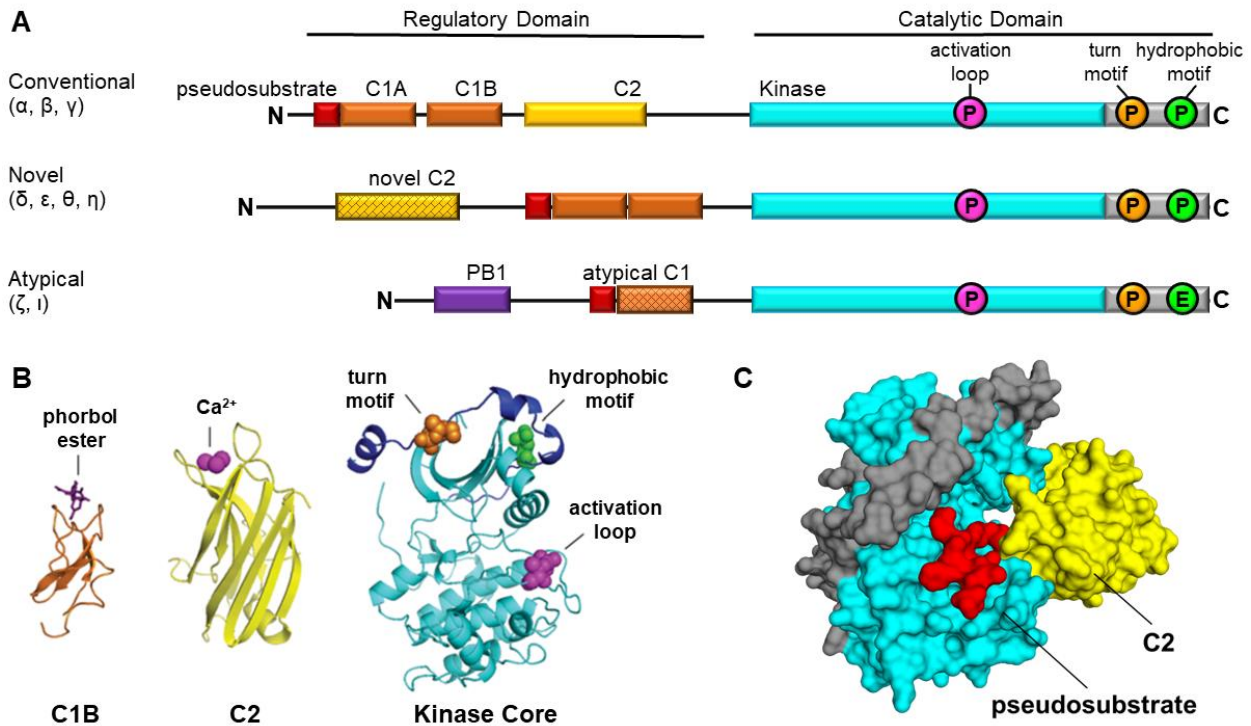


Figure 1.2: Domain composition of PKC family members and crystal structures. (A) Domain structure of the three PKC subclasses. General domain structure is comprised of a regulatory domain and a catalytic domain. The regulatory moiety of conventional isoforms includes the pseudosubstrate (red), C1 domains (orange), C2 domain (yellow). Novel isoforms contain a novel C2 domain (patterned yellow), and atypical isoforms possess a protein-binding PB1 domain (purple) as well as an atypical C1 domain (patterned orange). The catalytic moiety is conserved among the family members, containing a kinase domain (cyan) and a C-terminal tail. The catalytic moiety also contains the phosphorylation sites necessary for catalytic competency: the activation loop (pink), turn motif (orange), and hydrophobic motif (green). **(B)** Crystal structures of the PKC C1B (PDB code 1PTR), C2 (PDB code 1A25), and kinase (PDB code 2I0E) domains. **(C)** Model based on reinterpretation of crystal packing data from Hurley and colleagues containing the kinase (cyan) and C2 (yellow) domains with a docked pseudosubstrate (red).

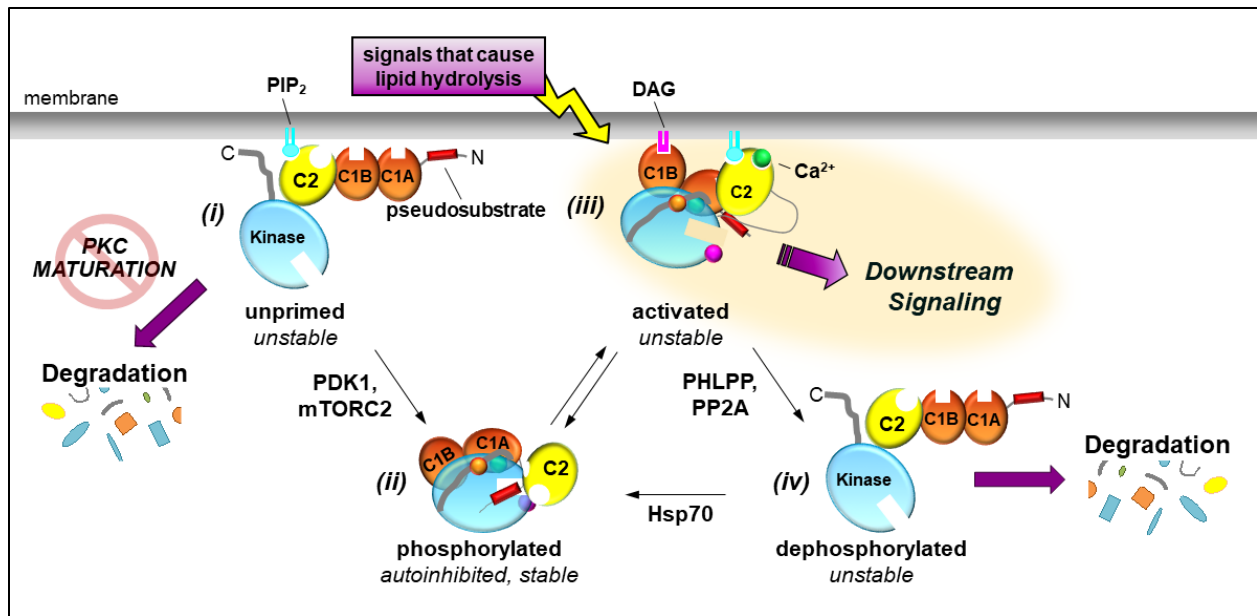


Figure 1.3: The life cycle of PKC. *(i)* Newly-synthesized, unprimed PKC is localized to the plasma membrane. *(ii)* It undergoes a series of tightly-coupled, constitutive phosphorylations in order to gain catalytic competency, mediated by PDK1 and mTORC2. Once phosphorylated, it is in a primed but inactive state. *(iii)* Hydrolysis of PIP₂ results in the generation of DAG and release of Ca²⁺ from intracellular stores. Ca²⁺ binding to the C2 domain recruits the kinase to the membrane where it is retained via electrostatic interactions with PIP₂. At the membrane, the C1 domain binds DAG, causing a conformational change that expels the pseudosubstrate from the substrate-binding cavity and activates the kinase. PKC can then engage in downstream signaling. *(iv)* In its active state, PKC adopts an open conformation that is sensitive to dephosphorylation by phosphatases, namely PHLPP and PP2A. This species is markedly unstable and is shunted off to degradative pathways. However, Hsp70 can facilitate rephosphorylation, returning PKC to the pool of signaling-competent enzyme. Impeding PKC maturation, such as through inhibition of PDK1 or mTORC2, also results in degradation of PKC.

Chapter 2

Protein Kinase C Fusions Reveal Mechanism for Loss of Protein Kinase C Function in Cancer

2.1 Abstract

While protein kinase C (PKC) has been identified as the most frequently fused kinase in the AGC superfamily, the proteins resulting from these cancer-associated PKC gene fusions have yet to be characterized. Here, we investigated both fusions that retain the transcript encoding the PKC catalytic domain and fusions that retain the transcript encoding the PKC regulatory domain. Overexpression of PKC catalytic domain fusions revealed that they were unphosphorylated at the three PKC priming sites yet were constitutively active. Although loss of the autoinhibitory pseudosubstrate permitted this constitutive activity, it also rendered the fusion proteins unstable, degrading at a faster rate compared to their wild-type counterparts. To assess whether the unstable fusion proteins would be detected in an endogenous context, we utilized CRISPR/Cas9-mediated gene editing to express a fusion in cells. While the fusion mRNA was detected in the CRISPR-edited cells, the fusion protein was not, demonstrating that the protein is too unstable to accumulate. Hence, PKC catalytic domain fusions are paradoxically loss-of-function due to their instability. Overexpression of a PKC regulatory domain fusion revealed that it suppressed both endogenous basal and agonist-induced PKC activity. Moreover, we identified the Golgi as a major site where this suppression occurs. Thus, in addition to being intrinsically loss-of-function due to loss of the catalytic domain, PKC regulatory domain fusions may also act in a dominant-negative manner. Taken together, our findings show that PKC gene fusions present a mechanism by which PKC activity is lost in cancer, supporting a tumor suppressive role for PKC.

2.2 Introduction

Advances in bioinformatics and next-generation sequencing technology have revolutionized our ability to appreciate the abundance and relevance of gene fusions in cancer, particularly with respect to solid tumors (111–113). While numerous studies have investigated point mutations, deletions, and amplifications, relatively little attention has been given to gene fusions. However, as exemplified by *BCR-ABL1* in chronic myeloid leukemia and *ALK* fusions in lung carcinomas and mesenchymal tumors, gene fusions may play critical roles in tumorigenesis and present as attractive targets for therapeutic intervention (114–117).

Previous analysis of RNA sequencing data from The Cancer Genome Atlas (TCGA) revealed that approximately 15% of in-frame kinase fusions belong to members of the AGC superfamily of serine/threonine kinases, second only to the tyrosine kinase family (114). Within the AGC kinases, protein kinase C (PKC) has been identified as the most frequently fused member, with the greatest abundance of gene fusions involving *PRKC* isozyms. The PKC family consists of nine isozyms, categorized into three classes: conventional (α , β , γ), novel (δ , ϵ , η , θ), and atypical (ζ , ι/λ) (100). While the C-terminal catalytic domain is conserved across all PKC family members, the regulatory moiety differs, revealing the distinct co-factor dependency of each PKC subclass. Conventional PKCs contain diacylglycerol (DAG)-binding C1A and C1B domains and a Ca^{2+} -binding C2 domain. Novel isozyms possess a C2 domain that lacks key residues required for coordinating Ca^{2+} , but compared to conventional isozyms, bind DAG with a 100-fold greater affinity (22, 23). Atypical isozyms respond to neither DAG nor Ca^{2+} but contain a protein-binding PB1 domain that mediates protein-protein interactions (49). All

PKC isozymes contain an autoinhibitory pseudosubstrate sequence that maintains PKC in an inactivated state, occupying the substrate-binding active site of the kinase domain. In this manner, PKC activity is tightly regulated, only able to phosphorylate downstream substrates in the presence of its second messengers (39).

PKC plays a critical role in cellular homeostasis, transducing signals initiated by receptor-mediated hydrolysis of phospholipids to regulate cellular processes such as apoptosis, migration, and proliferation (7, 15, 16). With its activity finely tuned, dysregulation of PKC has been implicated in a multitude of diseases, including metabolic disorders, neurodegeneration, and most notably, cancer (70, 88, 97). Since PKC was identified as a high-affinity receptor for the tumor-promoting compounds known as phorbol esters, it has been associated with an oncogenic role, its activation contributing to tumorigenesis (91–93). However, over the past three decades, PKC has remained an elusive target as therapeutics designed to inhibit it have failed in clinical trials and at times worsened patient outcome (94). We have since learned that phorbol esters lock PKC in an active conformation, ultimately promoting its downregulation (95, 96). Moreover, our laboratory's previous analysis of cancer-associated point mutations in PKC revealed most to be loss-of-function, with PKC inactivation conferring a survival advantage and promoting tumor growth (11). Furthermore, high protein levels of PKC are associated with improved survival in diverse cancers, including colon cancer and pancreatic cancer (101, 118). Thus, a tumor suppressive role for PKC was established, reversing the dogma of PKC as an oncogene. Given that both gain-of-function fusions involving oncogenes and loss-of-function fusions involving tumor suppressors have been identified, we sought to determine what function these newly identified PKC gene fusions may have in cancer.

Here, we investigated PKC gene fusions that yield proteins retaining the catalytic domain of PKC (3' PKC fusions) as well as fusions that yield proteins retaining the regulatory domain of PKC (5' PKC fusions). We found that while the catalytic domain fusions were unphosphorylated at the three PKC processing sites necessary for catalytic competency, they were constitutively active, as measured in cells with our genetically encoded PKC activity reporter. However, the open conformation facilitating this constitutive activity also rendered the catalytic domain fusions more sensitive to degradation compared to wild-type PKC. Utilizing CRISPR/Cas9-mediated gene editing to express a 3' PKC fusion, we were able to detect the fusion at the mRNA level in CRISPR-edited cells but not the protein level, suggesting that the fusion protein is too unstable to accumulate in cells. In our analysis of a 5' PKC fusion, we observed that overexpression of the regulatory domain fusion suppressed endogenous basal and agonist-induced PKC activity. Using a variant of our PKC activity reporter targeted to the Golgi, we determined that the Golgi is a primary site for this suppression. Thus, in addition to loss of the kinase domain, PKC regulatory domain fusions may also act in a dominant-negative manner. Our results show that like the majority of PKC point mutations, PKC gene fusions are loss-of-function, revealing a mechanism for loss of PKC activity in cancer and supporting a role for PKC as a tumor suppressor.

2.3 Results

A multitude of PKC fusions have been identified in cancer

In order to assess the landscape of PKC fusions in cancer, we queried the literature and several online databases to curate a comprehensive list of all PKC fusions identified

from patient tumor samples (Table 2.1). The online databases utilized in this study include the Mitelman Database of Chromosome Aberrations and Gene Fusions in Cancer, TCGA Tumor Fusion Gene Data Portal, ChimerDB v3.0, and COSMIC (112, 119). With this list of fusions, we were able to ascertain that each of the nine isozymes from the three subclasses of the PKC family (Figure 2.1A) was detected in at least one gene fusion (Figure 2.1B). Although there were only 5 isozymes for which there were fusions detected that retained the 5' end of PKC, there were fusions detected for all isozymes where the 3' end of PKC was retained. The greatest number of fusions was detected for *PRKCA* with 25 fusions identified, and the majority of these (12 fusions) were found in breast cancer samples. There were seven fusions identified for *PRKCB*, *PRKCE*, *PRKCH*, and *PRKCZ*, five fusions identified for *PRKCI*, and one fusion identified for *PRKCG*, *PRKCD*, and *PRKCQ*. In total, 61 fusions were identified across all PKC family members. PKC gene fusions were detected in 20 different cancer types, from bladder urothelial carcinoma (BLCA) to uterine corpus endometrial carcinoma (UCEC) (Figure 2.1C). Among these different cancer types, the greatest number of PKC gene fusions was identified in breast cancer with 22 fusions detected and lung adenocarcinoma with 9 fusions detected. Given that PKC is the most abundantly fused AGC kinase and the fusions were detected in a multitude of cancers, we sought to determine how these fusions might affect PKC signaling and contribute to tumorigenesis. To this end, we selected three 3' fusions (*TANC2-PRKCA*, *CTL1-PRKCA*, and *GGA2-PRKCB*) and one 5' fusion (*PRKCA-CDH8*) in this study for further analysis (115, 120).

PKC catalytic domain fusions are unphosphorylated yet constitutively active

3' PKC gene fusions yield proteins in which the N-terminal regulatory domain of PKC is truncated and replaced with the N-terminal domain of its gene partner. The 3' fusions *TANC2-PRKCA*, *SLC44A1-PRKCA*, and *GGA2-PRKCB*, found in lung squamous cell carcinoma (LUSC), papillary glioneuronal tumors (PGNT), and low-grade glioma (LGG), respectively, were selected for biochemical analysis (Figure 2.2A) (115, 120–122). *TANC2-PRKCA* encodes the first 45 amino acid residues of TANC2 fused to the last 496 residues of PKC α , and *SLC44A1-PRKCA* encodes the first 650 residues of CTL1 fused to the last 366 residues of PKC α . *GGA2-PRKCB* encodes the first 158 residues of GGA2 fused to the last 605 residues of PKC β II. While TANC2 is identified as a scaffolding protein in dendritic spines, CTL1 functions as a choline transporter (123–125). GGA2 is part of the Golgi-localized, gamma adaptin ear-containing, ARF-binding (GGA) family of adaptor proteins which localize to the trans-Golgi network and regulate protein trafficking (126). The protein products resulting from the fusion transcripts retain the complete catalytic domain of PKC with some portion of the regulatory domain. Specifically, *TANC2-PRKCA* retains the C2 domain and *GGA2-PRKCB* retains the C1B and C2 domains whereas *CTL1-PRKCA* only retains part of the hinge between the regulatory and catalytic moieties. Notably, the autoinhibitory pseudosubstrate, located at the far N-terminus, is lost in all three fusion proteins. In our biochemical analysis of these catalytic domain fusions, we also analyzed N-Deletion proteins in which we delete the fusion partner and retain only the PKC portion of the fusion. Additionally, we also analyzed a variant of the *CTL1-PRKCA* fusion protein in which there was an internal deletion within the choline transporter domain (CTD) of *CTL1* (120).

Phosphorylation at the three PKC priming sites, the activation loop, turn motif, and hydrophobic motif, is necessary for catalytic competency (127). Thus, we determined whether the fusion proteins and their variants are also phosphorylated at these sites. While wild-type PKC was constitutively phosphorylated at all three processing sites, the full-length fusion proteins TANC2-PKC α , CTL1-PKC α , and GGA2-PKC β II were not. The PKC α and PKC β II N-Deletion proteins as well as the CTL1-PKC α Internal Deletion (Int. Del.) protein were also not appreciably phosphorylated at the activation loop, turn motif, or hydrophobic motif. Lack of phosphorylation at the priming sites of these proteins is consistent with that of PKC α and PKC β II proteins where the pseudosubstrate is deleted (Δ PS). It is also of note that since CTL1 is a transmembrane protein, a large proportion of the overexpressed CTL1-PKC α fusion protein was unable to migrate through the separating gel. Altogether, we see that the fusion proteins and their variants are all unphosphorylated compared to wild-type PKC, potentially affecting their ability for catalysis.

To address this possibility, we sought to determine the cellular activity of the full-length and related fusion proteins compared to wild-type PKC utilizing the genetically-encoded, fluorescence resonance energy transfer (FRET)-based reporter for PKC activity, C Kinase Activity Reporter (CKAR) (128). In COS7 cells co-expressing CKAR and mCherry-tagged wild-type PKC, we observed a transient increase in CKAR phosphorylation, and thus PKC activity, with addition of the physiological agonist UTP, followed by maximal, sustained activity upon treatment with the phorbol ester PDBu (Figure 2.2C). Addition of inhibitor, either Gö6976 or Gö6983, resulted in a decrease in PKC activity to baseline levels. In contrast, the full-length fusion proteins did not respond

as robustly as wild-type PKC to the addition of UTP or PDBu. However, addition of inhibitor resulted in a sizeable decrease in PKC activity, and when comparing the activity of the fusion proteins to that of their wild-type counterparts prior to agonist addition, the fusion proteins display significantly higher basal activity. Introduction of a mutation to render the PKC kinase domain catalytically dead (V353F in PKC α and V356F in PKC β) abolishes this constitutive activity in the full-length fusion proteins. Moreover, the N-Deletion proteins exhibited similar activity to their corresponding full-length fusion proteins, with much greater basal activity compared to wild-type PKC that also does not significantly increase upon addition of agonist. To more precisely probe basal activity of the fusion proteins, we treated naïve COS7 cells expressing either CKAR alone or co-expressing mCherry-tagged PKC with a PKC inhibitor (BisIV or Gö6983) (Figure 2.2D). Upon addition of inhibitor, we see a very modest drop in CKAR phosphorylation in cells assaying endogenous activity as well as the activity of overexpressed wild-type PKC. This small drop suggests that there is very little basal activity in the absence of agonist. In contrast, addition of inhibitor in cells overexpressing the full-length fusion proteins exhibit a dramatic drop in CKAR phosphorylation, suggesting high basal activity. This activity is abolished when introducing the mutation rendering the kinase domain catalytically dead. The N-Deletion proteins mirror their full-length counterparts, exhibiting high basal activity as well. Thus, while the full-length fusion and N-Deletion proteins are unphosphorylated at the PKC priming sites, they exhibit constitutive, agonist-independent activity.

Although analysis of steady-state levels of the fusion protein indicate that they are not phosphorylated at the three PKC processing sites, it is important to note that having a phosphorylatable residue at those sites is necessary for activity. When the hydrophobic

motif of PKC α is mutated to an Ala (S657A) in TANC2-PKC α , the high basal activity exhibited by the unmutated fusion protein is abolished (Figure 2.3A). Similarly, mutation of the hydrophobic motif of PKC β II to Ala (S660A) in GGA2-PKC β II also abolished the high basal activity of the unmutated fusion protein (Figure 2.3B). Mutation of the turn motif and hydrophobic motif in PKC α to Glu (T638E and T657E, respectively) in TANC2-PKC α causes no significant change in basal activity compared to the unmutated fusion protein (Figure 2.3A). Mutation of the turn motif in PKC β II to Glu (T641E) in GGA2-PKC β II resulted in a decrease in basal activity compared to the unmutated fusion protein, but this activity was still significantly greater than that of wild-type PKC β II (Figure 2.3B). These studies therefore suggest that the fusion proteins may be phosphorylated at some point in time. To this end, we examined the phosphorylation status of wild-type PKC β II and GGA2-PKC β II fusion protein purified from baculovirus-infected insect cells, a system where low PHLPP activity permits retention of phosphate on aberrant PKC (Figure 2.3C). As expected, wild-type PKC β II is phosphorylated at the three priming sites. Interestingly, the GGA2-PKC β II fusion protein is also phosphorylated at all three sites, demonstrating that there is some context in which the fusion protein is phosphorylated.

Fusions of the PKC catalytic domain are unstable

Prolonged activation of PKC, such as that which occurs with phorbol ester treatment, ultimately results in PKC downregulation and degradation. To determine whether the constitutively active PKC fusion proteins are also sensitive to degradation, COS7 cells overexpressing YFP-tagged wild-type PKC, fusion protein, or pseudosubstrate-deleted PKC were treated with cycloheximide, and degradation of the

PKC proteins was monitored (Figure 2.4A). Wild-type PKC α and PKC β II degrade slowly, with appreciable levels of protein even at the end of the 48 h time course. The TANC2-PKC α and GGA2-PKC β II fusion proteins, however, degraded much more rapidly compared to their wild-type counterparts, with significantly less protein at the end of the time course. The rapid degradation of the fusion proteins is also observed in mutants of PKC wherein the pseudosubstrate segment is deleted, PKC α Δ PS and PKC β II Δ PS. Moreover, we observed that unphosphorylated wild-type PKC, represented by the faster mobility, lower band in wild-type PKC β II, undergoes rapid degradation similar to that of the fusion and Δ PS proteins. Interestingly, GGA2-PKC β II protein purified from HEK 293T cells was found to be in complex with other proteins, denoted by the additional bands observed with the pure protein on a Coomassie-stained gel (Figure 2.5A). Through western blot analysis, we identified Hsp90, Hsp70, and Cdc37 to be associated with the purified GGA2-PKC β II protein but not wild-type protein, suggesting that the molecular chaperones are attempting to stabilize the fusion protein (Figure 2.5B). This also indicates that the fusion protein maintains an open conformation that permits binding of these chaperones (27). Thus, these data demonstrate that unphosphorylated PKC, whether that be wild-type, fusion, or pseudosubstrated-deleted PKC, is more sensitive to degradation compared to the fully phosphorylated wild-type PKC.

Given that the fusion proteins were observed to be more sensitive to degradation, we next asked whether they were more ubiquitinated than wild-type PKC. To address this, we performed a cellular ubiquitination assay in which we overexpressed ubiquitin alone or in conjunction with wild-type PKC α or the TANC2-PKC α fusion in COS7 cells, immunoprecipitated the PKC protein, and assessed the degree of ubiquitination (Figure

2.4B). Additionally, we compared cells treated with the phorbol ester PDBu to vehicle (DMSO), as treatment with phorbol esters ultimately results in PKC degradation and would thus promote ubiquitination. In basal conditions, we observed that TANC2-PKC α is indeed more ubiquitinated compared to wild-type PKC α . Treatment with PDBu induced ubiquitination of wild-type PKC α but had no effect on ubiquitination of the fusion protein, which lacks the domains necessary to bind PDBu. However, this is not surprising since the fusion protein lacks the C1B domain responsible for binding to PDBu. These results indicate that the unstable fusion protein is indeed more ubiquitinated compared to wild-type PKC and is likely shunted off to downstream pathways facilitating its degradation.

CRISPR-edited cells exhibit detectable PKC fusion mRNA but not protein

Since our previous overexpression studies suggested that the catalytic domain fusion proteins are markedly unstable, we sought to determine whether they would be detected in an endogenous context. To accomplish this, we utilized CRISPR/Cas9-mediated gene editing to express the *TANC2-PRKCA* fusion in the MDA-MB-231 breast cancer cell line (Figure 2.6A) (129, 130). Employing two guide RNAs, one directed at an intron of *TANC2* and one directed at an intron of *PRKCA*, we were able to successfully generate a heterozygous clone (CRISPR Clone #93) with one wild-type allele of *PRKCA* and one allele of the *TANC2-PRKCA* fusion. We first validated expression of *TANC2-PRKCA* at the mRNA level, amplifying a product at the fusion junction (Figure 2.6B). Indeed, we were able to detect expression of the fusion mRNA in cells of the CRISPR-edited clone but not the parental. Next, we examined expression of *TANC2* and *PRKCA*, probing for products at the 5' and 3' ends of each mRNA which would correspond to the

respective “N-Term” and “C-Term” of the resulting proteins. Compared to the parental MDA-MB-231 cells, the CRISPR-edited cells exhibited an increase in expression of the *TANC2* “N-Term” product and a decrease in expression of the “C-Term” product (Figure 2.6C). A decrease in expression of the *TANC2* “C-Term” product is in concordance with the fusion-expressing cells containing only one copy of wild-type *TANC2* while the increase in expression of the *TANC2* “N-Term” product may be a compensatory effect from loss of the other copy of *TANC2*. When looking at *PRKCA* expression in the parental and CRISPR-edited cells, we see the reverse; while expression of the *PRKCA* “N-Term product” is decreased in the fusion-expressing cells, expression of the “C-Term” product is increased (Figure 2.6D). In this case, a decrease in expression of the “C-Term” product in the fusion-expressing cells can be attributed to loss of a copy of wild-type *PRKCA*, and as with *TANC2*, the increase in *PRKCA* expression may be compensatory. Moreover, the upregulation of *PRKCA* expression observed here is consistent with increased *PRKCA* expression reported in the tumor in which the fusion was originally detected (115).

Upon confirmation of *TANC2-PRKCA* expression in the CRISPR-edited cells, we next assessed whether the fusion could be detected at the protein level and if so, to what extent. Compared to the parental MDA-MB-231 line, we observed a decrease in both *TANC2* and PKC α protein in cells of the fusion-expressing clone (Figure 2.6E). Importantly, the *TANC2-PKC* α fusion protein, predicted to migrate at 65 kDa, was not detected in the CRISPR-edited cells. This suggests that the fusion protein is indeed too unstable to be able to appreciably accumulate in an endogenous context. In support of this, a titration of DNA transfected into COS7 cells, where both wild-type PKC and the fusion are under control of the same promoter, showed that less fusion protein was

detected at steady-state levels compared to wild-type PKC for the same amount of DNA transfected (Figure 2.7). We then sought to determine whether degradation of the fusion protein could be slowed. Inhibition of proteasomal or endosomal/lysosomal degradative pathways in our overexpression studies with cycloheximide did not slow degradation of the TANC2-PKC α fusion protein (Figure 2.8A, B). Additionally, knockdown of RINCK, the E3 ligase that catalyzes ubiquitin-mediated degradation of wild-type PKC, as well as CHIP, a “quality control” E3 ligase that cooperates with molecular chaperones to ubiquitinate unfolded proteins, did not allow for accumulation of the protein in the CRISPR-edited cells (Figure 2.9) (56, 131). These data thus suggest that the unstable fusion protein is degraded through a separate, proteasome- and endosome/lysosome-independent mechanism. Importantly, given that the fusion is unable to accumulate appreciably in cells, it is clearly loss-of-function.

CRISPR-edited fusion cells exhibit reduced apoptosis

We next sought to determine the functional relevance of the catalytic domain fusion, whose expression would invariably result in the loss of PKC activity. To this end, we determined whether there was any difference in apoptosis between the parental MDA-MB-231 cells and the CRISPR-edited fusion cells. We assessed basal apoptosis in the two cell lines via immunoblot analysis, probing for levels of cleaved caspase-3 (Figure 2.10A). Compared to the parental cells, cells expressing the *TANC2-PRKCA* fusion exhibited significantly decreased levels of cleaved caspase-3. While there was a clear difference in cleaved caspase-3 in basal conditions, there was no difference in cleaved caspase-3 between the two cell lines when apoptosis was induced by treatment with

etoposide (Figure 2.10B). This suggests that the difference in basal apoptosis is not due to an intrinsic difference in overall apoptotic capacity. Lastly, we generated heterozygous and homozygous knockouts of PKC α in the MDA-MB-231 cell line and compared their levels of cleaved caspase-3 to that of the parental and fusion-expressing lines (Figure 2.10C). Both heterozygous and homozygous knockout lines mirror what is observed in the fusion-expressing line; compared to the parental cells, all three CRISPR-edited cell lines had reduced levels of cleaved caspase-3, suggesting that the loss of PKC activity is coincident with decreased apoptosis. Overall, these results indicate that expression of the 3' PKC fusion and subsequent loss of PKC activity indeed have functional consequences, resulting in suppression of apoptosis.

PKC regulatory domain fusions are LOF and potentially dominant negative

While PKC catalytic domain fusions are loss-of-function due to their instability, regulatory domain fusions are intrinsically loss-of-function due to truncation of the transcript encoding the C-terminal kinase domain. However, expression of these 5' PKC fusions may have functional consequences beyond loss of the catalytic domain. Previous studies investigating loss-of-function mutations in PKC demonstrated that kinase-dead mutants may act in a dominant-negative manner (11). Thus, we addressed whether 5' PKC fusions, retaining various elements of the regulatory moiety, can also be dominant negative. For our biochemical analyses, we selected the fusion *PRKCA-CDH8*, originally detected in breast cancer (Figure 2.11A). *PRKCA-CDH8* translates to a protein containing the first 306 amino acid residues of PKC α fused to the last 715 residues of Cadherin-8 (CDH8). CDH8 is a type II classical cadherin that mediates cell-cell adhesion and

regulates proliferation of cortical interneurons (132). The portion of *PRKCA* retained in the fusion encodes the entire PKC regulatory moiety, including the inhibitory pseudosubstrate, the C1A and C1B domains, and the C2 domain. In addition to analyzing the full-length fusion, we also analyzed a C-Deletion (C-Del.) variant containing only the PKC portion of the fusion. First, we determined the effect of the regulatory fusion and the C-Deletion variant on endogenous PKC activity utilizing the genetically-encoded FRET reporter CKAR. In COS7 cells expressing CKAR, UTP treatment caused a transient increase in endogenous PKC activity, PDBu treatment caused a greater, more sustained induction in PKC activity, and inhibitor treatment reversed this induction, bringing activity back to baseline (Figure 2.11B). However, in cells co-expressing CKAR and the PKC α -CDH8 fusion, the UTP-mediated increase in PKC activity was ablated. While the response to a physiological stimulus (UTP) was altered with expression of the regulatory domain fusion, there was no change in PDBu-induced activity. Expression of the C-Deletion protein, which is essentially the isolated regulatory moiety of PKC, blunted UTP-induced PKC activity as well as PDBu-induced activity. To examine the effect of the fusion on basal activity, we treated cells expressing the reporter alone or co-expressing the full-length fusion or C-Deletion protein with the PKC inhibitor Gö6983 (Figure 2.11C). Expression of either PKC α -CDH8 or the C-Deletion variant suppressed endogenous PKC activity, indicated by the smaller drop in CKAR phosphorylation compared to that of cells expressing the reporter alone. Thus, these results show that the PKC α -CDH8 regulatory domain fusion and C-Deletion variant are able to suppress not only agonist-induced PKC activity but also basal PKC activity.

To complement our FRET studies, we also examined the effect of the PKC regulatory domain fusion on endogenous PKC activity through immunoblot analysis, probing for phosphorylation of PKC substrates with a phospho-Ser PKC substrate antibody (Figure 2.11D). We compared non-transfected (NT) COS7 cells to COS7 cells overexpressing YFP-tagged wild-type PKC α , PKC α -CDH8, or the C-Deletion in PDBu-treated and vehicle (DMSO) conditions. In the vehicle-treated condition, we detected basal phosphorylation in non-transfected cells that increased with overexpression of wild-type PKC α . Between non-transfected cells and cells expressing the fusion or C-Deletion variant, we were unable to detect a difference at basal conditions. In the PDBu-treated condition, we also saw an increase in substrate phosphorylation between the non-transfected cells and cells expressing wild-type PKC α . Importantly, there was significantly less PKC substrate phosphorylation in cells expressing either the regulatory fusion or the C-Deletion protein compared to non-transfected cells. These data demonstrate that expression of a PKC regulatory domain fusion (PKC α -CDH8) or the isolated regulatory domain (PKC α -CDH8 C.-Del.) can suppress agonist-evoked phosphorylation of PKC substrates, likely by sequestering DAG.

Lastly, we observed in our previous FRET studies with CKAR that the PKC α -CDH8 fusion appeared to be more localized to the Golgi compared to wild-type PKC α (Figure 2.11E). Given that the unmasked regulatory domains of PKC have a propensity to bind the DAG-rich Golgi, we addressed whether the regulatory fusion may have a more pronounced effect in suppressing PKC function at the Golgi. To assess PKC activity at the Golgi, we utilized a variant of CKAR targeted to the Golgi, known as GolgiCKAR (6). GolgiCKAR was generated through addition of sequence encoding the first 33 residues

of endothelial nitric-oxide synthase to the 5' end of CKAR. In COS7 cells, we expressed GolgiCKAR alone, to measure endogenous PKC activity at the Golgi, or in conjunction with the full-length PKC α -CDH8 fusion. For agonist-induced activity, we treated cells with the physiological agonist UTP, the phorbol ester PDBu, or the PKC inhibitor Gö6983 (Figure 2.11F). We observed an increase in PKC activity at the Golgi with UTP treatment, which was further induced with PDBu treatment. Treatment with the inhibitor reversed this induction. Expression of the PKC regulatory domain fusion greatly suppressed both UTP-induced and PDBu-induced PKC activity at the Golgi. For basal activity, we treated cells with the PKC inhibitor Gö6983 alone and observed the decrease in GolgiCKAR phosphorylation from baseline levels (Figure 2.11G). Here, we observed that expression of PKC α -CDH8 suppressed basal PKC activity at the Golgi, causing a much smaller drop in the FRET ratio, and thus phosphorylation of GolgiCKAR, upon inhibitor addition. These results corroborate the Golgi as an important intracellular compartment in which PKC regulatory domain fusions such as PKC α -CDH8 exert their effects, acting in a dominant-negative manner to suppress global PKC output.

2.4 Discussion

In this study, we identified PKC gene fusions to be a mechanism by which PKC function is lost in cancer. To assess the impact of gene fusion on PKC function, we biochemically characterized both 3' PKC fusions, retaining transcript encoding the PKC catalytic domain, and 5' PKC fusions, retaining transcript encoding the PKC regulatory domain. PKC catalytic domain fusions were found to be unphosphorylated at the three phosphorylation sites required for PKC to become catalytically competent. However,

despite the lack of phosphorylation at these priming sites, the fusion proteins exhibited agonist-independent, constitutive activity. We subsequently determined that the fusion proteins were more sensitive to degradation and more ubiquitinated compared to wild-type PKC. When we utilized CRISPR/Cas9-mediated gene editing to express a 3' PKC fusion in a cancer cell line, we were able to detect the fusion mRNA but unable to detect the fusion protein. These data are consistent with a model in which 3' PKC fusions yield proteins that are unable to adopt the stable, autoinhibited conformation of wild-type PKC and are subsequently shunted off to degradative pathways (Figure 2.12A). Due to truncation of the regulatory domain, specifically loss of the pseudosubstrate, the fusion proteins exist in an open conformation that renders them constitutively active and markedly unstable. Moreover, the degree of this instability is such that fusion protein is unable to accumulate in cells at steady-state levels, making 3' fusions paradoxically loss-of-function. Unprimed PKC that is unable to undergo appropriate maturation as well as PKC subjected to phorbol ester treatment also adopt an open, unstable conformation that results in their degradation. Together, these three cases illustrate that the ultimate consequence for loss of autoinhibition is degradation.

Since 5' PKC fusions result in proteins with a truncated catalytic domain, they are intrinsically loss-of-function with respect to PKC activity. However, we show that these regulatory domain fusions may have an additional role in suppressing wild-type PKC activity. Our data demonstrate that overexpression of a regulatory domain fusion suppressed endogenous PKC activity in basal and agonist-treated conditions. Furthermore, we identified the Golgi to be a primary site of interest for this fusion-mediated suppression of global PKC output, especially as the regulatory fusion was pre-

localized to that intracellular compartment. In the absence of the catalytic domain, the regulatory moiety is no longer constrained in the closed conformation characterized by wild-type PKC in basal conditions. Thus, the individual components of the regulatory domain, namely the C1 and C2 domains, are fully exposed and capable of binding to ligand. We have previously shown that the membrane affinity of full-length PKC is at least an order of magnitude less than the product of the affinities of the isolated C1B and C2 domains (133). This reduced affinity of full-length PKC for membranes results from significant masking of the C1 domains during the maturation of PKC to the phosphorylated and autoinhibited species (12). Indeed, in the context of the full-length PKC enzyme, only one of the DAG sensors binds ligand (22, 92), with several lines of evidence suggesting it is the C1B domain (12, 95). Furthermore, not only do the regulatory domain fusions have two unmasked C1 domains but the C1A domain binds DAG with two orders of magnitude higher affinity than the C1B domain (22, 23). As a result, the isolated regulatory domain is predicted to bind DAG with several orders of magnitude higher affinity than full-length PKC. This enhanced affinity for DAG is likely what directs the regulatory domain fusions to the DAG-rich Golgi, overriding the intrinsic affinity of the C2 domain for plasma membrane (33, 38). Since wild-type PKC adopts an autoinhibited conformation in the absence of second messengers, it exhibits very little basal activity. Therefore, the effect of the regulatory fusion in suppressing wild-type PKC activity in basal conditions is quite modest. However, in activating conditions where PKC's second messengers are present, the ability of the regulatory domain fusion to suppress PKC activity is more prominent. In our model, 5' PKC fusions yield proteins with exposed regulatory modules that have the potential to sequester common titratable components,

such as diacylglycerol, thereby competing with wild-type PKC and acting in a dominant-negative manner (Figure 2.12B). This ability to suppress endogenous activity is consistent with previous studies showing that kinase-dead mutants also act in a dominant-negative manner, suppressing global PKC output (11). Beyond loss of their own catalytic activity, these mutants acted in a dominant-negative manner, suppressing global PKC output. Our current results indicate that one mechanism for this dominant-negative effect is mediated by the membrane-targeting modules that are unmasked and can effectively compete for ligand binding.

Our data demonstrate that PKC gene fusions result in a loss of PKC activity, and here, we show that one consequence of losing PKC function is reduced apoptosis. Compared to parental cells containing two wild-type alleles of PKC, there was reduced cleaved caspase-3 levels in the CRISPR-edited, fusion-expressing cells, suggesting a reduction in apoptosis. This effect was also observed in both the heterozygous and homozygous PKC α knockout cells, of which the former we would expect to phenocopy the fusion-expressing cells since they, too, contain a single wild-type allele of PKC α . These results complement previous studies wherein a heterozygous loss-of-function mutation in PKC β was corrected to wild-type in DLD-1 colorectal cancer cells through CRISPR/Cas9 gene editing (11). When these cells were subcutaneously injected into nude mice, the resulting tumors were smaller and exhibited greater TUNEL staining compared to those from the parental cells. Thus, we see that increased PKC activity is associated with increased apoptosis while loss of PKC activity is associated with decreased apoptosis. PKC α , specifically, has been found to promote apoptosis in LNCaP cells, a model for androgen-dependent prostate cancer, through dephosphorylation and

inactivation of Akt (134). It has also been identified as a pro-apoptotic factor in other cancer contexts, including gastric cancer and leukemia (135, 136). There is also evidence that other isozymes of PKC, including PKC δ , PKC ϵ , and PKC θ , may also promote apoptosis (17, 52). Further studies are required to ascertain whether there are other functional effects that arise from these fusions, including effects on invasion, migration, and proliferation, and, more broadly, to dissect the precise mechanisms by which PKC exerts its tumor suppressive function.

Although the vast majority of PKC gene fusions are not highly recurrent, they serve altogether as an important general mechanism for loss of PKC function in cancer. The distribution of loss-of-function point mutations in the different domains of PKC revealed that there are no true mutational hotspots, indicating that there are a multitude of ways in which PKC can be inactivated (11). Similarly, while there are many different breakpoints among the PKC fusions, many of the truncation events would result in loss of PKC activity. For 5' PKC fusions, even minimal loss of the C-terminus would result in loss of PKC function as phosphorylation of the hydrophobic motif site is necessary for catalytic competence. For 3' PKC fusions, partial loss of the N-terminal regulatory moiety could also result in loss of PKC function as it would constitute a loss in autoinhibition, which could lead to subsequent degradation. Specifically, through the PKC α and PKC β II Δ PS mutants, we showed that deletion of the pseudosubstrate was sufficient to cause lack of phosphorylation at the PKC priming sites, agonist-independent cellular activity, and sensitivity to degradation exhibited by the fusion proteins. Hence, for conventional isozymes of PKC, any fusion with a minimal truncation of the 5' end of the gene would

constitute as loss-of-function. Overall, due to the potential deletion of functionally relevant domains, PKC gene fusions have a high probability of impacting PKC activity.

Our work supports a role for PKC as a tumor suppressor and thus underscores the importance of developing therapies that serve to stabilize or enhance PKC activity in cells. This is an important consideration as the initial identification of catalytic domain fusions immediately prompted discussion of PKC-targeted inhibitors (115, 137, 138). Our data demonstrate, however, that this would be detrimental. In addition to informing the development of PKC-targeted therapeutics, PKC fusions may also serve another important role in cancer as biomarkers. Recurrent fusions of *PRKCB* and *PRKCD* to membrane-associated proteins were identified in benign fibrous histiocytomas (BFHs), one of the most common neoplasms in the skin (138–140). The recurrent fusions *LAMTOR1-PRKCD* and *PDPN-PRKCB*, alongside *CD63-PRKCD* and *KIRREL-PRKCA*, were identified through fluorescent in situ hybridization (FISH) and RT-qPCR. In each of these cases, the N-terminus of PKC was replaced with membrane-binding domains of a partner protein while retaining the PKC catalytic domain. In total, roughly 15% of BFHs analyzed contained a PKC fusion. Moreover, tumors containing rearrangements in *PRKCB* did not have rearrangements in *ALK*, previously shown to occur in the majority of the epithelial subtype of BFHs. The *SLC44A1-PRKCA* fusion, characterized in this study, was identified in rare mixed neuronal-glia tumors known as papillary glioneuronal tumors (PGNTs) that are difficult to diagnose (120). In the initial analyses of these tumors, the sole karyotypic abnormality was the chromosomal translocation t(9;17)(q31;q24), resulting in the *SLC44A1-PRKCA* fusion. Out of the 10 documented cases of PGNTs, the fusion was detected in 9 of them (120–122). Furthermore, PGNTs harboring the PKC

fusion lacked BRAF and FGFR1 mutations characteristic of histologically similar tumors. Interestingly, the fusion was not detected in any of 15 PGNT “mimics,” tumors that shared many morphological similarities to bona fide PGNTs (121). Taken together, the recurrent fusions detected in BFHs and PGNTs may serve as effective biomarkers as they appear to be mutually exclusive of mutations and rearrangements in known drivers. Thus, PKC gene fusions, whether as targets or biomarkers, may have significant therapeutic relevance in cancer.

2.5 Materials and Methods

Curation of PKC Gene Fusions

5' and 3' PKC fusions organized in Table 2.1 and graphed in Figure 2.1A, B, and C were curated from the following online databases: TCGA Tumor Fusion Gene Data Portal, ChimerDB v3.0, the Mitelman Database of Chromosome Aberrations and Gene Fusions in Cancer, and COSMIC. PKC fusions found in multiple databases were only listed once.

Plasmid constructs

The C Kinase Activity Reporter (CKAR) and the Golgi-targeted C Kinase Activity Reporter (GolgiCKAR) were previously described (6, 128). Human PKC α and PKC β were N-terminally tagged with mCherry and YFP via Gateway cloning as previously described (11). PKC pseudosubstrate-deleted constructs (Δ PS) were generated by QuikChange site-directed mutagenesis (Agilent) as previously described (118). Human TANC2-PKC α and GGA2-PKC β constructs were generated using Gibson Assembly (NEB). Constructs containing human CTL1 (SLC44A1) and CDH8 were obtained through the DNASU

plasmid repository (HsCD00627280 and HsCD00403546, respectively). The CTL1-PKC α and PKC α -CDH8 fusions were generated through multiple iterations of PCR. Fragments of each protein were amplified by PCR with primers containing overhang homologous to their fusion partner. Once the fragments were annealed, the complete fusion was amplified from the reaction by PCR and subcloned into pcDNA3. N-Deletion and C-Deletion constructs were generated through amplification of regions of interest by PCR from constructs of wild-type PKC α and subsequent subcloning into pcDNA3. Constructs with an N-terminal mCherry tag were cloned into pcDNA3 containing mCherry between the BamHI and XbaI sites, and constructs with an N-terminal YFP tag were cloned into pcDNA3 containing YFP between the XhoI and XbaI sites. Point mutants were generated using QuikChange site-directed mutagenesis. The PX458 vector encoding the Cas9 nuclease was a gift from Feng Zhang (Plasmid # 48138, Addgene). The pAAV-SEPT-Acceptor vector was a gift from Todd Waldman (Plasmid #25648, Addgene).

Antibodies and reagents

The antibodies used in this study are as listed: PKC α (610108, BD Transduction), PKC β (610128, BD Transduction), phospho-specific PKC turn motif (PKC α/β pT638/641, 9375S, Cell Signaling), phospho-specific PKC hydrophobic motif (PKC β pS660, 9371S, Cell Signaling), HA (clone 16B12, 901515, Biolegend), GST (sc-138, Santa Cruz), Hsp70 (610608, BD Transduction), Hsp90 (610418, BD Transduction), Cdc37 (D28H7, 4222S, Cell Signaling), TANC2 (D-11, sc-515710, Santa Cruz), caspase-3 (9662S, Cell Signaling), cleaved caspase-3 (Asp175, 9661S, Cell Signaling), pSer PKC Substrate (2261S, Cell Signaling), GFP (2555S, Cell Signaling), β -actin (A2228, Sigma-Aldrich),

and α -tubulin (T6074, Sigma-Aldrich). The phospho-specific PKC activation loop antibody has been previously described (141). The RINCK antibody was also previously described (56). The pharmacological reagents used in this study are as listed: UTP (6701, Calbiochem), PDBu (524390, Calbiochem), Gö6976 (365253, Calbiochem), Gö6983 (80051-928, Calbiochem), BisIV (203297, Calbiochem), cycloheximide (239764, Calbiochem), MG-132 (474790, Calbiochem), chloroquine (C6628, Sigma-Aldrich), and wortmannin (W1628, Sigma-Aldrich).

Cell culture and transfection

All cells were maintained in Dulbecco's modified Eagle's medium (DMEM, 10-013-CV, Corning) containing 10% fetal bovine serum (S11150, Atlanta Biologicals) and 1% penicillin/streptomycin (15140-122, Gibco) at 37C in 5% CO₂ (v/v). Cells were tested for *Mycoplasma* contamination and showed no contamination. Transient transfection was carried out using the Lipofectamine 3000 transfection reagent (Life Technologies).

Cell lysis and immunoblotting

Most cells were lysed in buffer containing 50 mM Tris (pH 7.4), 1% Triton X-100, 50 mM NaF, 10 mM Na₄P₂O₇, 100 mM NaCl, 5 mM EDTA, 1% deoxycholic acid that was supplemented with 1 mM Na₃VO₄, 1 mM phenylmethyl-sulfonyl fluoride, 50 μ g/ml leupeptin, 1 μ M microcystin, 1 mM DTT, and 2 mM benzamidine. Whole cell lysates were briefly sonicated and boiled in sample buffer containing 250 mM Tris HCl, 8% (w/v) SDS, 40% (v/v) glycerol, 80 μ g/mL bromophenol blue, and 2.86 M β -mercaptoethanol for 5 min at 95°C. Cells used in the analysis of the CTL1-PKC α fusion protein were lysed in RIPA

buffer (50 mM Tris (pH 7.4), 150 mM NaCl, 2 mM EDTA, 1% Triton X-100, 1% deoxycholic acid, 0.1% SDS, 10 mM NaF) supplemented with 1 mM Na_3VO_4 , 1 mM phenylmethylsulfonyl fluoride, 50 $\mu\text{g}/\text{ml}$ leupeptin, 1 μM microcystin, 1 mM DTT, and 2 mM benzamidine. Whole cell lysates from these studies were neither sonicated nor boiled to minimize protein aggregation. Lysates were analyzed by SDS-PAGE and immunoblotting via chemiluminescence on a FluorChem Q imaging system (ProteinSimple).

FRET imaging and analysis

Cells were imaged as described previously (6). As indicated, COS7 cells were transfected with CKAR or GolgiCKAR alone or co-expressed with mCherry-tagged PKC. Cells were rinsed once with and imaged in Hanks' balanced salt solution (Corning) containing 1 mM CaCl_2 . Images were acquired on a Zeiss Axiovert microscope (Carl Zeiss Microimaging Inc.) using a MicroMax digital camera (Roper-Princeton Instruments) controlled by MetaFluor software (Universal Imaging Corp.). Baseline values were acquired for at least 2 min prior to reagent addition. For experiments measuring agonist-induced activity, data were normalized to FRET ratios after addition of inhibitor. For experiments measuring basal activity, data were normalized to FRET ratios at baseline. Normalized FRET ratios from at least three independent experiments were combined, and traces represent average of these ratios \pm SEM.

Purification of GST-tagged PKC protein from Sf9 insect cells

Human PKC β II and GGA2-PKC β II were subcloned into a pFastBac HT/B vector (Invitrogen) modified with a N-terminal GST tag. Baculovirus was made using the Bac-to-

Bac Baculovirus Expression System (Invitrogen). The pFastBac plasmids were transformed into DH10Bac cells, and the resulting bacmid DNA was transfected into Sf9 insect cells (11496015, Thermo Fisher Scientific) in Sf-900 II SFM media (10902-088, Gibco) via CellFECTIN (Thermo Fisher Scientific). The recombinant baculoviruses were harvested and amplified, with Sf9 insect cells grown in shaking cultures at 27°C. GST-tagged PKC β II and GGA2-PKC β II were batch-purified from baculovirus-infected Sf9 insect cells using glutathione sepharose beads. Sf9 insect cells were infected with baculovirus for either protein and incubated for 3 days in shaking cultures at 27°C. Infected cells were then pelleted, rinsed in PBS, and lysed in buffer containing 50 mM HEPES (pH 7.5), 1 mM EDTA, 100 mM NaCl, 0.1% Triton X-100, 0.1 mg/mL BSA, 100 μ M PMSF, 1 mM DTT, 2 mM benzamide, 50 μ g/mL leupeptin, and 1 μ M microcystin. The soluble lysate was then incubated with the glutathione beads for 2.5 h at 4°C. The beads were washed three times in buffer containing 50 mM HEPES (pH 7.5), 1 mM EDTA, 100 mM NaCl, 0.1 mg/mL BSA, and 1 mM DTT. Protein was eluted in wash buffer supplemented with 10 mM glutathione. The eluted protein was concentrated using 50 kDa Amicon centrifugal filter units (EMD Millipore), exchanged into buffer containing 20 mM HEPES (pH 7.5), 1 mM EDTA, 1 mM EGTA, and 1 mM DTT. An equal volume of glycerol was added, and the protein stock was stored at -20°C. Protein was quantified utilizing BSA standards run alongside the purified protein on an SDS-PAGE gel stained with Coomassie Brilliant Blue.

Purification of FLAG-tagged PKC protein from HEK 293T cells

HEK 293T cells were transfected with 3XFLAG-tagged PKC β II and GGA2-PKC β II in 15

cm plates via Effectene (301427, QIAGEN). After 48 h incubation, cells were pelleted, rinsed in PBS, and lysed in buffer containing 20 mM Tris (pH 7.5), 150 mM NaCl, 1 mM EDTA, 1 mM EGTA, 1% Triton X-100, 2.5 mM sodium pyrophosphate, 1 mM β -glycerophosphate that was supplemented with 1 mM Na_3VO_4 , 1 mM DTT, 1 mM PMSF, 10 $\mu\text{g}/\text{mL}$ leupeptin, 1 μM microcystin, and 10 $\mu\text{g}/\text{mL}$ aprotinin. Detergent-solubilized lysates were incubated with anti-FLAG M2 affinity gel (A2220, Sigma-Aldrich) for 1 h at 4°C. Beads were washed twice in lysis buffer and twice in elution buffer, containing 50 mM HEPES (pH 7.4), 0.01% NP40, 100 mM NaCl, 5 mM β -glycerophosphate, 0.1 mM Na_3VO_4 , and 10% glycerol. Beads were then incubated in elution buffer containing 0.5 mg/mL of FLAG peptide (F4799, Sigma) for 1 h at 4°C. The supernatant was divided into aliquots, snap frozen, and stored at -80°C. Protein was quantified using the Pierce Coomassie (Bradford) Protein Assay Reagent (1856209, Thermo Fisher Scientific): 5 μl of protein or BSA standard was mixed with 45 μl of buffer containing 0.05 M NaOH and 20 mM Tris, 500 μl of the Coomassie reagent was added to the mixture, and the sample was incubated for 10 min at room temperature. Samples were read via spectrophotometer at 595 nm.

Cellular ubiquitination assay

COS7 cells were transfected with HA-tagged ubiquitin alone or co-transfected with the indicated YFP-tagged PKC. After 24 h, cells were lysed in 50 mM Tris (pH 7.4), 1% Triton X-100, 50 mM NaF, 10 mM $\text{Na}_4\text{P}_2\text{O}_7$, 100 mM NaCl, 5 mM EDTA, 1% deoxycholic acid that was supplemented with 1 mM Na_3VO_4 , 1 mM phenylmethyl-sulfonyl fluoride, 50 $\mu\text{g}/\text{ml}$ leupeptin, 1 μM microcystin, 1 mM DTT, and 2 mM benzamidine. Lysis buffer was also

supplemented with 10 mM N-ethylmaleimide to preserve ubiquitinated species. After centrifugation, 500 µg of the detergent-solubilized lysates were incubated with an anti-PKCα antibody overnight at 4°C and subsequently with protein A/G beads (Santa Cruz) for 1 h at 4°C. The immunocomplexes were washed three times with lysis buffer (un-supplemented) and eluted by boiling in sample buffer for 5 min at 95°C. Samples were separated by SDS-PAGE and analyzed by immunoblotting.

Generation of CRISPR constructs for *TANC2-PRKCA* expression

The TANC2-PKCα protein is generated from the fusion of exon 1-2 of TANC2 fused to exon 6-17 of PKCα. To generate the *TANC2-PRKCA* gene fusion, sgRNAs targeting intron 2 of *TANC2* (*TANC2* gRNA: GTTGGAGTATCATCACACAC) and intron 6 of *PRKCA* (*PRKCA* gRNA: GACCGGAATTCCCTATCCAG) were cloned into the PX458 vector. Left and right homology arms to target *TANC2* and *PRKCA*, respectively, were approximately 1 kb each and generated using the following oligonucleotides:

TANC2 LHA forward: GTTTTAGCTTTTCTTAACATGCATGAGGG

TANC2 LHA reverse: CAAATGTTGGTGTGAAAATTCACTTTTGG

PRKCA RHA forward: GGGCCTGGTTACTCCCTCCTCGGGGCTG

PRKCA RHA reverse: CTCGGCTGCAAATCTGCTCCCCCATAACATGG

Homology arms were cloned into the pAAV-SEPT-Acceptor vector.

Generation of rAAV for *TANC2-PRKCA* expression

Recombinant AAV (rAAV) particles were generated in 293T cells (ATCC CRL-3216) via co-transfection of pAAV-SEPT containing the *TANC2* and *PRKCA* homology arms with

the packaging plasmids pAAV-RC and pHELPER. Five days after transfection, cells were collected in media and subjected to three freeze/thaw cycles to release rAAV particles followed by a 15 min spin to remove cellular debris. Released and clarified rAAV were stored in media at -80°C.

Generation of CRISPR-edited cell lines for *TANC2-PRKCA* expression

MDA-MB-231 cells at 50-60% confluence in a 10 cm dish were placed in serum-free media and transfected with 6 µg each of PX458-*TANC2* sgRNA and PX458-*PRKCA* sgRNA using Lipofectamine 3000. After 4 h, cells were fed with complete media and incubated for 2 h. To transduce the cells with rAAV, media was replaced with 50/50 media/rAAV and incubated for 2 days. To select recombinant clones, cells were trypsinized and collected in 120 mL of media containing 2 mg/ml G418 and seeded at 200 µl/well into six 96 well plates. Plates were wrapped in plastic wrap to reduce evaporation, and incubated for 20-30 days. Single colonies were expanded into 48-well plates and screened for generation of the fusion product by PCR. To screen for recombinant clones, gDNA was isolated using the *Quick-DNA* Microprep Kit (D3020, Zymo Research) from 90% of the cells with the remaining 10% re-seeded in a 48-well plate. For clones that successfully integrated the repair template, the floxed Neo cassette was removed. To remove the cassette from the clonal cell lines, cells were grown in a 6-well plate to 50% confluence and treated with Adenovirus-Cre (Ad5CMVCre-eGFP high titer, Iowa U.) in serum-free media overnight before replacing with complete medium. Efficiency of cassette removal was verified by splitting the well into two in the presence and absence of 2 mg/ml G418.

mRNA isolation and RT-qPCR analysis

RNA was isolated from cells using the RNeasy Mini Kit (74104, Qiagen). Total mRNA was reverse-transcribed into cDNA using the SuperScript III First Strand Synthesis System (18080-051, Invitrogen) and 20 ng of the resulting cDNA was used to perform real-time PCR. Real-time PCR was performed with SYBR Premix Ex TaqII (RR820A, Takara Bio) and a 100 nM mix of forward and reverse primers on a QuantStudio 3 Real-Time PCR System (Applied Biosystems). The real-time PCR values were normalized to the housekeeping gene actin (*ACTB*) using the $\Delta\Delta CT$ method (Livak 2001). The primer sequences used in this study are as follows:

human *PRKCA* 5'

forward: CGGCGGAGGCAAGAGGTGGT

reverse: TGCGGGCGAAGCGGTTG

human *PRKCA* 3'

forward: ATTCAAGCCCAAAGTGTGTGG

reverse: GATCAGGTGGTGTAAAGACGGG

human *TANC2* 5'

forward: CAGGTCAAGTGATGGAGGG

reverse: CAGAGCGGCTTTGGCGAG

human *TANC2* 3'

forward: GCTTTGCACCTTATAGGCCTCC

reverse: GGAAAACCCAATCTCGGCCAAC

human *TANC2-PRKCA*

forward: GAGGAACCACCGGATCGAAG

reverse: GGATCTGAAAGCCCGTTTGG

human *ACTB*

forward: AGGCACCAGGGCGTGAT

reverse: GCCCACATAGGAATCCTTCTGAC

siRNA knockdown of RINCK (TRIM41) and STUB1 (CHIP)

MDA-MB-231 cells were transfected with 200 nM siRNA for TRIM41 (L-007105-00-0005, Dharmacon), STUB1 (L-007201-00-0005, Dharmacon), or both via Lipofectamine 3000 in serum-free media. After 3 h, serum-free media was removed from cells, and complete media was added. Cells were incubated for 72 h and then harvested. Cells were lysed in buffer containing 50 mM Tris (pH 7.4), 1% Triton X-100, 50 mM NaF, 10 mM Na₄P₂O₇, 100 mM NaCl, 5 mM EDTA, 1% deoxycholic acid that was supplemented with 1 mM Na₃VO₄, 1 mM phenylmethyl-sulfonyl fluoride, 50 µg/ml leupeptin, 1 µM microcystin, 1 mM DTT, and 2 mM benzamidine. Whole cell lysates were briefly sonicated and boiled in sample buffer for 5 min at 95°C.

Generation of CRISPR-edited cell lines for knockout of PKC α

To generate PKC α knockout lines, gRNAs were selected using Synthego's CRISPR Design Tool. Two sgRNAs targeting exon 4 of *PRKCA* were cloned into the PX458 vector (*PRKCA* gRNA 2: AAGTTCAAATCCACACTTA and *PRKCA* gRNA 3: AGGTGGGGCTTCCGTAAGTG). MDA-MB-231 cells were nucleofected with 2 µg of either sgRNA using the Amaxa Nucleofector II (Amaxa) and incubated for 3 days. Cells

were then single-cell sorted for GFP-positive cells into two 96-well plates per sgRNA and incubated for 20-30 days. Single colonies were expanded into 48-well plates and screened for potential *PRKCA* knockout by PCR. To screen clones, gDNA was isolated using the Quick-DNA Microprep Kit from 90% of the cells with the remaining 10% re-seeded in a 48-well plate. An approximately 1 kb fragment around the targeting region of the sgRNAs was amplified by PCR and submitted for Sanger sequencing (GENEWIZ). The results were analyzed using Synthego's Inference of CRISPR Edits (ICE) CRISPR Analysis Tool and validated by immunoblotting following sufficient expansion of the clones.

2.6 Acknowledgments

We thank the members of the Newton Laboratory and the laboratory of Dr. Jack E. Dixon for helpful discussion. We thank Dr. Sourav Banerjee for his advice and performing cell sorting in the development of the MDA-MB-231 PKC α knockout lines. We also thank Manuel Kaulich for introducing us to the CRISPR approach used in this study.

This work was supported by NIH R35 GM122523 and NIH GM43154 (A.C.N.). A.-A.N.V. and C.E.A. were supported in part by the University of California, San Diego Graduate Training Program in Cellular and Molecular Pharmacology (T32 GM007752). C.E.A. was supported by the NSF Graduate Research Fellowship (DGE1144086).

Chapter 2, in full, is currently being prepared for submission under the title "Protein Kinase C Fusions Reveal Mechanism for Loss of Protein Kinase C Function in Cancer." The authors include An-Angela N. Van. Maya T. Kunkel, Corina E. Antal, and Alexandra

C. Newton. The dissertation author was the primary investigator and author of this material.

2.7 Table and Figures

Table 2.1: PKC gene fusions identified in cancer. Table of PKC fusions that were curated from TCGA Tumor Fusion Gene Data Portal, ChimerDB v3.0, and the Mitelman Database of Chromosome Aberrations and Gene Fusions in Cancer. Symbols (*, #, and %) represent fusions that are detected in different cancer types. Fusions listed in red and italicized are recurrent, detected in more than one tumor sample for the same cancer.

PKC Isozyme	Cancer	Fusion Pair	5' Gene Junction	3' Gene Junction	Sample ID	Frame	Unique fusions per specific breakpoint	Unique fusion partners per cancer
PRKCA	BLCA	PRKCA-NF1	Chr17:64302245	Chr17:29652838	TCGA-4Z-AA86-01A	Out-of-Frame		
PRKCA	BRCA	PRKCA-CDH8	Chr17:64685165	Chr16:61935377	TCGA-AC-A5XU-01A	In-Frame		
PRKCA	BRCA	PRKCA-CRYBA1	Chr17:64302245	Chr17:27576160	TCGA-A2-A1FW-01A	In-Frame		
PRKCA	BRCA	PRKCA-IGF2BP1	Chr17:64302245	Chr17:47126714	TCGA-AC-A6IV-01A	Out-of-Frame		
PRKCA	BRCA	PRKCA-RGS9	Chr17:64637584	Chr17:63221120	TCGA-3C-AALI-01A	Out-of-Frame		
PRKCA	BRCA	PRKCA-ST6GALNAC2	Chr17:64492401	Chr17:74574898	TCGA-A2-A0YE-01A	Out-of-Frame		
PRKCA	BRCA	ACACA-PRKCA	Chr17:35468465	Chr17:64637472	TCGA-3C-AALI-01A	Out-of-Frame		
PRKCA	BRCA	INO80-PRKCA	Chr15:41371899	Chr17:64728806	TCGA-C8-A1HI-01A	In-Frame		
PRKCA	BRCA	MMD-PRKCA	Chr17:53499030	Chr17:64728805	TCGA-A8-A08O-01A	Out-of-Frame		
PRKCA	BRCA	PITPNC1-PRKCA						
PRKCA	BRCA	PSMD12-PRKCA	Chr17:65340721	Chr17:64492318	TCGA-C8-A12P-01A	Out-of-Frame		
PRKCA	BRCA	TUFT1-PRKCA	Chr1:151512901	Chr17:64782984	TCGA-A2-A1FW-01A	In-Frame		
PRKCA	KIRC	UNK-PRKCA	Chr17:73781065	Chr17:64492319	TCGA-BP-4983-01A	CDS-SUTR		
PRKCA	LUAD	PRKCA-PITPNC1	Chr17:64492401	Chr17:65528918	TCGA-05-5429-01A	In-Frame		
PRKCA	LUSC	PRKCA-IGF2BP3	Chr17:64492401	Chr7:23358873	TCGA-33-4587-01A	In-Frame		
PRKCA	LUSC	PRKCA-SDK1	Chr17:64641629	Chr7:3990555	TCGA-66-2793-01A	In-Frame		
PRKCA	LUSC	IGF2BP3-PRKCA	Chr7:23381683	Chr17:64637473	TCGA-33-4587-01A	In-Frame		
PRKCA	LUSC	TANC2-PRKCA	Chr17:61151375	Chr17:64683229	TCGA-43-2581-01A	In-Frame		
PRKCA	COAD	PRKCA-TMEM100	Chr17:64492401	Chr17:53805343	TCGA-AY-A8YK-01A	Out-of-Frame		
PRKCA	LIHC	PRKCA-PPP4R4	Chr17:64302245	Chr14:94633881	TCGA-2Y-A9H0-01A			
PRKCA	LIHC	PRKCA-RPS6KB1	Chr17:64683385	Chr17:57987923	TCGA-DD-AADC-01A	Out-of-Frame		
PRKCA	PGNT	SLC44A1-PRKCA	Chr9	Chr17		In-Frame		
PRKCA	SARC	PRKCA-PIK4	Chr17:64302245	Chr22:21161746	TCGA-HS-A5N9-01A	Out-of-Frame		
PRKCA	SARC	PRKCA-RAB40B	Chr17:64302245	Chr17:80617533	TCGA-3B-A9HS-01A	Out-of-Frame		
PRKCA	SKCM	PRKCA-PITPNC1	Chr17:64302245	Chr17:65665624	TCGA-EB-A4XL-01A	Out-of-Frame	25	25
PRKCB	BLCA	USP31-PRKCB	Chr16:23159959	Chr16:23999829	TCGA-4Z-AA7M-01A	Out-of-Frame		
PRKCB	GBM	TNRC6A-PRKCB	Chr16:24741621	Chr16:24192111	TCGA-06-0882-01A	In-Frame		
PRKCB	LGG	GGA2-PRKCB	Chr16:23502998	Chr16:23999829	TCGA-HT-A5RC-01A	In-Frame		
PRKCB	LUAD	SPNS1-PRKCB	Chr16:28986878	Chr16:23999829	TCGA-83-5908-01A	In-Frame		
PRKCB	LUSC	ADCY9-PRKCB	Chr16:4163751	Chr16:23999829	TCGA-33-4533-01A	In-Frame		
PRKCB	PRAD	ABCC1-PRKCB	Chr16:16184445	Chr16:23999829	TCGA-KK-A8I7-01A	In-Frame		
PRKCB	ESCA	KIF22-PRKCB	Chr16:29802150	Chr16:24043456	TCGA-R6-A6XG-01B	Out-of-Frame		
PRKCB	ESCA	KIF22-PRKCB	Chr16:29802150	Chr16:24043457	TCGA-R6-A6XG-01B	Out-of-Frame	8	8
PRKCG	HNSC	NDUFA7-PRKCG	Chr19:8381379	Chr19:54406326	TCGA-D6-6515-01A	Out-of-Frame		
PRKCG	HNSC	NDUFA7-PRKCG	Chr19:8381380	Chr19:54406327	TCGA-D6-6515-01A	Out-of-Frame	2	1
PRKCD	BRCA	CACNA1D-PRKCD	Chr3:53535747	Chr3:53217468	TCGA-GM-A2DD-01A	In-Frame	1	1
PRKCE	BRCA	PRKCE-CAMKMT	Chr2:45879587	Chr2:44934538	TCGA-EW-A3UO-01A	In-Frame		
PRKCE	BRCA	BRE-PRKCE	Chr2:28268666	Chr2:46313347	TCGA-C8-A134-01A	In-Frame		
PRKCE	LUAD	MAP4K3-PRKCE						
PRKCE	LUAD	XRN1-PRKCE	Chr3:142089327	Chr2:46411874	TCGA-69-7979-01A	In-Frame		
PRKCE	SKCM	PRKCE-GPR126	Chr2:46070202	Chr6:142758571	TCGA-EB-A6L9-06A	Out-of-Frame		
PRKCE	PRAD	PRKCE-QPCT	Chr2:45879587	Chr2:37579932	TCGA-XK-AAJA-01A	In-Frame		
PRKCE	PCPG	HECW2-PRKCE	Chr2:197458232	Chr2:46070139	TCGA-RW-A688-01A	NA	7	7
PRKCH	BRCA	HIF1A-PRKCH*	Chr14:62162557	Chr14:61952219	TCGA-AO-A0JF-01A	Out-of-Frame		
PRKCH	BRCA	RP11-47I22.3-PRKCH	Chr14:62037478	Chr14:61995793	TCGA-BH-A0C0-01A	Out-of-Frame		
PRKCH	HNSC	HIF1A-PRKCH	Chr14:62162557	Chr14:61995792	TCGA-CV-7435-01A	In-Frame		
	HNSC	HIF1A-PRKCH#	Chr14:62162557	Chr14:61857942	TCGA-BA-4076-01A	Out-of-Frame		
PRKCH	HNSC	RP11-47I22.3-PRKCH%	Chr14:62037478	Chr14:61952220	TCGA-BB-4227-01A	In-Frame		
PRKCH	KIRC	RP11-47I22.3-PRKCH	Chr14:62037478	Chr14:61909829	TCGA-CJ-5681-01A	Out-of-Frame		
PRKCH	LGG	PRKCH-MNAT1	Chr14:61789182	Chr14:61434947	TCGA-TQ-A7RS-01A	Out-of-Frame		
PRKCH	LGG	HIF1A-PRKCH	Chr14:62162557	Chr14:61912409	TCGA-DU-5872-01A	In-Frame		
PRKCH	LUAD	HIF1A-PRKCH	Chr14:62211426	Chr14:61968341	TCGA-44-2668-01B	Out-of-Frame		
PRKCH	LUAD	HIF1A-PRKCH*	Chr14:62162557	Chr14:61952219	TCGA-44-6147-11A	Out-of-Frame		
PRKCH	LUAD	HIF1A-PRKCH	Chr14:62207905	Chr14:61991769	TCGA-44-2668-01B	Out-of-Frame		
PRKCH	LUAD	HIF1A-PRKCH	Chr14:62207905	Chr14:61995792	TCGA-44-2668-01A	In-Frame		
		<i>HIF1A-PRKCH</i>	<i>Chr14:62207905</i>	<i>Chr14:61995792</i>	<i>TCGA-44-2668-01B</i>	<i>In-Frame</i>		
PRKCH	LUAD	HIF1A-PRKCH	Chr14:62207906	Chr14:61995792	TCGA-44-2668-01A	In-Frame		
		<i>HIF1A-PRKCH</i>	<i>Chr14:62207906</i>	<i>Chr14:61995792</i>	<i>TCGA-44-2668-01B</i>	<i>In-Frame</i>		
PRKCH	LUAD	HIF1A-PRKCH	Chr14:62207906	Chr14:61995793	TCGA-44-2668-01A	In-Frame		
		<i>HIF1A-PRKCH</i>	<i>Chr14:62207906</i>	<i>Chr14:61995793</i>	<i>TCGA-44-2668-01B</i>	<i>In-Frame</i>		
PRKCH	LUAD	RP11-47I22.3-PRKCH%	Chr14:62037478	Chr14:61952220	TCGA-69-7978-01A	In-Frame		

Table 2.1: PKC gene fusions identified in cancer. Table of PKC fusions that were curated from TCGA Tumor Fusion Gene Data Portal, ChimerDB v3.0, and the Mitelman Database of Chromosome Aberrations and Gene Fusions in Cancer. Symbols (*, #, and %) represent fusions that are detected in different cancer types. Fusions listed in red and italicized are recurrent, detected in more than one tumor sample for the same cancer, Continued.

PKC Isozyme	Cancer	Fusion Pair	5' Gene Junction	3' Gene Junction	Sample ID	Frame	Unique fusions per specific breakpoint	Unique fusion partners per cancer
PRKCH	LUSC	HIF1A-PRKCH*	Chr14:62162557	Chr14:61952219	TCGA-77-6844-01A	Out-of-Frame		
	LUSC	HIF1A-PRKCH	Chr14:62162557	Chr14:62014460	TCGA-60-2712-01A	Out-of-Frame		
PRKCH	OV	HIF1A-PRKCH	Chr14:62162557	Chr14:61909829	TCGA-20-0987-01A	Out-of-Frame		
PRKCH	SKCM	DAAM1-PRKCH	Chr14:59758024	Chr14:61995793	TCGA-D3-A8GM-06A	Out-of-Frame		
PRKCH	SKCM	GPHN-PRKCH	Chr14:66975309	Chr14:61857943	TCGA-FW-A3I3-06A	Out-of-Frame		
PRKCH	CESC	HIF1A-PRKCH*	Chr14:62162557	Chr14:61952219	TCGA-EA-A5O9-01A	Out-of-Frame		
PRKCH	ESCA	HIF1A-PRKCH	Chr14:62188541	Chr14:61909828	TCGA-Q9-A6FU-01A	In-Frame		
PRKCH	ESCA	HIF1A-PRKCH*	Chr14:62162557	Chr14:61952219	TCGA-VR-AA7D-01A	Out-of-Frame		
		<i>HIF1A-PRKCH</i>	<i>Chr14:62162557</i>	<i>Chr14:61952219</i>	<i>TCGA-LN-A49X-01A</i>	<i>Out-of-Frame</i>		
		<i>HIF1A-PRKCH</i>	<i>Chr14:62162557</i>	<i>Chr14:61952219</i>	<i>TCGA-LN-A4A6-01A</i>	<i>Out-of-Frame</i>		
PRKCH	ESCA	HIF1A-PRKCH#	Chr14:62162557	Chr14:61857942	TCGA-Z6-A8JD-01A	Out-of-Frame		
PRKCH	ESCA	HIF1A-PRKCH	Chr14:62162557	Chr14:61919943	TCGA-LN-A49U-01A	Out-of-Frame		
PRKCH	ESCA	AKAP7-PRKCH	Chr6:131540948	Chr14:61952219	TCGA-IG-A7DP-01A	Out-of-Frame		
PRKCH	STAD	HIF1A-PRKCH	Chr14:62162557	Chr14:61857943	TCGA-HU-A4GH-01A	Out-of-Frame		
PRKCH	UCEC	HIF1A-PRKCH	Chr14:62162557	Chr14:61995793	TCGA-EO-A22U-01A	In-Frame		
	UCEC	HIF1A-PRKCH*	Chr14:62162557	Chr14:61952219	TCGA-EO-A22Y-01A	Out-of-Frame	23	19
PRKCO	BRCA	GALNT2-PRKCO	Chr1:230203153	Chr10:6506366	TCGA-AR-A2LR-01A	In-Frame	1	1
PRKCI	BRCA	PRKCI-TNIK	Chr3:169953139	Chr3:170912424	TCGA-D8-A27N-01A	Out-of-Frame		
PRKCI	BRCA	GPR160-PRKCI						
PRKCI	PRAD	PRKCI-SLC30A4	Chr3:170009641	Chr15:45806160	TCGA-YL-A8SJ-01B	Out-of-Frame		
PRKCI	PRAD	PRKCI-SLC30A4	Chr3:170011170	Chr15:45806160	TCGA-YL-A8SJ-01B	In-Frame		
PRKCI	PRAD	PRKCI-TMPRSS2	Chr3:169955312	Chr21:42845251	TCGA-HC-7078-01A	In-Frame		
PRKCI	PRAD	PRKCI-TMPRSS2	Chr3:169956122	Chr21:42845251	TCGA-HC-7078-01A	In-Frame		
PRKCI	PRAD	PRKCI-TMPRSS2	Chr3:169999364	Chr21:42843798	TCGA-HC-7078-01A	In-Frame		
PRKCI	COAD	SKIL-PRKCI	Chr3:170079217	Chr3:169981167	TCGA-DM-A0XF-01A	Out-of-Frame	8	5
PRKCO	BLCA	SKI-PRKCO	Chr1:2161174	Chr1:2087434	TCGA-4Z-AA7Q-01A	In-Frame		
PRKCO	BRCA	PRKCO-GABRD	Chr1:1991030	Chr1:1956381	TCGA-UL-AAZ6-01A	Out-of-Frame		
PRKCO	BRCA	SKI-PRKCO	Chr1:2161174	Chr1:2066701	TCGA-A7-A26G-01A	Out-of-Frame		
		<i>SKI-PRKCO</i>	<i>Chr1:2161174</i>	<i>Chr1:2066701</i>	<i>TCGA-E9-A1NA-01A</i>	<i>Out-of-Frame</i>		
PRKCO	ESCA	PRKCO-IFLTD1	Chr1:1991030	Chr12:25679889	TCGA-IG-A4QS-01A	Out-of-Frame		
PRKCO	ESCA	PRKCO-IFLTD1	Chr1:1991030	Chr12:25702480	TCGA-IG-A4QS-01A	In-Frame		
PRKCO	ESCA	PRKCO-KRAS	Chr1:1982140	Chr12:25398329	TCGA-IG-A4QS-01A	5'UTR-5'UTR		
PRKCO	LIHC	ARID1A-PRKCO	Chr1:27088810	Chr1:2066701	TCGA-DD-A11D-01A	In-Frame		
PRKCO	SARC	TMCO3-PRKCO	Chr13:114193822	Chr1:2100957	TCGA-KF-A41W-01A	Out-of-Frame	8	7
TOTAL FUSIONS							83	74

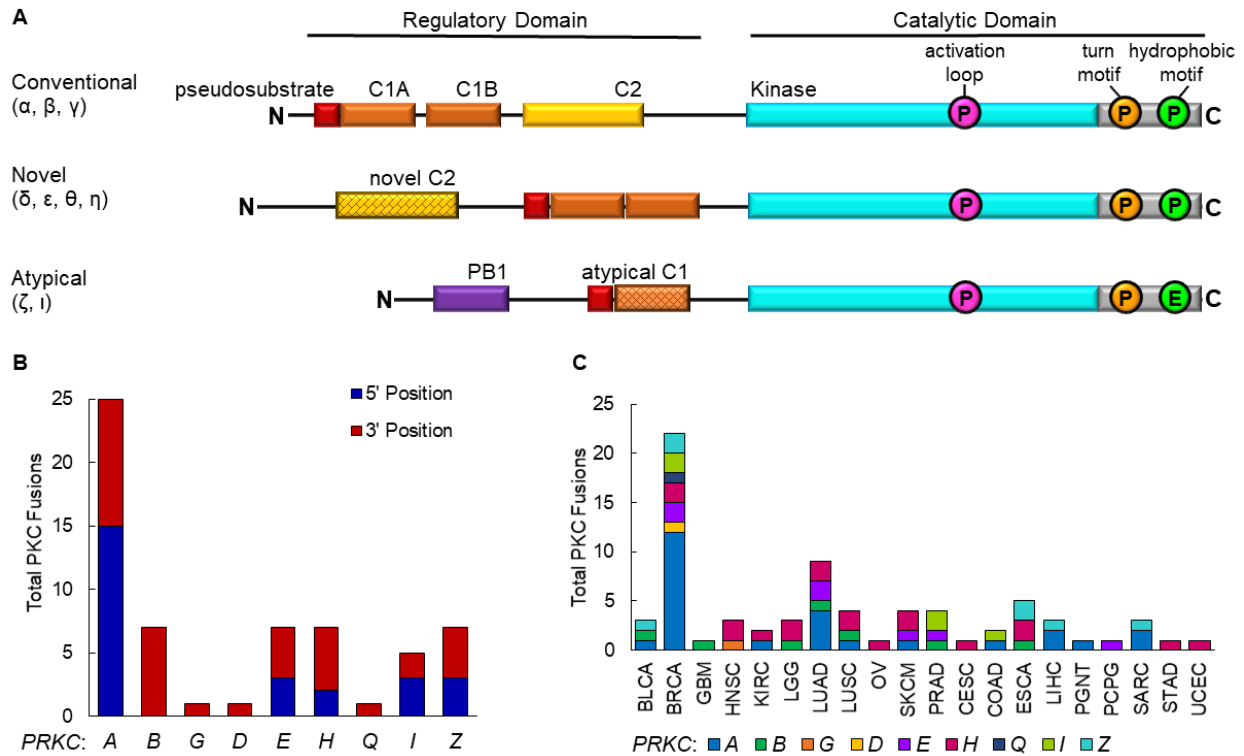
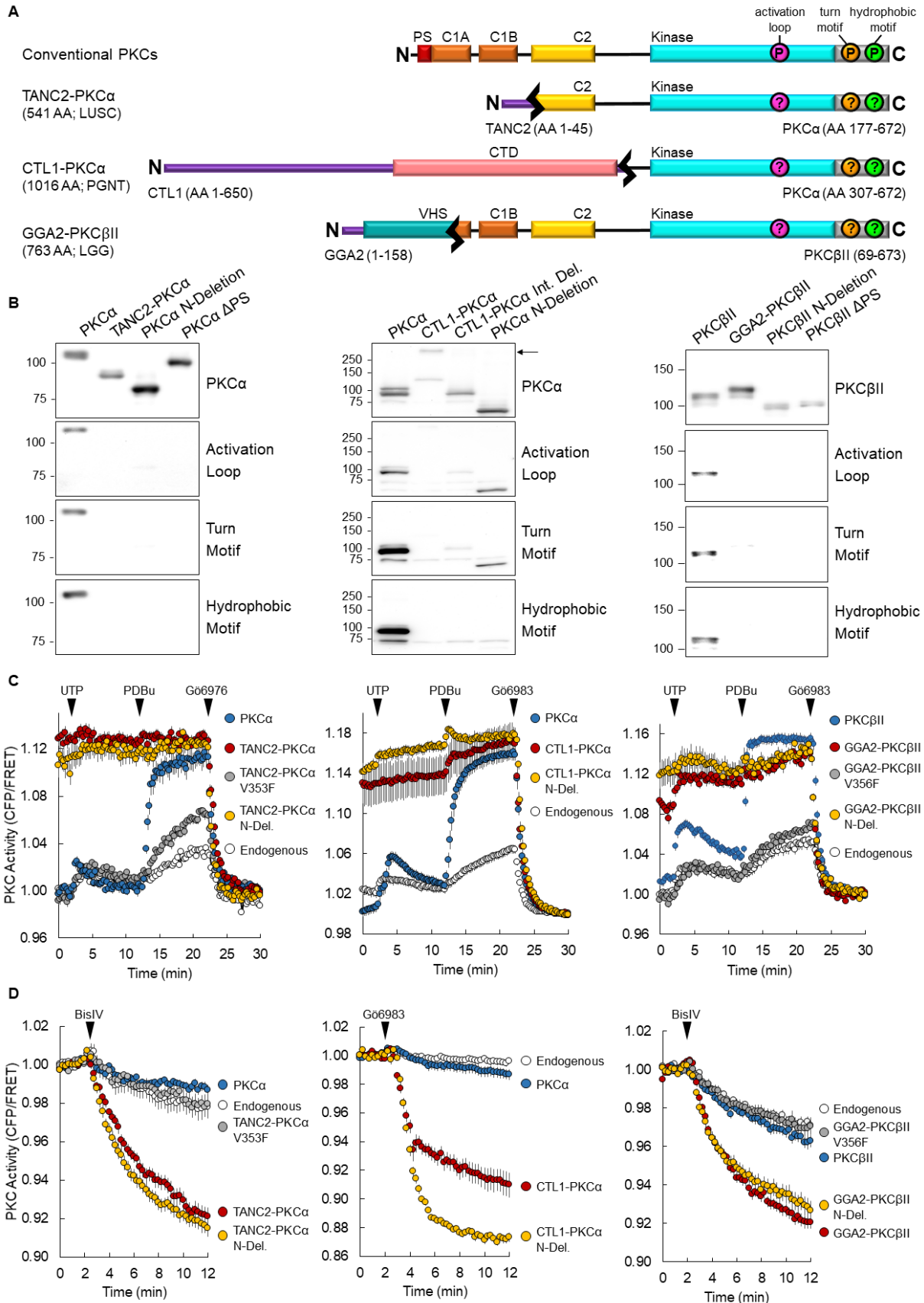


Figure 2.1: Fusions of the protein kinase C regulatory and catalytic moieties are detected in a multitude of cancers. (A) Domain structure of the three PKC subclasses, including pseudosubstrate (red), C1 domains (orange), C2 domain (yellow), and kinase domain (cyan). PKC structure consists of a variable N-terminal regulatory domain followed by a conserved C-terminal catalytic domain. The activation loop, turn motif, and hydrophobic motif phosphorylation sites necessary for catalytic competency are indicated (pink, orange, and green, respectively). (B) Curated from TCGA Tumor Fusion Gene Data Portal, ChimerDB v3.0, and the Mitelman Database of Chromosome Aberrations and Gene Fusions in Cancer, number of 5' and 3' gene fusions for each PKC isozyme is depicted. (C) Curated PKC fusions in (B) categorized by cancer type in which they were detected (BLCA: bladder urothelial carcinoma; BRCA: breast cancer; GBM: glioblastoma multiforme; HNSC: head and neck squamous cell carcinoma; KIRC: clear cell renal cell carcinoma; LGG: low grade glioma; LUAD: lung adenocarcinoma; LUSC: lung squamous cell carcinoma; OV: ovarian serous cystadenocarcinoma; SKCM: skin cutaneous melanoma; PRAD: prostate adenocarcinoma; CESC: cervical squamous cell carcinoma and endocervical adenocarcinoma; COAD: colon adenocarcinoma; ESCA: esophageal carcinoma; LIHC: liver hepatocellular carcinoma; PGNT: papillary glioneuronal tumor; PCPG: pheochromocytoma and paraganglioma; SARC: sarcoma; STAD: stomach adenocarcinoma, UCEC; uterine corpus endometrial carcinoma).

Figure 2.2: 3' PKC fusions yield proteins that are unphosphorylated at the PKC priming sites yet constitutively active. (A) Schematic of wild-type and PKC fusion constructs used in this study. In addition to full-length PKC fusions, N-Deletion constructs were generated in which the N-terminal fusion partner is deleted. A construct representing a variant of the CTL1-PKC α fusion in which there is an internal deletion in the transmembrane choline transporter domain (CTD) was also generated (CTL1-PKC α Int. Del.). (B) Immunoblot analysis of lysates from COS7 cells transfected with the indicated YFP-tagged constructs. Blots probed with the indicated total PKC or phospho-specific antibodies. Arrow indicates border between stacking and separating gels. Data is representative from three independent experiments. (C) Analysis of agonist-induced PKC activity in COS7 cells transfected with CKAR alone (Endogenous) or co-transfected with the indicated mCherry-tagged PKC construct. Cells treated with agonists UTP (100 μ M), PDBu (200 nM), and either inhibitor Gö6976 or Gö6983 (1 μ M). Graphs depict normalized FRET ratio changes (mean \pm SEM) from three independent experiments. (D) Analysis of basal PKC activity in COS7 cells transfected with CKAR alone (Endogenous) or co-transfected with the indicated mCherry-tagged PKC construct. Cells treated with inhibitor BisIV (2 μ M) or Gö6983 (1 μ M). Graphs depict normalized FRET ratio changes (mean \pm SEM) from three independent experiments.



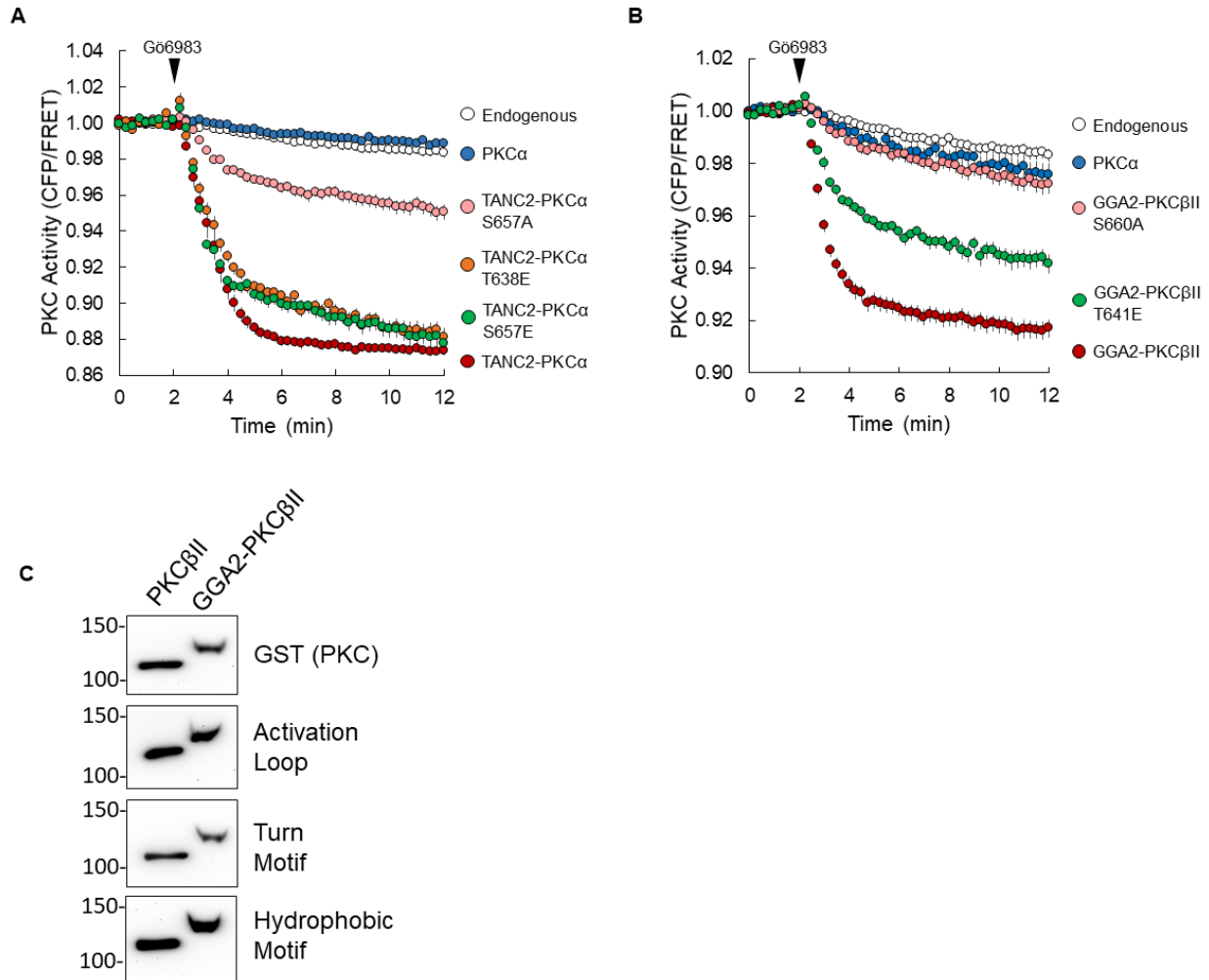


Figure 2.3: PKC fusion proteins require phosphorylatable residues at priming sites for activity. (A) Analysis of basal PKC activity in COS7 cells transfected with CKAR alone (Endogenous) or co-transfected with the indicated mCherry-tagged PKC α construct and treated with inhibitor Gö6983 (1 μ M). Constructs of the fusion in which the turn and hydrophobic motif residues are mutated to glutamate (T638E and T657E, respectively) represent constitutive phosphorylation at those sites while mutation to alanine represents an unphosphorylatable site (T657A). Graphs depict normalized FRET ratio changes (mean \pm SEM) from three independent experiments. (B) Analysis of basal PKC activity in COS7 cells transfected with CKAR alone (Endogenous) or co-transfected with the indicated mCherry-tagged PKC β construct and treated with inhibitor Gö6983 (1 μ M). While the T641E mutant phenocopies constitutive phosphorylation at the turn motif, the S660A mutant cannot be phosphorylated at the hydrophobic motif. Graphs depict normalized FRET ratio changes (mean \pm SEM) from three independent experiments. (C) Immunoblot analysis of purified wild-type PKC β II or GGA2-PKC β II fusion protein. PKC purified from baculovirus-infected insect cells via GST pulldown and elution with GST peptide. Blots probed for total PKC and phosphorylation at priming sites with indicated antibodies.

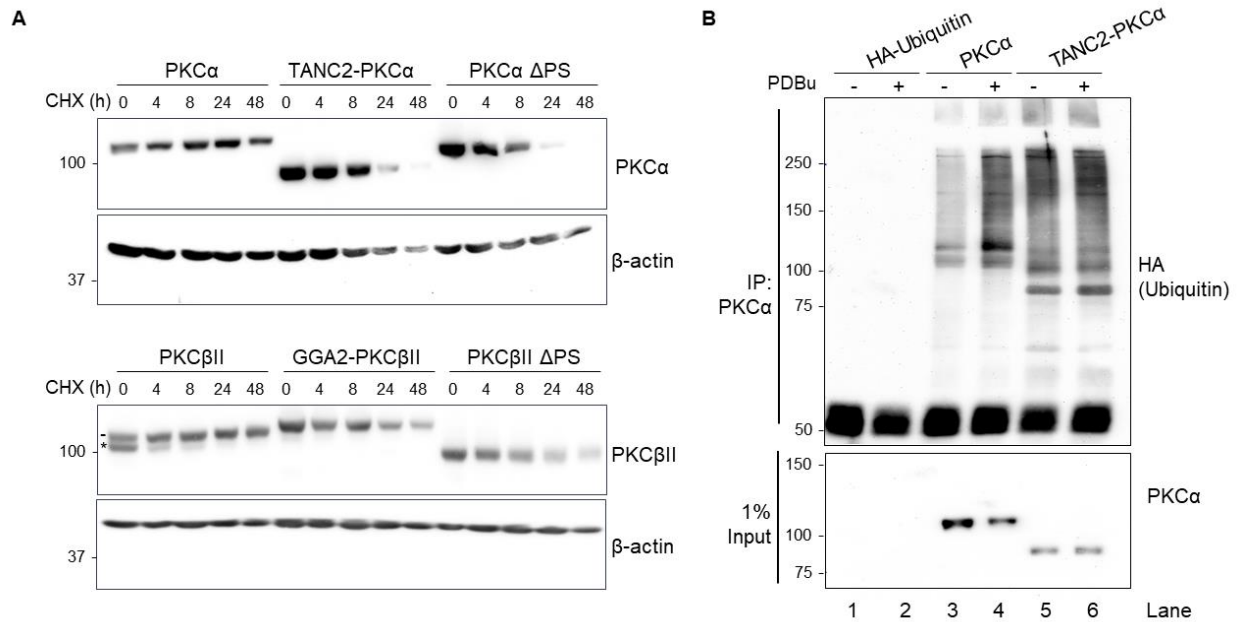


Figure 2.4: The open conformation that renders fusions of the PKC catalytic domain to be constitutively active also cause them to be markedly unstable. (A) Immunoblot analysis of lysates from COS7 cells transfected with the indicated YFP-tagged constructs, treated with cycloheximide (CHX, 355 μ M), and harvested at the indicated timepoints. Blots probed for indicated PKC and β -actin. For wild-type PKC, dash depicts slower mobility phosphorylated PKC while asterisk depicts faster mobility unphosphorylated PKC. Data is representative from three independent experiments. **(B)** Immunoblot analysis of PKC α immunoprecipitates from COS7 cells transfected with HA-tagged ubiquitin alone or co-transfected with indicated YFP-tagged PKC and treated with PDBu (200 nM) or vehicle (DMSO). Blots probed for HA to assess ubiquitination of wild-type PKC compared to the fusion. Data is representative from three independent experiments.

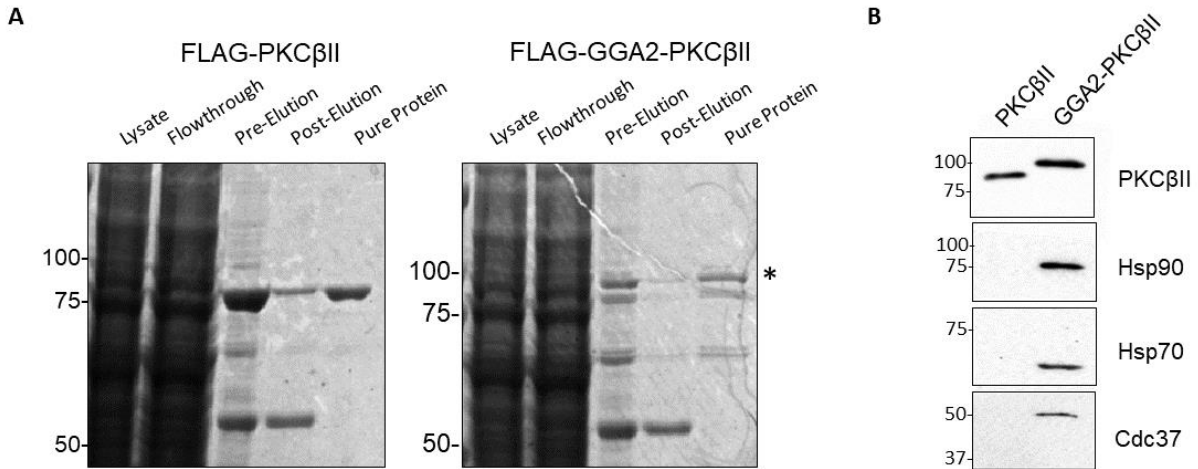
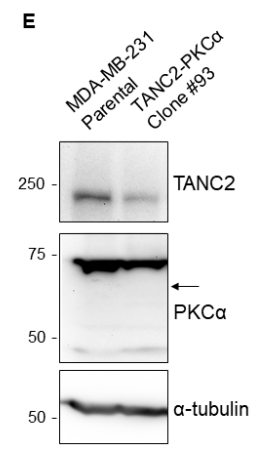
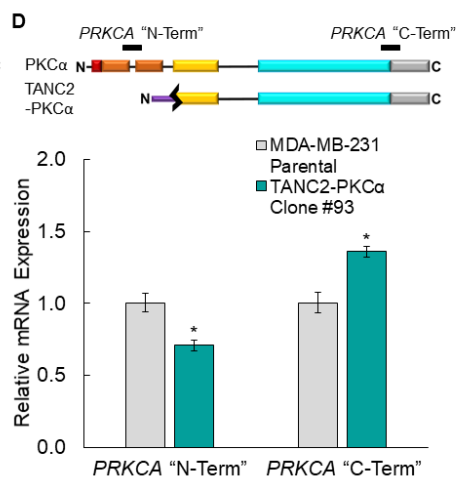
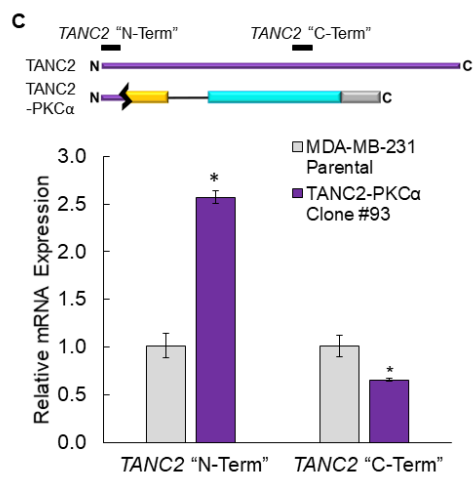
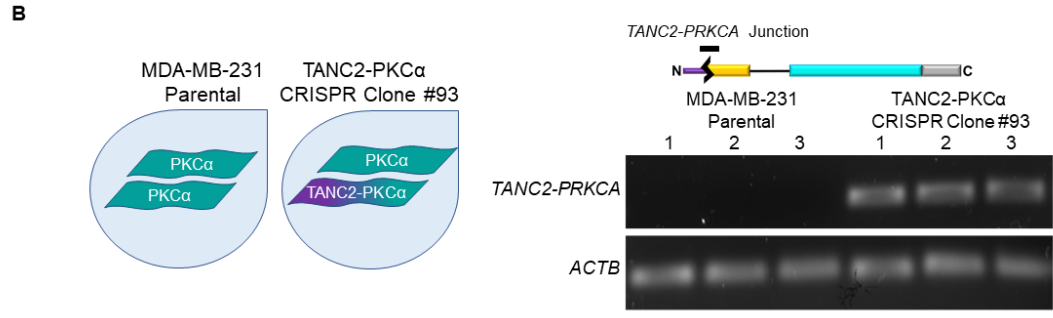
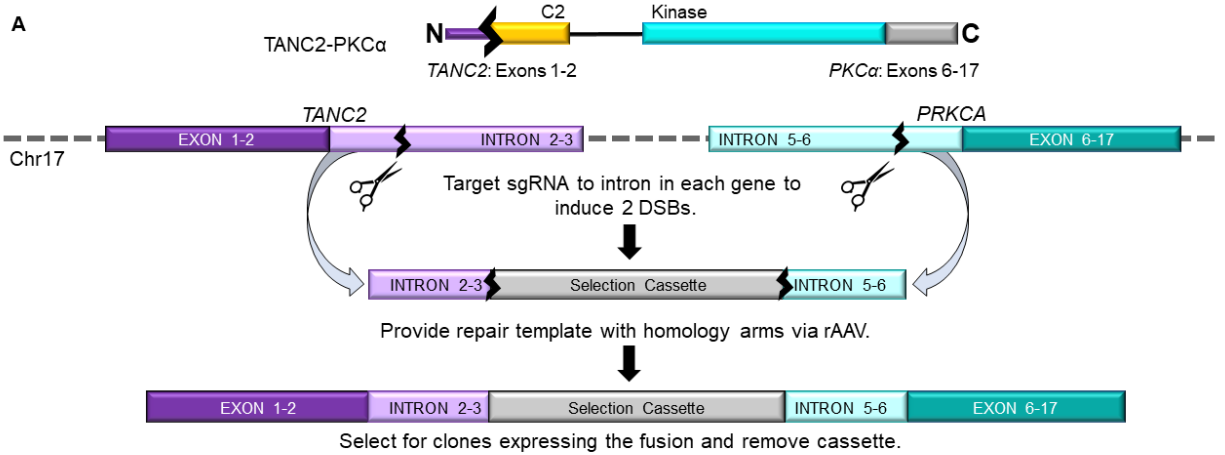


Figure 2.5: Purified GGA2-PKC β II fusion protein is in complex with other proteins, notably molecular chaperones. (A) Coomassie Blue-stained SDS/PAGE gel from different stages during purification of FLAG-tagged wild-type PKC β II or GGA2-PKC β II fusion protein. Protein purified from HEK 293T cells via FLAG pulldown and elution with FLAG peptide. Asterisk (*) indicates band corresponding to fusion protein. (B) Immunoblot analysis of purified PKC β II or GGA2-PKC β II protein, probing for PKC or the molecular chaperones Hsp70, Hsp90, and Cdc37.

Figure 2.6: The *TANC2-PRKCA* fusion is detected at the mRNA level but not the protein level in CRISPR-edited cells. (A) Schematic illustrating strategy to generate cells expressing the *TANC2-PRKCA* fusion via CRISPR/Cas9 gene editing. (B) mRNA expression of the *TANC2-PRKCA* fusion in the parental and CRISPR-edited clone analyzed by RT-qPCR and normalized to actin (*ACTB*). Product indicated by black bar on schematic. Reactions analyzed on agarose gel, with each lane representing individual biological replicate. (C) *TANC2* mRNA expression at the 5' ("N-Term") and 3' ("C-Term") ends in the parental and CRISPR-edited clone analyzed by RT-qPCR and normalized to actin (*ACTB*). Products indicated by black bars on schematic. Data represent means \pm SEM from three independent experiments. * $p < 0.05$ (Student's t-test). (D) *PRKCA* mRNA expression at the 5' ("N-Term") and 3' ("C-Term") ends in the parental and CRISPR-edited clone analyzed by RT-qPCR and normalized to actin (*ACTB*). Products indicated by black bars on schematic. Data represent means \pm SEM from three independent experiments. * $p < 0.05$ (Student's t-test). (E) Immunoblot analysis of lysates from parental and CRISPR-edited cells, probing for TANC2, PKC α , and α -tubulin. Arrow indicates predicted mobility of the fusion protein. Data is representative from three independent experiments.



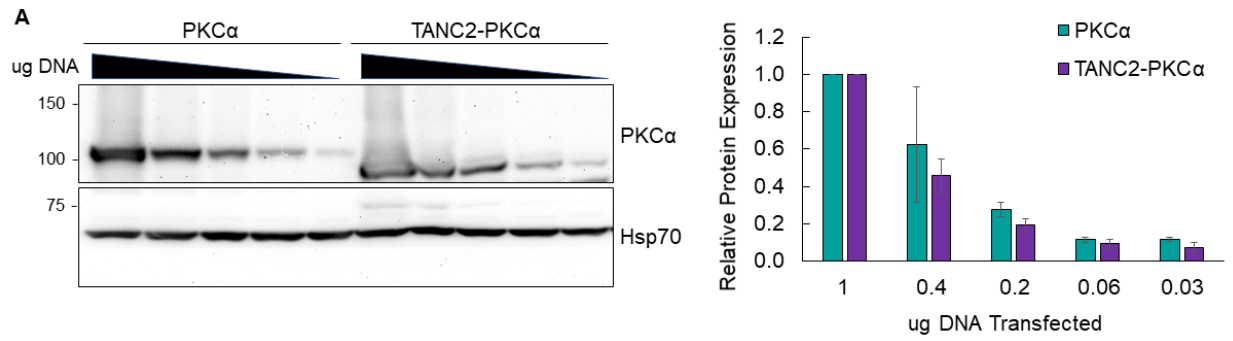
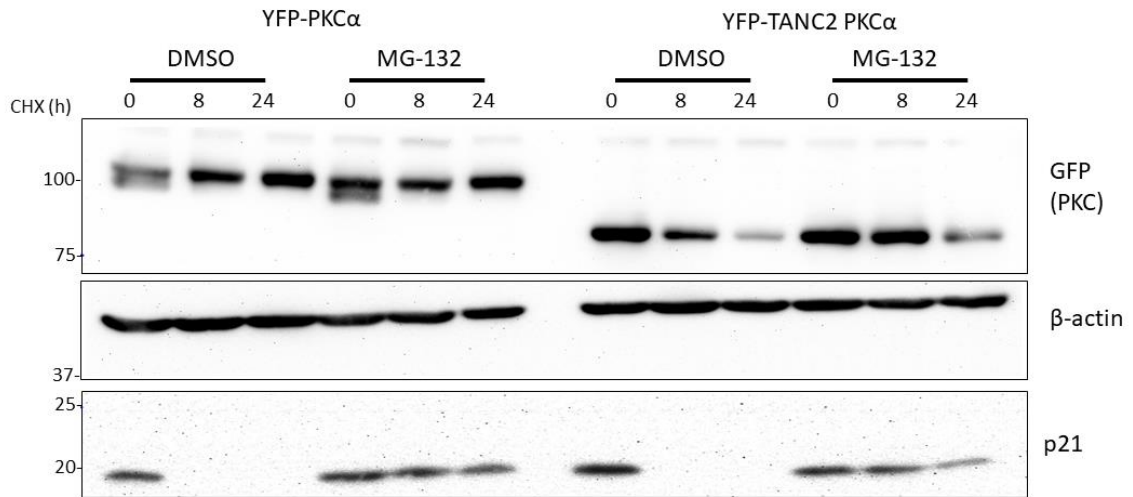
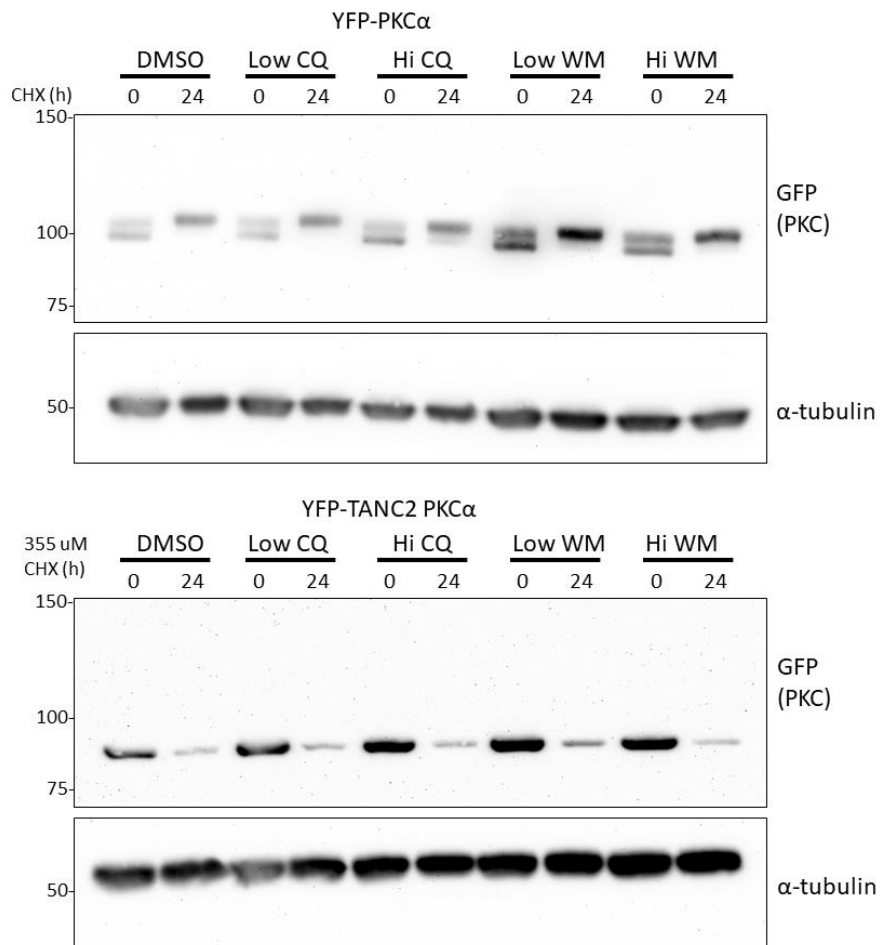


Figure 2.7: Less TANC2-PKC α protein is detected compared to wild-type PKC α in a titration of DNA transfected into cells. (A) Immunoblot analysis of lysates from COS7 cells transfected with varying amounts of YFP-tagged PKC α or TANC2-PKC α . Blots probed for PKC α and loading control (Hsp70). In quantification of blot, ratio of PKC α to Hsp70 signal is normalized to protein expression with 1 μ g of DNA transfected. Blot is representative, and data represent mean \pm SEM from three independent experiments.

Figure 2.8: Inhibition of proteasomal or endosomal/lysosomal degradative pathways does not prevent degradation of TANC2-PKC α fusion protein upon cycloheximide treatment. (A) Immunoblot analysis of lysates from COS7 cells transfected with YFP-tagged PKC α or TANC2-PKC α , pre-treated with MG-132 (20 μ M) or vehicle (DMSO), and treated with cycloheximide (355 μ M). Cells were harvested at indicated timepoints. Blots probed for GFP, β -actin, and p21. (B) Immunoblot analysis of lysates from COS7 cells transfected with YFP-tagged PKC α or TANC2-PKC α , pre-treated with chloroquine, wortmannin, or vehicle (DMSO), and treated with cycloheximide (355 μ M). Cells were harvested at indicated timepoints. Blots probed for GFP and α -tubulin.

A**B**

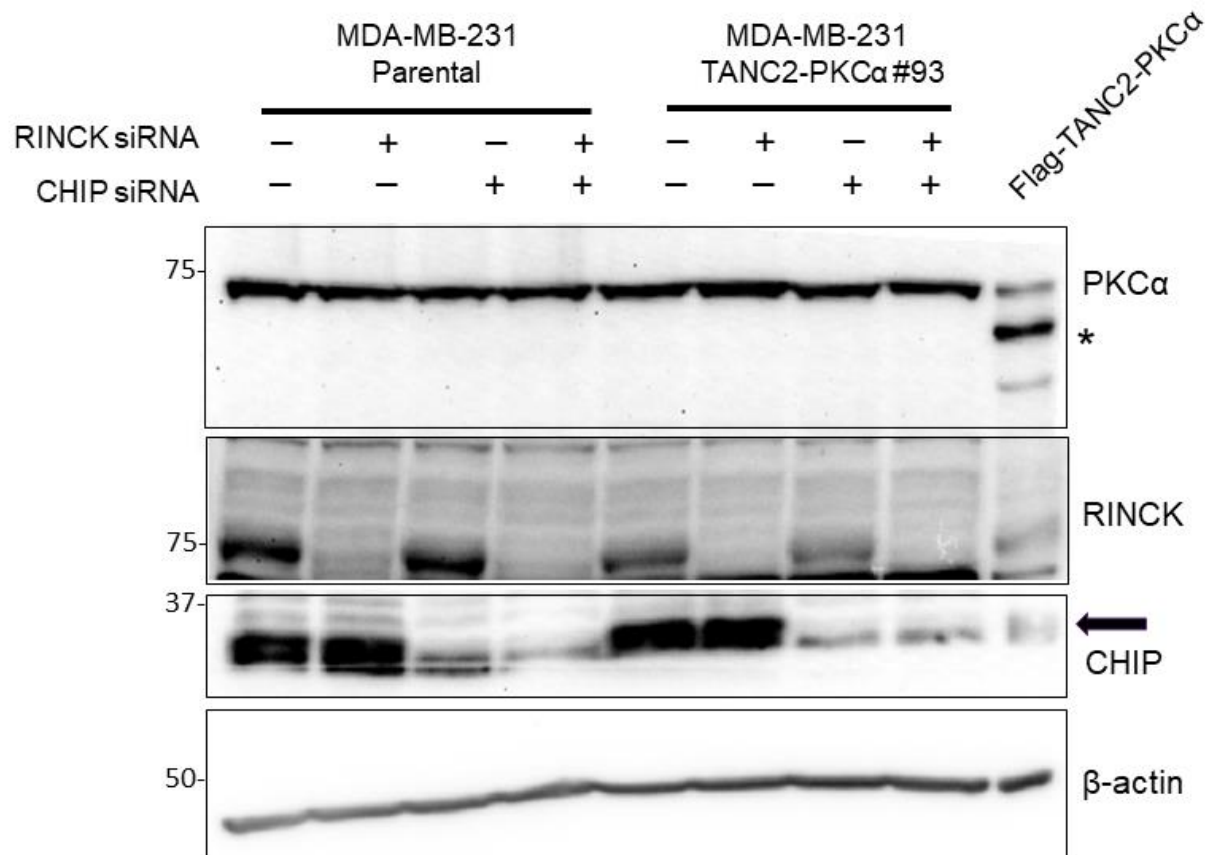


Figure 2.9: Knockdown of E3 ligases does not allow for accumulation of the TANC2-PKCα fusion protein in CRISPR-edited cells. (A) Immunoblot analysis of lysates from MDA-MB-231 parental and CRISPR-edited fusion-expressing cells. Parental and CRISPR-edited cells were transfected with control siRNA, TRIM41 (RINCK) siRNA, STUB1 (CHIP) siRNA, or both RINCK and CHIP siRNAs. Lysate from parental MDA-MB-231 cells overexpressing FLAG-tagged fusion protein was included as a control. Blots probed for PKCα, RINCK, CHIP, and β-actin. Asterisk indicates predicted mobility of the fusion protein. Data is representative from three independent experiments for knockdown of RINCK and CHIP, separately.

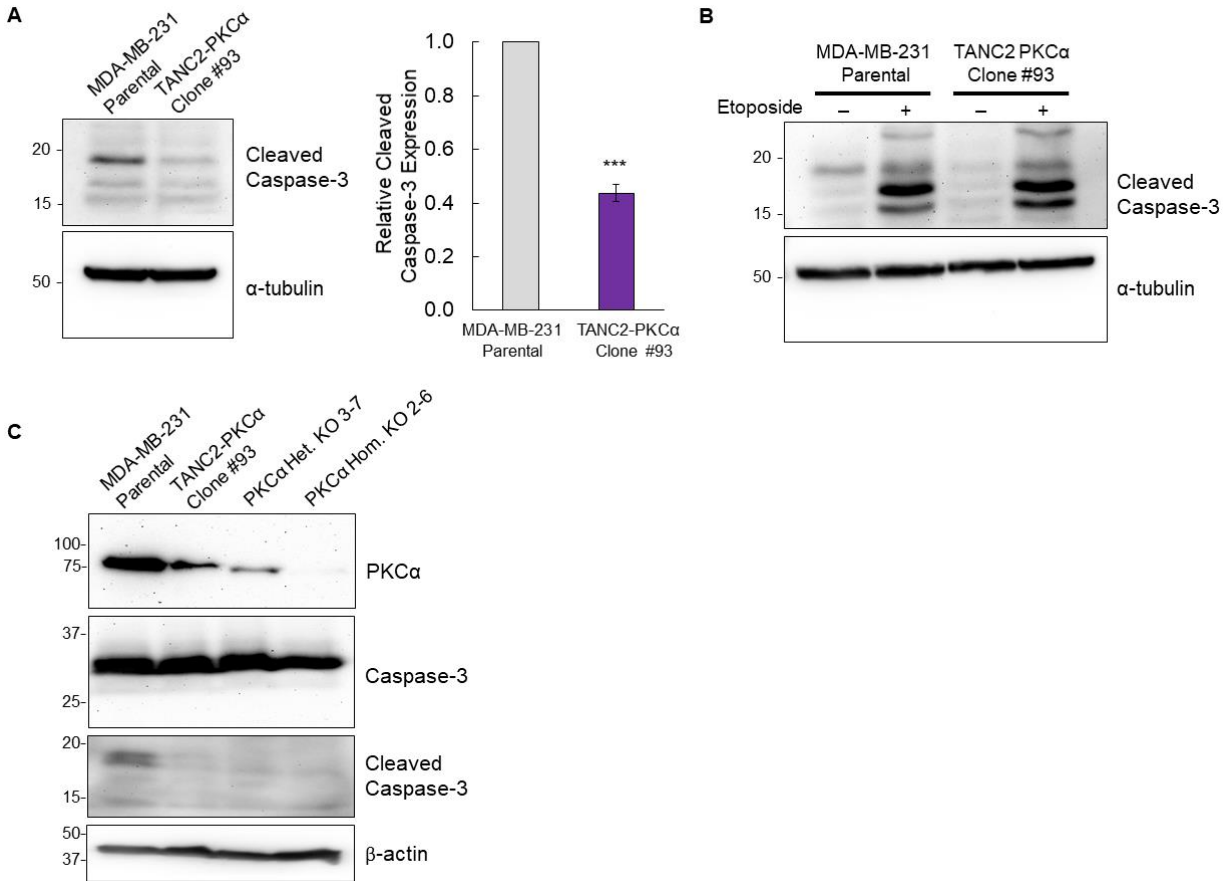
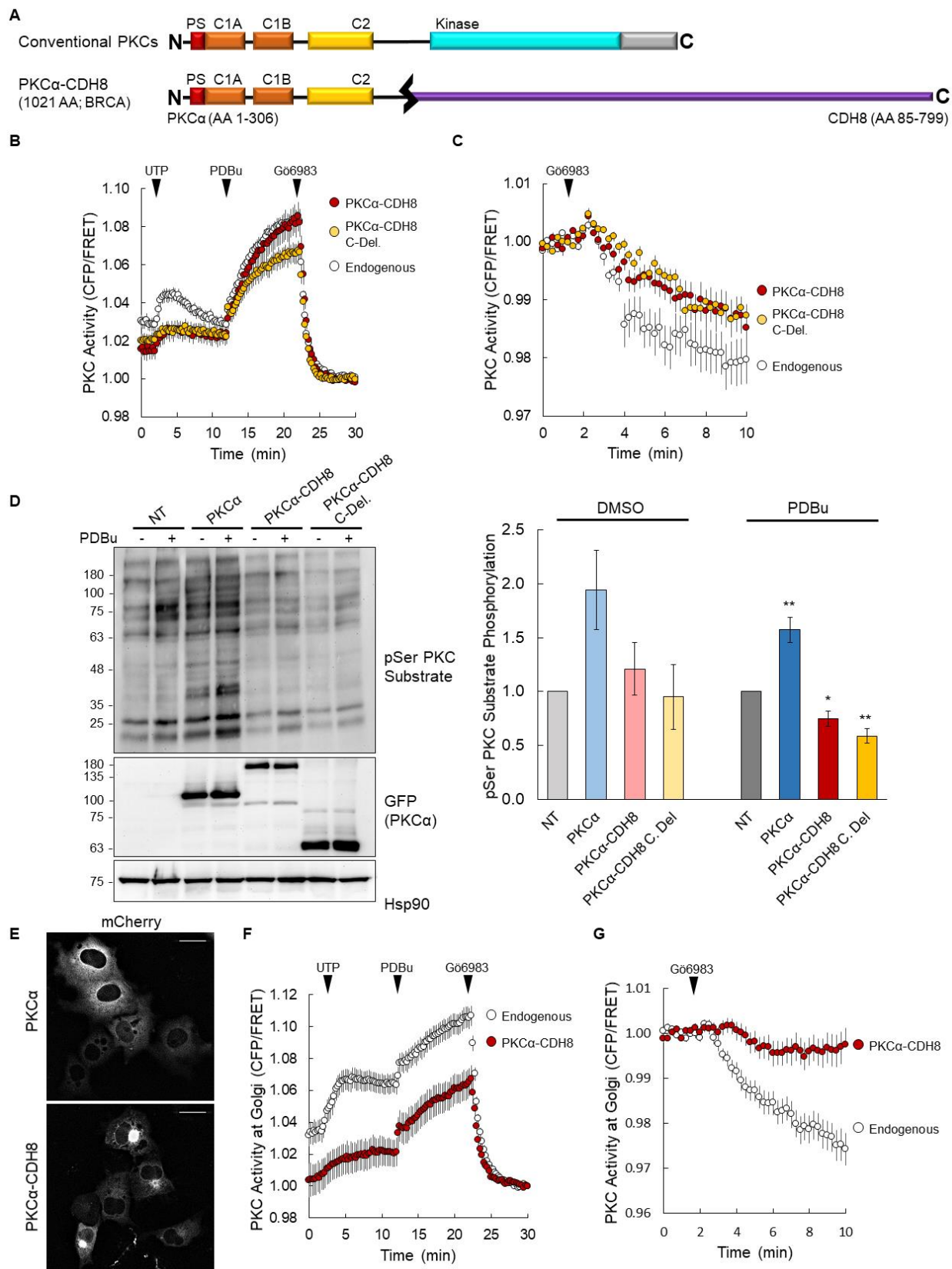


Figure 2.10: *TANC2-PRKCA*-expressing cells display a reduction in apoptosis as indicated by reduced cleaved caspase 3 levels. (A) Immunoblot analysis of lysates from parental and CRISPR-edited cells, probing for cleaved caspase-3 and α -tubulin. Blot is representative, and graph depicts mean \pm SEM from three independent experiments. *** $p < 0.001$ (Student's t-test). (B) Immunoblot analysis of lysates from parental and CRISPR-edited cells treated with etoposide (50 μ M) or vehicle (DMSO). Blots probed for cleaved caspase-3 and α -tubulin. Data is representative from three independent experiments. (C) Immunoblot analysis of lysates from parental, CRISPR-edited fusion, heterozygous PKC α knockout, and homozygous PKC α knockout cells, probing for caspase-3, cleaved caspase-3, PKC α , and β -actin. Data is representative from three independent experiments.

Figure 2.11: 5' PKC fusions may act in a dominant-negative manner, suppressing the activity of wild-type PKC. (A) Schematic of wild-type and PKC α -CDH8 fusion construct used in this study. In addition to the full-length fusion, a C-Deletion construct in which the C-terminal fusion partner is deleted was also generated (PKC α C-Del.). (B) Analysis of agonist-induced PKC activity in COS7 cells transfected with CKAR alone (Endogenous) or co-transfected with the indicated mCherry-tagged PKC construct. Cells treated with agonists UTP (100 μ M), PDBu (200 nM), and inhibitor Gö6983 (1 μ M). Graphs depict normalized FRET ratio changes (mean \pm SEM) from three independent experiments. (C) Analysis of basal PKC activity in COS7 cells transfected with CKAR alone (Endogenous) or co-transfected with the indicated mCherry-tagged PKC construct. Cells treated with inhibitor Gö6983 (1 μ M). Graphs depict normalized FRET ratio changes (mean \pm SEM) from three independent experiments. (D) Immunoblot analysis of lysates from COS7 cells transfected with the indicated YFP-tagged PKC and treated with PDBu (200 nM) or vehicle (DMSO). Blots probed with antibodies for pSer PKC substrate and GFP. Quantification of pSer PKC substrate signal normalized to loading control (Hsp90) depicts mean \pm SEM from three independent experiments. (E) Images of cells from (B) depicting mCherry fluorescence at baseline. Scale bar, 20 μ m (F) Analysis of agonist-induced PKC activity at the Golgi in COS7 cells transfected with Golgi-targeted CKAR alone (Endogenous) or co-transfected with mCherry-tagged PKC α -CDH8. Cells treated with agonists UTP (100 μ M), PDBu (200 nM), and inhibitor Gö6983 (1 μ M). Graphs depict normalized FRET ratio changes (mean \pm SEM) from three independent experiments. (G) Analysis of basal PKC activity at the Golgi in COS7 cells transfected with Golgi-targeted CKAR alone (Endogenous) or co-transfected with mCherry-tagged PKC α -CDH8. Cells treated with inhibitor Gö6983 (1 μ M). Graphs depict normalized FRET ratio changes (mean \pm SEM) from three independent experiments.



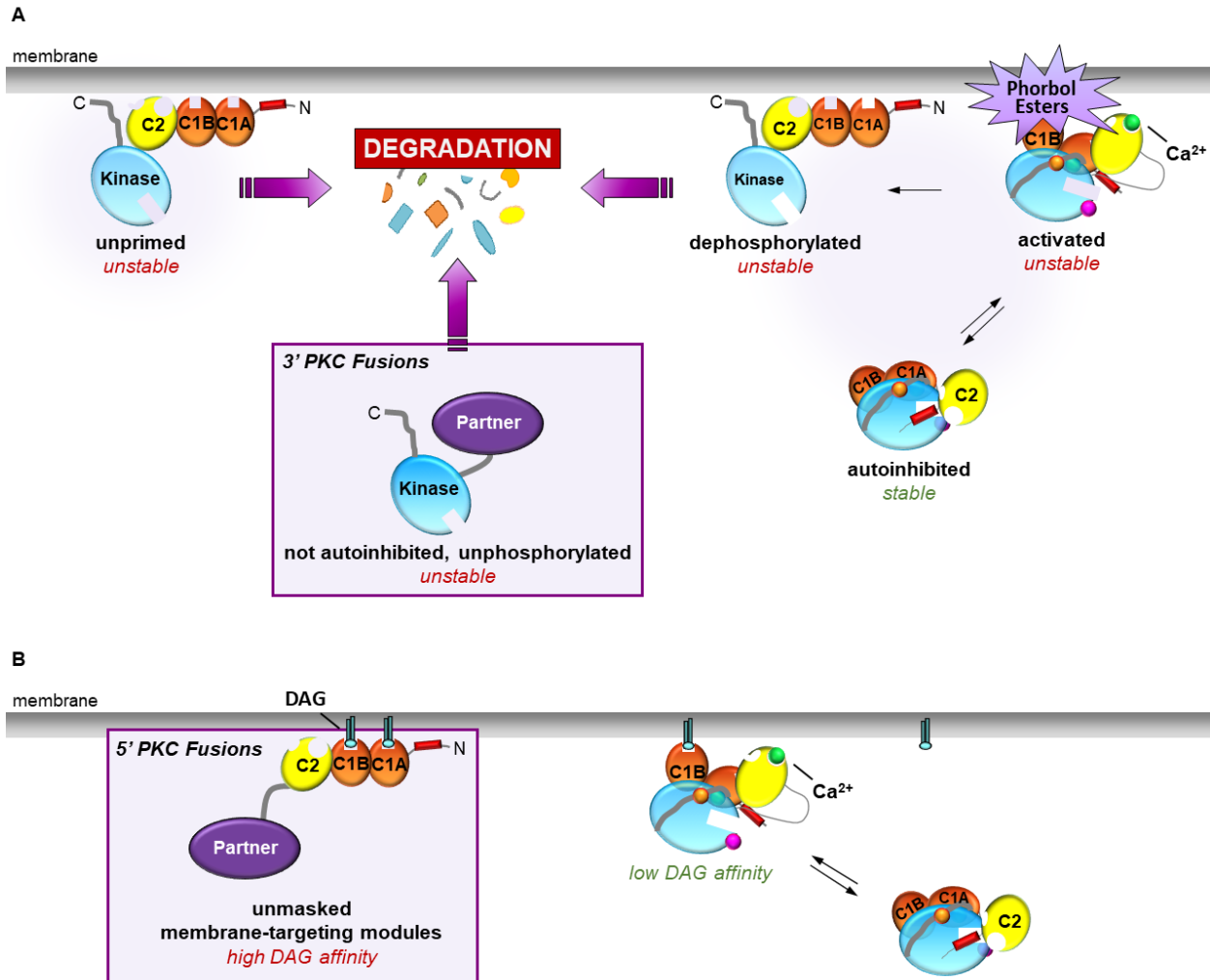


Figure 2.12: Model of PKC fusions as mechanism for loss of PKC activity in cancer. (A) 3' PKC fusions are constitutively active yet markedly unstable. Their instability renders them sensitive to degradation, and thus, they are unable to accumulate to any detectable level in cells. (B) 5' PKC fusions are intrinsically loss-of-function due to loss of the kinase domain but may also act in a dominant-negative manner by sequestering common titratable components, such as diacylglycerol (DAG).

Chapter 3

Mechanisms of Protein Kinase C

Dysregulation in Cancer

3.1 Abstract

While protein kinase C (PKC) has been regarded as an oncogene since its identification as the receptor for the tumor-promoting phorbol esters, recent studies have revealed a role for PKC as a tumor suppressor. With the paradigm for PKC as an oncogene brought into serious question, further studies are required to probe the multitude of ways in which loss of PKC function occurs. In this study, we examine some of those mechanisms, both through analysis of various PKC mutants and through probing physiological regulation of PKC. First, we showed that mutants associated with adult t-cell leukemia/lymphoma are activating yet are still able to retain phosphate at their processing sites. However, they still present as loss-of-function due to their increased sensitivity to dephosphorylation and subsequent degradation. We also revealed the presence of potential chaperones that may serve to stabilize PKC mutants. Furthermore, we examined the mechanism by which inactivating PKC mutants are able to act in a dominant-negative manner, specifically by sequestering common titratable components. Additionally, we demonstrated that in addition to perturbing PKC activity, PKC function can be altered through mislocalization of the protein upon stimulation. This may result in decreased phosphorylation of its substrates at its intended subcellular location and aberrant phosphorylation of substrates at its new location. Lastly, we assessed the interaction between PHLPP and PKC, with PHLPP serving as the negative regulator of PKC steady-state levels by regulating dephosphorylation and thus stability of the kinase. Taken together, these findings provide insight into dysregulation of PKC occurs in cancer, increasing our understanding of the kinase and allowing for the development of more effective therapies.

3.2 Introduction

Since protein kinase C (PKC) was identified as the high-affinity receptor for the tumor-promoting compounds known as phorbol esters, it has been associated with an oncogenic role, its activation contributing to tumorigenesis (16, 17, 142). However, PKC has remained an elusive target as therapeutics designed to inhibit it have failed in clinical trials and at times worsened patient outcome (94). Since then, it has become apparent that while phorbol esters acutely activate the enzyme, they also lock PKC in an active conformation, promoting its dephosphorylation and subsequent downregulation (95, 96). Moreover, an analysis of approximately 50 cancer-associated point mutations in PKC revealed most to be loss-of-function, with PKC inactivation conferring a survival advantage and promoting tumor growth (11). Thus, a tumor suppressive role for PKC was established, reversing the dogma of PKC as an oncogene (97).

The PKC family of Ser/Thr kinases consists of nine isozymes, categorized into three subclasses based on the composition of their regulatory domains: conventional, novel, and atypical (9, 18–21). Accordingly, the nature of the regulatory moiety reveals the distinct co-factor dependency of each PKC subclass. Conventional isozymes include α , the alternatively spliced β I and β II, and γ . These isozymes contain adjacent C1A and C1B domains that bind diacylglycerol (DAG) in membranes and a C2 domain that binds membranes in the presence of Ca^{2+} . Novel isozymes include δ , ϵ , η , and θ . These isozymes also contain tandem C1A and C1B domains but have a novel C2 domain which lacks key residues required for coordinating Ca^{2+} . Thus, while novel isozymes are sensitive to DAG, they are not responsive to Ca^{2+} . However, while they are regulated by only one membrane-targeting module, the C1B domain of novel isozymes has an affinity

for DAG that is two orders of magnitude greater than that of conventional isozymes. Atypical isozymes include ζ and ι/λ . These isozymes respond to neither DAG nor Ca^{2+} and possess an atypical, non-ligand binding C1 domain and a protein-binding PB1 domain that mediates protein-protein interactions, specifically with scaffolds such as Par6 (49). Finally, all three PKC subclasses contain a short pseudosubstrate segment in their regulatory moieties that functions to maintain PKC in a stable, autoinhibited state by occupying the substrate-binding site of the kinase domain. While the amino-terminal regulatory domains vary significantly based on the subclass, the carboxy-terminal catalytic domain is conserved across the PKC family member, consisting of a kinase domain followed by a c-terminal tail.

When translated, PKC is considered to be unprimed and localizes to the plasma membrane. In order to become catalytically competent, PKC undergoes a series of tightly coupled, constitutive phosphorylations. These processing phosphorylations stabilize the PKC protein and occur at three sites within the kinase domain, the activation loop, the turn motif, and the hydrophobic motif (18). Phosphoinositide-dependent kinase PDK1 mediates phosphorylation of PKC at the activation loop and is constitutive for conventional, novel, and atypical isozymes (43). For conventional isozymes of PKC, subsequent phosphorylation occurs at the turn motif and hydrophobic motif, dependent on the mammalian target of Rapamycin complex 2 (mTORC2) (45). Conventional and novel isozymes PKCs, in their mature but inactive form, are retained within the cytosol. Here PKC is in a closed conformation and is subject to autoinhibition by the pseudosubstrate. Agonist-induced generation of second messengers resulting from hydrolysis of phosphatidylinositol-4,5-bisphosphate (PIP_2) triggers activation of PKC.

Conventional PKCs are targeted to the membrane upon binding of Ca^{2+} to the C2 domain. Retention of the C2 domain at the membrane is facilitated by bridge interactions with anionic phospholipids, namely PIP_2 . At the membrane, the C1 domain binds DAG, resulting in a conformational change in which the pseudosubstrate is expelled. PKC is then effectively activated, able to engage in downstream signaling. Unlike conventional isoforms of PKC, novel isoforms are activated by DAG alone. Activation of atypical PKC isoforms is dependent upon protein-protein interactions, specifically with protein scaffolds that bring the enzyme in close proximity to its substrates. When PKC is active, it adopts an open conformation. This conformation is sensitive to dephosphorylation by phosphatases, such as PH domain leucine-rich repeat protein phosphatase (PHLPP) (54). Prolonged activation of PKC, such as through treatment with phorbol esters, results in dephosphorylation of the protein, which destabilizes the kinase and ultimately causes its subsequent ubiquitination and degradation (118).

While analysis of point mutations in various cancers have highlighted some mechanisms by which PKC is inactivated, much is still to be learned regarding dysregulation of PKC in cancer. Here we investigate the different ways in which PKC biology can be altered in cancer, both by analyzing various cancer-associated PKC mutants and by probing the mechanisms that serve to regulate PKC. We characterized mutations in PKC that were identified in adult T-cell leukemia and lymphoma, which exhibit basal activity yet are phosphorylated at the priming sites. However, they are sensitive to dephosphorylation and thus are conceivably loss-of-function. We investigated the existence of potential chaperones that may stabilize PKC mutants. Additionally, we assessed how inactivating mutants of PKC are able to exert their dominant-negative

effects, particularly through sequestration of common titratable components. Using live-cell imaging studies, we determined how loss of certain regulatory domains affects PKC translocation, resulting in their mislocalization to other subcellular compartments. Finally, we examined PHLPP-mediated regulation of PKC, wherein PHLPP negatively regulates steady-state levels of the kinase through dephosphorylation of its hydrophobic motif. Taken together, we illustrate additional ways in which loss of PKC function may occur in a cancer context.

1.3 Results

Activating PKC mutants in ATLL are phosphorylated yet loss-of-function

PKC mutations have been identified in adult T-cell leukemia/lymphoma (ATLL). In an analysis of 426 patient samples, *PRKCB* was found to be the second most frequently mutated gene, mutated in 33% of cases (143). Among these mutations, 93% were located within the catalytic domain with a particular hotspot at D427. Mutation of the Asp to Asn (D427N) is purported to activate the kinase by interfering with the interaction between the NFD motif and the C1B domain. To assess the cellular activity of the D427N mutant compared to that of wild-type PKC β II, we utilized the genetically-encoded fluorescence resonance energy transfer (FRET)-based reporter for PKC activity, C Kinase Activity Reporter (CKAR) (128). In COS7 cells, we expressed the reporter alone or co-expressed mCherry-tagged wild-type PKC β II or the D427N mutant (Figure 3.1A). Stimulation with the physiological agonist UTP resulted in a very modest increase in activity for the D427N mutant compared to wild-type PKC. Similarly, we observed a greater increase in activity for wild-type PKC than the mutant upon stimulation with the phorbol ester PDBu.

However, addition of the PKC inhibitor Gö6983 revealed a more substantial drop in activity relative to baseline with the D427N mutant. Indeed, prior to agonist treatment, the D427N mutant appears to be more basally active than its wild-type counterpart. In order to probe the basal activity of the mutant more precisely, we treated naïve cells with the PKC inhibitor alone (Figure 3.1B). Addition of inhibitor to cells co-expressing the reporter and wild-type PKC resulted in a decrease in CKAR phosphorylation comparable to that of cells expressing the reporter alone. This suggests that wild-type PKC β II exhibits very little basal activity, subject to autoinhibition in the absence of agonist. In contrast, addition of inhibitor causes a greater drop in CKAR phosphorylation in cells expressing PKC β II D427N, indicating that the mutant exhibits agonist-independent activity.

While the catalytic domain mutations comprise the majority of ATLL-associated PKC mutations, other mutations were identified, namely in the autoinhibitory pseudosubstrate segment. To determine the cellular activity of two such mutants (G24D and G24V), we again performed live-cell imaging utilizing CKAR. As with the D427N mutant, both G24D and G24V mutants exhibited more modest increases in activity upon stimulation with UTP and PDBu compared to wild-type PKC β II. Additionally, these data revealed that like the catalytic domain mutant, the pseudosubstrate mutants are also basally active. Thus, the PKC β II D427N, G24D, and G24V mutations all serve to activate the kinase, albeit by targeting different components of the kinase.

In order to become catalytically competent, PKC undergoes phosphorylation at the activation loop, turn motif, and hydrophobic motif. Previously, we demonstrated that cancer-associated fusion proteins which retain the catalytic domain are constitutively active yet unphosphorylated at steady-state levels. To determine whether this also

applied to the ATLL mutants, we assessed their phosphorylation state at the three processing sites. Like wild-type PKC β II, the D427N mutant was phosphorylated at all three sites (Figure 3.1D). Similarly, the G24D and G24V mutants were also phosphorylated at the three priming sites. In contrast to the catalytic domain fusions, the ATLL-associated mutants thus retained their processing phosphorylations.

The agonist-independent activity of the ATLL mutants suggests that they adopt an open conformation. While they are phosphorylated, their open conformation may render them sensitive to dephosphorylation compared to wild-type PKC. To assess the sensitivity of the mutants to dephosphorylation, we treated cells expressing wild-type PKC β II, PKC β II D427N, PKC β II G24D, or PKC β II G24V with PDBu over a 24-hour time course (Figure 3.1F). For wild-type PKC, we observe a single band at the start of the time course, corresponding to the phosphorylated species of PKC. After 3 h, we observe the appearance of a lower molecular weight band, corresponding to the unphosphorylated species of PKC. Over time, the phosphorylated species decreases as more of it is subject to dephosphorylation, facilitated by PHLPP1 and PP2A. While wild-type PKC does not appear to be significantly degraded over the time course, approximately half of the total PKC present is phosphorylated and half is unphosphorylated by 24 h. In contrast, the D427N mutant is more sensitive to PDBu-induced dephosphorylation. At $t = 0$, while the majority of the mutant PKC is phosphorylated, the presence of a lower band indicates that there is already a pool of unphosphorylated PKC present. The phosphorylated species of the mutant decreases more rapidly over time compared to wild-type PKC. Furthermore, unlike wild-type PKC, the mutant appreciably degrades over the time course. As with the catalytic domain mutant, the pseudosubstrate mutants are more

readily dephosphorylated with the phosphorylated species decreasing more rapidly compared to that of wild-type. While the pseudosubstrate mutants may not degrade as rapidly as the catalytic domain mutant, they have greater initial pools of unphosphorylated PKC basally and possess smaller ratios of phosphorylated:unphosphorylated PKC beginning at 3 h post-PDBu treatment. Taken together, these data show that the ATLL mutants are basally active and phosphorylated but are more sensitive to dephosphorylation and subsequently, degradation, compared to wild-type PKC, revealing another biochemical profile of cancer-associated PKC mutations.

Catalytic domain fusions are stabilized by chaperones and the pseudosubstrate

Purification of the GGA2-PKC β II fusion protein from HEK 293T cells revealed that it existed in complex with the chaperones Hsp90, Hsp70, and Cdc37. In addition to these proteins, other unidentified proteins also appeared to be purified with the fusion protein, evidenced by the Coomassie-stained gel with the pure protein (Figure 2.S2A). Purification from Sf9 insect cells similarly showed other proteins in complex with the fusion protein, indicated by the higher molecular weight bands present on the Coomassie-stained gel containing the eluate (Figure 3.2A). To determine whether these proteins may have an effect on the activity of the fusion protein, we performed an *in vitro* kinase assay comparing the activities of wild-type PKC β II, the GGA2-PKC β II fusion, and a 50:50 combination of the two proteins (Figure 3.2B). We assessed activity in four conditions: no lipid, no Ca²⁺; Ca²⁺ only; lipid only; and lipid and Ca²⁺. While wild-type PKC β II was only active in the presence of both lipid and Ca²⁺, the fusion protein exhibited activity in all conditions, corroborating the cellular studies that revealed its agonist-independent

activity. With the wild-type/fusion protein combination in the no lipid, no Ca^{2+} and Ca^{2+} only conditions, we observed a level of intermediate activity that was reflective of the sum of each individual protein. However, in the lipid only as well as the lipid and Ca^{2+} conditions, we observed a synergistic effect where the apparent activity exceeded the sum of each individual protein. In the combination of the two proteins, wild-type PKC β II is exposed to the proteins that are co-purified with the fusion protein. This suggests that the proteins purified in conjunction with the fusion protein may play a role in potentiating PKC activity, perhaps by stabilizing the protein. While the identified chaperones, namely the heat shock proteins, are in great abundance in the cell, the unidentified proteins may be limiting. PKC mutants may thus sequester these proteins away from PKC or other proteins.

Purification of the fusion protein in conjunction with the *in vitro* kinase data demonstrate that activating mutants of PKC may be targeted by chaperones and other proteins to counteract its intrinsic instability. Activating mutants, such as the catalytic domain fusions, adopt an open conformation that is permissive for activity in the absence of the appropriate second messengers. However, this open conformation renders it unstable. Given that the pseudosubstrate plays a crucial role in the autoinhibition and therefore stability of the kinase, addition of the pseudosubstrate in *trans* may serve to increase autoinhibition and stability of the fusion protein. To address whether this is possible, we performed live-cell imaging studies with CKAR, assaying basal activity in the absence or presence of the GST-tagged PKC β II pseudosubstrate segment. We expressed CKAR alone or co-expressed wild-type PKC β II, the GGA2-PKC β II fusion protein, the GGA2-PKC β II N-Deletion variant, or PKC β II Δ PS, wherein the

pseudosubstrate is deleted (Figure 3.2C, D, E). For each of the four conditions, we also co-expressed a vector control or GST-tagged pseudosubstrate (PS). As observed previously, wild-type PKC is autoinhibited and thus has very little basal activity (Figure 3.2C). As such, addition of the pseudosubstrate has very little effect. In contrast, addition of the pseudosubstrate significantly decreases the basal activity of the fusion protein, though not to the level of wild-type PKC. For the N-Deletion protein, we observe an even greater suppression of activity in the presence of the pseudosubstrate (Figure 3.2D). Finally, we observed that the basal activity of PKC β II Δ PS can also be inhibited by introduction of the pseudosubstrate. These data demonstrate the pseudosubstrate is capable of exerting an appreciable autoinhibitory effect *in trans* by way of suppressing aberrant basal activity, which may serve to stabilize the protein to some extent.

Catalytically-dead PKC mutants are dominant negative

The regulatory domain fusion proteins were observed to act in a dominant-negative manner, suppressing the activity of wild-type PKC. Similarly, inactivating PKC mutants may also be dominant negative. One such mutant, PKC β II A509T, was detected in the DLD1 colorectal cancer cell line. Cells with heterozygous expression of the A509T allele with wild-type PKC exhibited greater anchorage-independent growth compared to cells expressing a single wild-type allele (11). However, the mechanism by which the mutant allele suppresses wild-type activity is unknown. Inactivating point mutations in PKC yield proteins that are unable to phosphorylate substrates but may still interact with the proteins that serve to regulate wild-type PKC. The mutants may thus exert their dominant-negative effect by sequestering such proteins from wild-type PKC. To address this possibility, we

compared the association of wild-type PKC β II and the A509T mutant to PDK1, a protein critical in the processing of PKC, by co-immunoprecipitation (Figure 3.3A). In addition to wild-type PKC β II and PKC β II A509T, we also assessed association of PDK1 with the kinase-dead mutant PKC β II K371R. In HEK 293T cells, we overexpressed Myc-tagged PDK1 and HA-tagged wild-type PKC β II, PKC β II A509T, or PKC β II K371R, immunoprecipitating PDK1 via the Myc tag. From wild-type PKC β II, we observed that PDK1 has a preference for the unphosphorylated species of PKC, binding lower band, unphosphorylated PKC despite the abundance of phosphorylated PKC. Comparing the mutants with wild-type PKC, PDK1 appears to co-immunoprecipitate with both PKC β II A509T and PKC β II K371R more than wild-type (Figure 3.3B). Thus, the inactivating mutants may be able to outcompete wild-type PKC for PDK1.

In addition to PDK1, we performed co-immunoprecipitation studies with mTOR, another protein critical for PKC maturation (Figure 3.3C). Here, we co-expressed Myc-tagged mTOR with HA-tagged wild-type PKC β II, PKC β II A509T, or PKC β II K371R, immunoprecipitating mTOR via the Myc tag. Compared to PDK1, mTOR appears to have an even greater preference for the unphosphorylated species of PKC, binding to the lower band of wild-type PKC β II that is difficult to detect at steady-state. Consequently, mTOR preferentially binds the A509T and K371R mutants substantially more than wild-type PKC, enriching for the mutants despite their low initial abundance. As with PDK1, the inactivating mutants may thus sequester mTOR away from wild-type PKC, interfering with PKC processing and potentially reducing steady-state levels of wild-type protein in the cell.

While PDK1 and mTOR are critical in the processing of PKC, they also play crucial roles in other proteins, such as Akt. In order to address the effect of an inactive PKC mutant on Akt, we utilized the DLD1 colorectal cancer cell line, which expresses the heterozygous PKC β II A509T mutation (A509T/WT), and three cell lines in which the mutation has been corrected through CRISPR/Cas9-mediated gene editing (WT/WT). We also utilized the previously described CRISPR-edited cell line in which the A509T mutant allele was knocked out, producing a hemizygous cell line expressing only one allele of wild-type PKC β II (WT/-). As with PKC, Akt is phosphorylated at 3 sites: the activation loop (Thr308), the turn motif (Thr450), and the hydrophobic motif (Ser473). Akt is constitutively phosphorylated at Thr450 by mTORC2 whereas the other two sites are phosphorylated upon activation (45). PDK1 phosphorylates Thr308 while mTORC2 is involved in Ser473 phosphorylation (47). We investigated whether the PKC β II A509T could affect Akt processing or activity by probing for its total levels and phosphorylation state at the three sites in the parental and CRISPR-edited DLD1 cell lines (Figure 3.3D). In terms of total Akt, we observed no statistically-significant difference between the cell lines. We observed an increase in basal phosphorylation at the activation loop (Thr308) in the WT/WT and WT/- lines compared to the parental and no statistically-significant difference in the constitutive phosphorylation site (Thr450) among the cell lines. Lastly, for the hydrophobic motif (Ser473), there was increased basal phosphorylation in the WT/- line compared to the parental line and a trend towards increased phosphorylation in the WT/WT lines. While we were able to observe differences in basal phosphorylation among the different cell lines, we also investigated differences in phosphorylation upon stimulation with EGF (Figure 3.3F). As we saw basally, there was no difference in

phosphorylation at the turn motif among the different cell lines. However, with EGF stimulation, we observed a marked increase in phosphorylation at the Thr308 and Ser470 sites in the WT/WT and WT/- lines compared to the parental. Compared to the CRISPR-edited lines, Akt is very weakly activated by EGF at these sites in the parental line. Together, these data demonstrate that presence of the mutant allele results in suppression of Akt phosphorylation at the activation loop and hydrophobic motif sites, supporting a dominant-negative role for the A509T mutant with respect to the phosphorylation of Akt.

PKC fusions demonstrate potential loss of PKC function via mislocalization

Cancer-associated point mutations have been identified in all of the functional domains of PKC. In addition to impeding catalysis and phosphorylation of PKC, inactivation of PKC can also occur by altering second messenger binding. While this can be accomplished by mutating critical residues in the regulatory domains of PKC, it can also be observed with the PKC catalytic domain fusions which have truncations in their regulatory domains. In the case of these fusions, rather than toggling the affinity of a particular component of the regulatory moiety for a given second messenger, the mutant PKC is unable to respond to the second messenger due to deletion of the domain. A potential consequence of altering second messenger binding is altering the localization of PKC upon stimulation. To this end, we performed live-cell imaging studies with different catalytic domain fusions, namely TANC2-PKC α and GGA2-PKC β II, to observe the impact of different regulatory domain truncations on translocation following agonist stimulation. While TANC2-PKC α retains only the C2 domain of the regulatory moiety, GGA2-PKC β II

retains the C1B and C2 domains. In addition to the two fusion proteins, we also observed translocation of the corresponding N-Deletion mutants, in which the partner protein is deleted, as well as the Δ PS mutants, in which the pseudosubstrate segment is deleted. We treated cells with thapsigargin, an inhibitor of the sarco/endoplasmic reticulum Ca^{2+} ATPase that increases intracellular Ca^{2+} levels, and the phorbol ester PDBu.

Upon agonist stimulation, conventional isozymes of PKC translocate to the plasma membrane. We thus first examined translocation of wild-type PKC and the mutants to the plasma membrane. In COS7 cells, we co-expressed myristoylated-palmitoylated mCFP (targeted to the plasma membrane) and YFP-tagged wild-type PKC α , the TANC2-PKC α fusion, or the TANC2-PKC α N-Deletion variant (Figure 3.4A). We monitored translocation of the proteins following treatment with thapsigargin, followed by PDBu. From the cytosol, wild-type PKC α translocates weakly to the plasma membrane following addition of thapsigargin and translocates strongly following PDBu treatment. In contrast, both the TANC-PKC α fusion and N-Deletion proteins do not translocate from the cytosol to the plasma membrane following treatment with either compound. Next, we monitored plasma membrane translocation of wild-type PKC β II, GGA2-PKC β II, GGA2-PKC β II N-Deletion, and PKC β II Δ PS proteins (Figure 3.4B). As with PKC α , we observed weak plasma membrane translocation of PKC β II following thapsigargin addition and strong translocation following phorbol ester treatment. While the GGA2-PKC β II and N-Deletion proteins did not respond significantly to thapsigargin, they appeared to weakly translocate to the plasma membrane following PDBu addition. This occurred to an even greater extent with the PKC β II Δ PS mutant, though not to the degree of wild-type PKC β II. Overall,

the mutant proteins indeed exhibited altered translocation upon stimulation compared to their wild-type counterparts.

Examining the images from the translocation studies, we observed whether the mutant proteins were translocating to different subcellular compartments upon stimulation. In the case of the TANC-PKC α fusion and N-Deletion proteins, they do not appear to translocate anywhere following treatment with either compound (Figure 3.4C). However, in the case of the GGA2-PKC β II, N-Deletion, PKC β II Δ PS proteins, they appear to translocate to the Golgi following drug treatment, the effect being most prominent in the Δ PS mutant (Figure 3.4D).

To quantify the extent of this Golgi translocation, we co-expressed Golgi-targeted mCFP and YFP-tagged PKC in COS7 cells and again, treated with thapsigargin and PDBu. Here we measured changes in YFP fluorescence in the Golgi region, demarcated by the Golgi-targeted mCFP. For wild-type PKC α , we observed a decrease in Golgi localization following thapsigargin treatment and a further decrease following PDBu treatment (Figure 3.4E). This coincides with translocation of the wild-type protein to the plasma membrane. Both the TANC-PKC α and N-Deletion proteins translocated weakly, if at all, to the Golgi following stimulation. In contrast, the PKC α Δ PS mutant translocated strongly to the Golgi after addition of PDBu. Golgi translocation of PKC β II mirrored that of PKC α with decreases following drug treatment as PKC β II translocates to the plasma membrane instead of the Golgi (Figure 3.4F). Finally, the GGA2-PKC β II fusion protein and, to a greater extent, the N-Deletion and Δ PS mutants indeed exhibited increases in translocation to the Golgi following drug treatment, corroborating the cellular images from the plasma membrane translocation studies. Taken together, these data illustrate how

loss of different regulatory domains affects PKC translocation, resulting in mislocalization of the mutants at different subcellular locations.

PKC is negatively regulated by PHLPP1

PHLPP1 catalyzes the first step in the downregulation of PKC: dephosphorylation of the hydrophobic motif (Ser657 in PKC α , Ser660 in PKC β II). As such, PHLPP plays an important role in negatively regulating the steady-state levels of PKC (118). To further investigate PHLPP1-mediated regulation of PKC, we performed experiments in Sf9 insect cells, which exhibit a different phosphatase environment than mammalian cells, and in mouse embryonic fibroblasts (MEFs) where PHLPP has been deleted (*Phlpp1*^{-/-}).

The GGA2-PKC β II fusion protein was found to be unphosphorylated at the three PKC priming sites in mammalian cells but phosphorylated at the sites when purified from Sf9 insect cells. Given that the Sf9 cells provide a cellular context in which a constitutively active and unstable PKC can retain its processing phosphorylations, we investigated whether expression of PHLPP can facilitate dephosphorylation of such a mutant. Specifically, we infected Sf9 cells with baculovirus to express GST-tagged wild-type PKC β II or PKC β II Δ PS protein and the His-tagged PP2C domain of PHLPP1 (Figure 3.5A). We compared total PKC levels and phosphorylation at the turn motif and hydrophobic motif in the absence and presence of the PHLPP1 PP2C domain. As observed for the GGA2-PKC β II fusion protein, the PKC β II Δ PS mutant was phosphorylated at the turn motif and hydrophobic motif. Thus, the PKC β II Δ PS mutant is phosphorylated at some point in time but is rapidly dephosphorylated due to lack of autoinhibition. Expression of the PHLPP1 PP2C domain resulted a decrease in

phosphorylation at both sites for the wild-type and Δ PS proteins. However, this was accompanied by a 4-fold decrease in total PKC protein (Figure 3.5B). Therefore, the decrease in phosphorylation at the turn and hydrophobic motifs is actually commensurate with the decrease in total protein and not indicative of an increase in the unphosphorylated species of PKC (Figure 3.5C, D). These data show that unphosphorylated PKC does not accumulate in insect cells, reflected by the decrease in steady-state levels of PKC and no statistically-significant difference in phosphorylation in the absence or presence of the PP2C domain. The PHLPP1 PP2C domain thus mediates dephosphorylation of PKC and consequently shunts it off to degradative pathways.

Considering the negative regulatory role of PHLPP, we next compared the sensitivity of endogenous PKC α to dephosphorylation and subsequent degradation in *Phlpp1^{+/+}* and *Phlpp1^{-/-}* MEFs (Figure 3.5E). We treated wild-type and knockout MEFs with PDBu over a 24 h time course, monitoring the levels of PKC α protein from whole cell lysates. Compared to *Phlpp1^{+/+}* MEFs, PKC α was more resistant to PDBu-induced downregulation in the *Phlpp1^{-/-}* MEFs with a half-time of 14 ± 2 h in *Phlpp1^{-/-}* MEFs vs. a half-time of 6.6 ± 0.9 h in *Phlpp1^{+/+}* MEFs (Figure 3.5F). In the absence of PHLPP, PKC α is able to evade PHLPP-mediated dephosphorylation of its hydrophobic motif which triggers the events leading to its degradation.

In the wild-type and knockout MEFs, we investigated the effect of PHLPP on the phosphorylation of overexpressed PKC β II (WT) and a mutant of PKC β II in which the position of positively charged amino acids in the pseudosubstrate is scrambled (Sc) (Figure 3.5G). We expressed HA-tagged PKC in *Phlpp1^{+/+}* and *Phlpp1^{-/-}* MEFs, analyzing the triton-soluble and triton-insoluble fractions separately. In *Phlpp1^{+/+}* MEFs, PKC β II was

primarily phosphorylated with a minor fraction of unphosphorylated PKC, indicated by the faster mobility lower band. In contrast, the scrambled mutant exhibited a greater proportion of unphosphorylated PKC. In *Phlpp1*^{-/-} MEFs, the proportion of phosphorylated PKC significantly increases for wild-type PKC (Figure 3.5H). Consequently, the proportion of unphosphorylated PKC significantly decreases for wild-type PKC in the *Phlpp1*^{-/-} MEFs, indicated by the absence of lower band on the immunoblot (Figure 3.5I). No significant difference was observed for the scrambled mutant in the proportion of the phosphorylated or unphosphorylated species in the *Phlpp1*^{+/+} and *Phlpp1*^{-/-} MEFs. Finally, we observe a decrease in wild-type protein in the triton-insoluble fraction, where unphosphorylated PKC is typically enriched, from *Phlpp1*^{+/+} MEFs to *Phlpp1*^{-/-} MEFs. Overall, in the absence of PHLPP, PKC β II maintains its phosphorylated state with very little of the species unphosphorylated.

Steady-state levels of PKC are under the pervasive regulation of PHLPP. We examined the levels of PKC α in *Phlpp1*^{+/+} and *Phlpp1*^{-/-} MEFs to determine the extent of this regulation (Figure 3.5J). Compared to wild-type MEFs, there is a 2-fold increase in PKC α in the knockout MEFs (Figure 3.5K). Altogether, these data essentially highlight the unstable nature of unphosphorylated PKC. By facilitating dephosphorylation of PKC which ultimately results in its degradation, PHLPP1 serves as a prominent negative regulator of the kinase.

3.4 Discussion

With its role as a tumor suppressor a relatively recent discovery, ongoing studies continue to reveal different ways in which PKC function is lost in cancer (97). An analysis

characterizing cancer-associated point mutations demonstrated that loss of PKC function can occur by interfering with the kinase's ability to phosphorylate substrate, preventing its own processing by phosphorylation, and disrupting the interaction between the kinase and its second messengers (11). Here we investigated different aspects of PKC regulation that might be targeted in cancer. Namely, through characterization of mutations in ATLL, we observed a new profile of mutants that are activating, phosphorylated, and sensitive to dephosphorylation. We explored the ability of PKC mutants to be stabilized in a cellular context. We demonstrated how mutant isozymes of PKC can act in a dominant-negative manner. We showed that mutations which perturb PKC's regulatory domains can result in mislocalization of the kinase. Finally, we assessed the nature of PHLPP's role in negatively regulating PKC.

Our characterization of the ATLL-associated mutations, PKC β II D427N, G24D, and G24V, demonstrated the specific effects of these mutations on PKC function and more generally, provided insight into a potential trend of PKC mutations in ATLL. However, beyond that, it yielded information on an additional kind of mutational profile of PKC in cancer. Analyses of PKC point mutations in cancer thus far have shown that a majority of them are directly inactivating (11). Analysis of proteins resulting from PKC 3' fusions where the catalytic domain is retained revealed that they were paradoxically activating yet loss-of-function due to their marked instability. Although the ATLL mutants were also activating, they were phosphorylated, unlike the fusion proteins. This suggests that the open conformation adopted by the ATLL mutants to permit basal activity independent of agonist differs from that adopted by the catalytic domain fusions. In this case, the conformation of the ATLL mutants is sufficient to protect the enzymes from

dephosphorylation. However, while the mutants are phosphorylated at steady-state levels, they are still more sensitive to PDBu-induced dephosphorylation compared to wild-type protein. This suggests that the mutants may also be more readily degraded, but further studies are required to more precisely assess stability of these mutants. Nevertheless, our analysis of the ATLL mutants shed light on how different PKC mutations can alter kinase structure and function.

We have demonstrated that the open conformation of the catalytic domain fusions renders the protein unstable to the extent that it cannot accumulate in cells in an endogenous context. However, we were able to sufficiently overexpress the protein in cells. This may have been aided by proteins serving to stabilize the protein. Purification of a catalytic domain fusion from mammalian cells corroborated this as the fusion was purified in conjunction with well-known molecular chaperones. In addition to these chaperones, other proteins also appeared to be purified in conjunction with the fusion, both from purification from mammalian cells and from insect cells. An *in vitro* kinase assay revealed that a combination of wild-type protein with fusion protein had a synergistic effect, with the resulting activity greater than the sum of the activity from each protein. The unidentified proteins potentiating the observed synergism may be stabilizing the PKC proteins, protecting them from degradation. While these stabilizing proteins may not be able to protect the catalytic domain fusions from degradation, they may act on other mutants of PKC.

There has been evidence that suggests inactivating mutants of PKC may act in a dominant-negative manner, but the mechanism by which this occurs is unclear. Through co-immunoprecipitation studies with PDK1 and mTOR, we showed that these two

proteins preferentially bind unphosphorylated mutant PKC over phosphorylated wild-type PKC. While the preference for unphosphorylated PKC was more substantial for mTOR, the amount of PDK1 in the cell is limiting with respect to the total sum of different PKC isozymes (144). Thus, a small (<2-fold) preference for mutant PKC over wild-type PKC may still be functionally relevant. Furthermore, both PDK1 and mTOR play crucial roles in the processing and activation of other substrates, namely Akt. Analyzing total and phosphorylated Akt in DLD1 parental and CRISPR-edited cells, presence of the mutant allele was associated with decreased phosphorylation at the activation loop and hydrophobic motif of Akt. The effect, appreciable in basal conditions, was more substantial following activation with EGF. We therefore illustrated that mutant PKC can exert its dominant-negative effects by sequestering common titratable components, hindering the processing and activation of PKC and Akt, respectively

Many cancer-associated mutations in PKC alter PKC activity, but loss of PKC function may also occur through other mechanisms, such as mislocalization of the kinase. Utilizing PKC fusion proteins and PKC Δ PS mutants, we observed the contribution of some of the regulatory domains to appropriate translocation of PKC following stimulation. TANC2-PKC α , retaining only the C2 domain, remained in the cytosol, failing to respond to either thapsigargin or PDBu. GGA2-PKC β II, retaining the C1B and C2 domains, weakly translocated to the plasma membrane and moderately translocated to the Golgi. Interestingly, both PKC α and PKC β II Δ PS mutants translocated moderately to the plasma membrane and strongly to the Golgi following stimulation. Deletion of the pseudosubstrate appears to unmask the C1A domain, favoring translocation of the mutants to the Golgi rather than the plasma membrane. Deletion of the regulatory

domains or, more conservatively, mutation of critical residues in the regulatory domains may thus alter agonist-induced translocation of PKC to its appropriate subcellular compartment, with mislocalization leading to alterations in the substrates which it phosphorylates.

Lastly, we probed the interaction of PKC with its negative regulator, PHLPP. Overexpression of the PHLPP1 PP2C domain in insect cells and PDBu-induced downregulation in *Phlpp1*^{-/-} MEFs underscored the marked instability of unphosphorylated PKC in the presence of PHLPP. PHLPP mediates the initial dephosphorylation event which triggers complete dephosphorylation of the enzyme. PKC is then subsequently shunted off to degradative pathways. In the absence of PHLPP, PKC is able to maintain its phosphorylated state, evidenced by the 2-fold increase in PKC α in *Phlpp1*^{-/-} MEFs compared to *Phlpp1*^{+/+} MEFs. The interaction between PKC and PHLPP may be targeted in cancer given that there is a survival advantage to reducing the steady-state levels of PKC and this can be readily accomplished by PHLPP-mediated dephosphorylation of PKC.

In summary, these findings shed insight into additional mechanisms by which loss of PKC function occurs in cancer. By understanding the mechanisms which serve to regulate PKC, we can appreciate the vulnerabilities which may be targeted in cancer. Conversely, analysis of cancer-associated PKC mutations also yields insight into the regulation of PKC in physiological conditions. While there are a multitude of studies which examine the role of PKC in cancer through an oncogenic lens, the tumor suppressive function of PKC has not been well-studied. As we continue to investigate alterations in

PKC biology in the context of cancer, we will be more apt to develop effective therapeutics, particularly those that serve to restore, rather than inhibit, PKC activity.

3.5 Materials and Methods

Plasmid constructs

The C Kinase Activity Reporter (CKAR) has been previously described (128). Human PKC β II and PKC α were N-terminally tagged with mCherry via Gateway cloning as previously described (11). N-terminal mCherry-tagged and HA-tagged constructs of PKC β II D247N, G24D, and G24V were generated through QuikChange site-directed mutagenesis of the respective wild-type PKC β II constructs (Agilent). GST-tagged PKC β II pseudosubstrate was generated through QuikChange mutagenesis of a previously described construct in which the N-terminus of PKC β II through the C1 domain (residues 1-156) was subcloned into the pEBG vector. The C1 domain was looped out from the construct, retaining the N-terminus through PKC β II pseudosubstrate segment (residues 1-36) (Gao 2001). Human TANC2-PKC α and GGA2-PKC β II constructs were generated using Gibson Assembly (NEB). N-Deletion constructs were generated through amplification of regions of interest by PCR from constructs of wild-type PKC α and PKC β II subsequent subcloning into pcDNA3. Constructs with an N-terminal mCherry tag were cloned into pcDNA3 containing mCherry between the BamHI and XbaI sites, and constructs with an N-terminal YFP tag were cloned into pcDNA3 containing YFP between the XhoI and XbaI sites. Human PKC pseudosubstrate-deleted (Δ PS) and scrambled pseudosubstrate constructs were generated by QuikChange mutagenesis as previously described (118). Plasma membrane-targeted CFP was previously described, with the N-

terminal 7 residues of Lyn kinase attached to the 5' end of monomeric CFP (128). Golgi-targeted CFP was also previously described, with the N-terminal 33 residues of endothelial nitric-oxide synthase fused in frame to the 5' end of CFP (6).

Antibodies and reagents

The antibodies used in this study are as listed: DsRed (632496, Clontech), phospho-specific PKC turn motif (PKC α/β pT638/641, 9375S, Cell Signaling), phospho-specific PKC hydrophobic motif (PKC β pS660, 9371S, Cell Signaling), HA (clone 16B12, 901515, Biologend), β -actin (A2228, Sigma-Aldrich), Myc tag (9B11, 2276S, Cell Signaling), Akt (9272S, Cell Signaling), phospho-specific Akt activation loop (Thr308, 4056S, Cell Signaling), phospho-specific Akt turn motif (Thr450, 9267S, Cell Signaling), phospho-specific Akt hydrophobic motif (Ser473, 9721L, Cell Signaling), Hsp90 (610419, Cell Signaling), α -tubulin (T6074, Sigma-Aldrich), GST (sc-138, Santa Cruz), His (H1029, Sigma-Aldrich), PHLPP1 (22789-1-AP, Proteintech), and PKC α (610108, BD Transductions). The phospho-specific PKC activation loop antibody has been previously described (Dutil 1998). The pharmacological reagents used in this study are as listed: UTP (6701, Calbiochem), PDBu (524390, Calbiochem), Gö6983 (80051-928, Calbiochem), and thapsigargin (586005, Calbiochem). The lipids used in the *in vitro* kinase assays included diacylglycerol (800811C, Avanti Polar Lipids) and phosphatidylserine (840034C, Avanti Polar Lipids).

Mammalian cell culture and transfection

Mammalian cells were maintained in Dulbecco's modified Eagle's medium (DMEM, 10-

013-CV, Corning) containing 10% fetal bovine serum (S11150, Atlanta Biologicals) and 1% penicillin/streptomycin (15140-122, Gibco) at 37°C in 5% CO₂ (v/v). Cells were tested for Mycoplasma contamination and showed no contamination. Transient transfection was carried out using the Lipofectamine3000 transfection reagent (L3000-075, Thermo Fisher Scientific). Parental and CRISPR-edited DLD1 cells were previously described (Corina).

FRET imaging and analysis

Cells were imaged as described previously (6). As indicated, COS7 cells were transfected with CKAR alone or co-expressed with mCherry-tagged PKC for activity experiments. For translocation studies, cells were co-transfected with either plasma-membrane targeted or Golgi-targeted mCFP and YFP-tagged PKC. Cells were rinsed once with and imaged in Hanks' balanced salt solution (Corning) containing 1 mM CaCl₂. Images were acquired on a Zeiss Axiovert microscope (Carl Zeiss Microimaging Inc.) using a MicroMax digital camera (Roper-Princeton Instruments) controlled by MetaFluor software (Universal Imaging Corp.). Baseline values were acquired for at least 2 min prior to reagent addition. For experiments measuring agonist-induced activity, data were normalized to FRET ratios after addition of inhibitor. For experiments measuring basal activity, data were normalized to FRET ratios at baseline. For plasma membrane translocation studies, data were normalized to FRET ratios at baseline. For Golgi translocation studies, data were normalized to YFP fluorescence at the Golgi at baseline. Normalized FRET ratios, or YFP fluorescence for the Golgi translocation studies, from at least three independent experiments were combined, and traces represent average of these ratios \pm SEM.

Cell lysis and immunoblotting

Mammalian cells were lysed in buffer containing 50 mM Tris (pH 7.4), 1% Triton X-100, 50 mM NaF, 10 mM Na₄P₂O₇, 100 mM NaCl, 5 mM EDTA, and 1% deoxycholic acid that was supplemented with 1 mM Na₃VO₄, 1 mM phenylmethyl-sulfonyl fluoride, 50 µg/ml leupeptin, 1 µM microcystin, 1 mM DTT, and 2 mM benzamidine. Whole cell lysates were used, unless otherwise stated, and were briefly sonicated and boiled in sample buffer containing 250 mM Tris HCl, 8% (w/v) SDS, 40% (v/v) glycerol, 80 µg/mL bromophenol blue, and 2.86 M β-mercaptoethanol for 5 min at 95°C. Insect cells were lysed directly in sample buffer, sonicated, and boiled for 5 min at 95°C. Lysates were analyzed by SDS-PAGE and immunoblotting via chemiluminescence on a FluorChem Q imaging system (ProteinSimple).

Insect cell culture and baculovirus generation

Human PKCβII, GGA2-PKCβII, and PKCβII ΔPS were subcloned into a pFastBac HT/B vector (Invitrogen) modified with a N-terminal GST tag. The PP2C phosphatase domain of PHLPP1 (residues 1154-1422) were subcloned into a pFastBac HT/B vector modified with an N-terminal His tag. Baculovirus was made using the Bac-to-Bac Baculovirus Expression System (Invitrogen). The pFastBac plasmids were transformed into DH10Bac cells, and the resulting bacmid DNA was transfected into Sf9 insect cells (11496015, Thermo Fisher Scientific) in Sf-900 II SFM media (10902-088, Gibco) via CellFECTIN (Thermo Fisher Scientific). The recombinant baculoviruses were harvested and amplified,

scaling up to 125 mL flasks to yield approximately 50 mL of baculovirus. In flasks, Sf9 insect cells were grown in shaking cultures at 27°C.

Purification of GST-tagged PKC protein

GST-tagged PKC β II and GGA2-PKC β II were batch-purified from baculovirus-infected Sf9 insect cells using glutathione sepharose beads. Sf9 insect cells were infected with baculovirus for either protein and incubated for 3 days in shaking cultures at 27°C. Infected cells were then pelleted, rinsed in PBS, and lysed in buffer containing 50 mM HEPES (pH 7.5), 1 mM EDTA, 100 mM NaCl, 0.1% Triton X-100, 0.1 mg/mL BSA, 100 μ M PMSF, 1 mM DTT, 2 mM benzamidine, 50 μ g/mL leupeptin, and 1 μ M microcystin. The soluble lysate was then incubated with the glutathione beads for 2.5 h at 4°C. The beads were washed three times in buffer containing 50 mM HEPES (pH 7.5), 1 mM EDTA, 100 mM NaCl, 0.1 mg/mL BSA, and 1 mM DTT. Protein was eluted in wash buffer supplemented with 10 mM glutathione. The eluted protein was concentrated using 50 kDa Amicon centrifugal filter units (EMD Millipore), exchanged into buffer containing 20 mM HEPES (pH 7.5), 1 mM EDTA, 1 mM EGTA, and 1 mM DTT. An equal volume of glycerol was added, and the protein stock was stored at -20°C. Protein was quantified utilizing BSA standards run alongside the purified protein on an SDS-PAGE gel stained with Coomassie Brilliant Blue.

In vitro kinase assay

The activity of purified PKC β II towards the PKC-selective peptide substrate Ac-FKKSFKL-NH₂ was previously described (keranan). Standard conditions for the assay

included Ca^{2+} (200 μM free Ca^{2+} with 500 μM EGTA), 100 μM ATP, 100 μM peptide substrate, 5 mM MgCl_2 , 200 μM CaCl_2 , 0.06 mg/mL BSA, and Triton X-100 (0.1% w/v) mixed micelles containing 15 mol % PS and 5 mol % DG in 50 mM HEPES (pH 7.5), 1 mM DTT, as previously described (JC PNAS). For reactions containing PKC β II or GGA2-PKC β II alone, 20 ng of protein was used per reaction. For reactions containing both PKC β II and GGA2-PKC β II, 10 ng of each protein was used for a total of 20 ng per reaction.

Co-infection of PKC and PHLPP1 PP2C baculoviruses

Sf9 cells were seeded in 6-well plates (1×10^6 cells/well) and infected with baculovirus for His-PHLPP1 PP2C alone or co-infected with baculovirus for GST-tagged wild-type PKC β II or PKC β II Δ PS. Following 2 days of incubation at 27°C, Sf9 cells were lysed directly in 1x Laemmli sample buffer, sonicated, and boiled at 95°C for 5 min.

Co-Immunoprecipitation

HEK 293T cells were co-transfected with HA-tagged PKC and Myc-tagged PDK1 or mTOR via Lipofectamine3000. Following 24 h incubation, cells were washed once in PBS and lysed in buffer containing 50 mM Tris (pH 7.4), 1% Triton X-100, 50 mM NaF, 10 mM $\text{Na}_4\text{P}_2\text{O}_7$, 100 mM NaCl, 5 mM EDTA, and 1% deoxycholic acid supplemented with 1 mM Na_3VO_4 , 1 mM phenylmethyl-sulfonyl fluoride, 50 $\mu\text{g}/\text{ml}$ leupeptin, 1 μM microcystin, 1 mM DTT, and 2 mM benzamide. Detergent-solubilized lysates were incubated with an anti-Myc antibody overnight at 4°C. Lysates were then incubated with protein A/G PLUS-Agarose beads (sc-2003, Santa Cruz) for 1 h at 4°C and washed in the previously

mentioned lysis buffer (unsupplemented) three times. Bound proteins were eluted in sample buffer and boiled for 5 min at 95°C. Samples were separated by SDS-PAGE and analyzed by immunoblotting.

3.6 Acknowledgments

This work was supported by NIH R35 GM122523 and NIH GM43154 (A.C.N.). A.-A.N.V. was supported in part by the University of California, San Diego Graduate Training Program in Cellular and Molecular Pharmacology (T32 GM007752).

Chapter 3, in part, contains material that appears in the publication “Protein kinase C quality control by phosphatase PHLPP1 unveils loss-of-function mechanism in cancer,” as published by Timothy R. Baffi, An-Angela N. Van, Wei Zhao, Gordon B. Mills, and Alexandra C. Newton in *Molecular Cell* 2019 Apr 18, 74(2):378-392. The dissertation author was a co-author of the publication and the primary investigator and author of the material included in this chapter of the dissertation (Figure 3.5A, B, C, D, E, F, J, and K). The remainder of Chapter 3 is unpublished material for which the dissertation author is the primary investigator and author of the work.

3.7 Figures

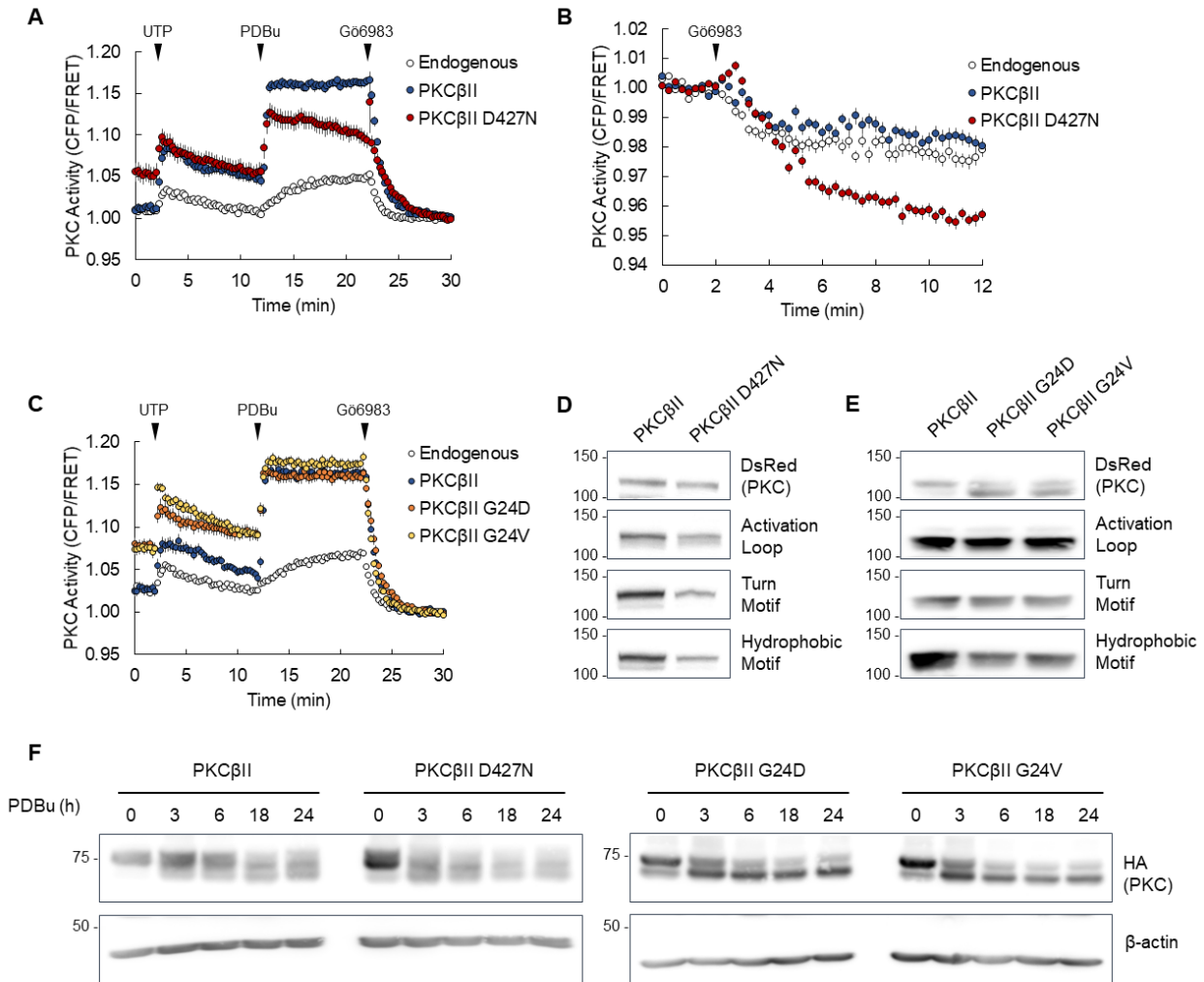


Figure 3.1: ATLL mutants are activating, phosphorylated, and sensitive to dephosphorylation. (A) Analysis of agonist-induced PKC activity in COS7 cells transfected with CKAR alone (Endogenous) or co-transfected with the indicated mCherry-tagged PKC construct. Cells treated with agonists UTP (100 μ M), PDBu (200 nM), and inhibitor Gö6983 (1 μ M). Graphs depict normalized FRET ratio changes (mean \pm SEM) from three independent experiments. (B) Analysis of basal PKC activity in COS7 cells transfected with CKAR alone (Endogenous) or co-transfected with the indicated mCherry-tagged PKC construct. Cells treated with inhibitor Gö6983 (1 μ M). Graphs depict normalized FRET ratio changes (mean \pm SEM) from three independent experiments. (D) and (E) Immunoblot analysis of lysates from COS7 cells transfected with mCherry-tagged wild-type PKC β II and PKC β II D427N (D) or wild-type PKC β II, PKC β II G24D, and PKC β II G24V (E). Blots probed with the indicated DsRed antibody for total PKC or phospho-specific antibodies for the activation loop, turn motif, and hydrophobic motif sites. Data is representative from three independent experiments. (F) Immunoblot analysis of lysates from COS7 cells transfected with the indicated HA-tagged constructs and treated with PDBu (200 nM) for the indicated times. Blots probed with HA antibody for total PKC.

Figure 3.2: Cancer-associated PKC fusions maintain an open conformation that attracts potential chaperones and can be inhibited *in trans* by the pseudosubstrate.

(A) Coomassie blue-stained SDS-PAGE gel of samples taken throughout purification of GST-tagged GGA2-PKC β II fusion protein from Sf9 insect cells. Band corresponding to the GGA2-PKC β II fusion is indicated by the asterisk (*). Unidentified proteins co-purified with the fusion protein are indicated by the blue arrows. The 66 kDa band corresponds to BSA. (B) Activity of wild-type PKC β II, GGA2-PKC β II, or an even mixture of the two proteins in the indicated conditions from an *in vitro* kinase assay. Data represent the average \pm SEM of two independent experiments with triplicate samples. (C), (D), and (E) Analysis of basal PKC activity in COS7 cells transfected with CKAR alone (Endogenous) or co-transfected with mCherry-tagged wild-type PKC β II, GGA2-PKC β II (C), GGA2-PKC β II N-Deletion (D), or PKC β II Δ PS (E), with vector control or GST-tagged PKC β II pseudosubstrate. Endogenous activity and activity of wild-type PKC β II from (C) is reproduced in (D) and (E) for comparison. Cells treated with inhibitor Gö6983 (1 μ M). Graphs depict normalized FRET ratio changes (mean \pm SEM) from three independent experiments.

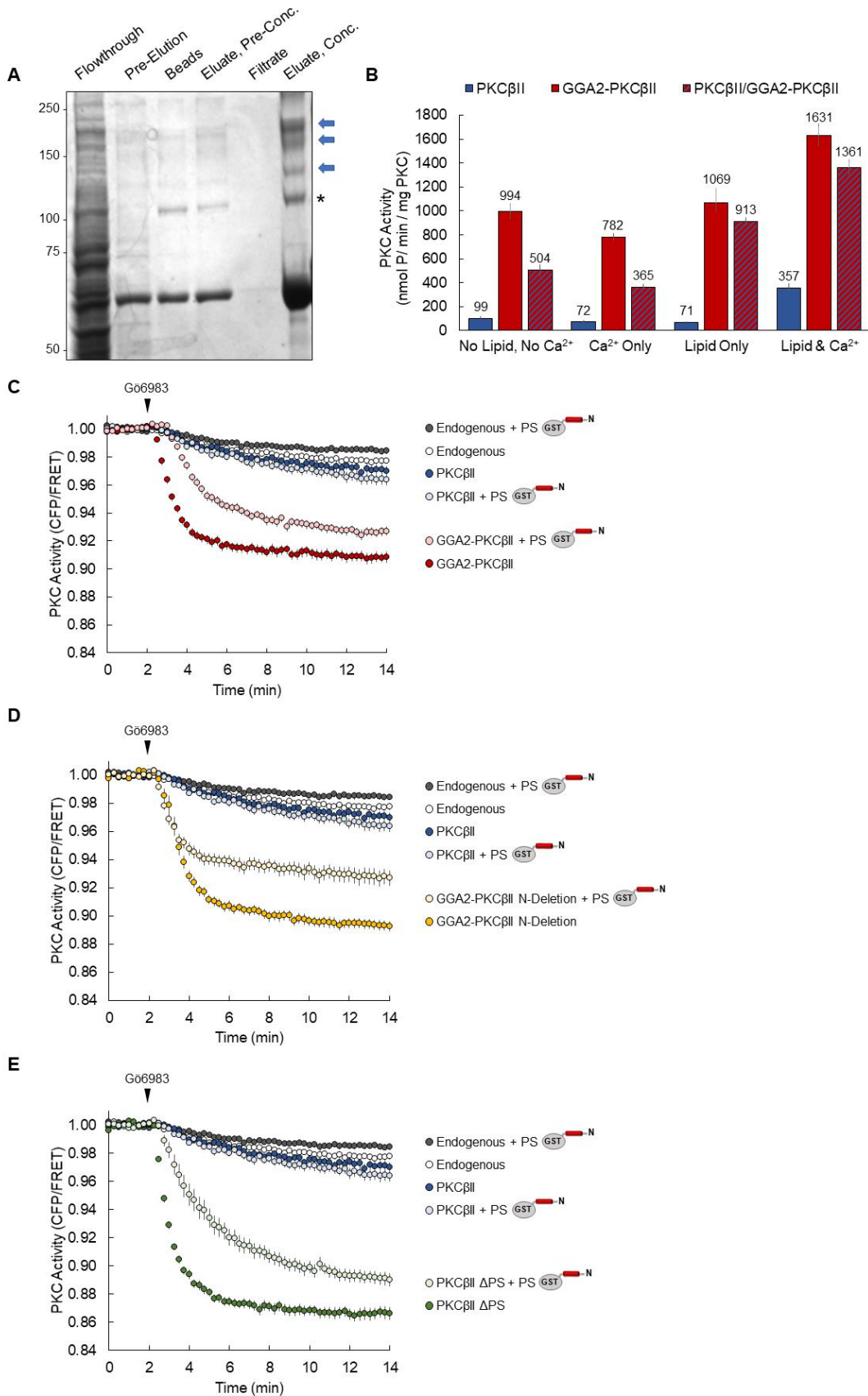


Figure 3.3: Inactivating mutants of PKC act in a dominant-negative manner by sequestering common titratable components. (A) Immunoblot analysis of detergent-solubilized lysates from HEK 293T cells transfected with Myc-tagged PDK1 alone or co-transfected with the indicated HA-tagged PKC construct and immunoprecipitated using the Myc tag antibody. Blots were probed for co-immunoprecipitation of PKC with the HA antibody. Data is representative from three independent experiments. (B) Quantification of PDK1-PKC co-immunoprecipitation from (A). HA-PKC IP was divided by Myc-PDK1 IP and normalized to HA-PKC β II. Graph represents the average \pm SEM of three independent experiments. * $p < 0.05$ (Student's t-test). (C) Immunoblot analysis of detergent-solubilized lysates from HEK 293T cells transfected with Myc-tagged mTOR alone or co-transfected with the indicated HA-tagged PKC construct and immunoprecipitated using the Myc tag antibody. Blots were probed for co-immunoprecipitation of PKC with the HA antibody. Data is representative from three independent experiments. (D) Immunoblot analysis of lysates from DLD1 parental or CRISPR-edited cells. Blots probed with antibody against Akt or phospho-specific antibodies for the activation loop (p308), turn motif (p450), or hydrophobic motif (p473) sites. Data is representative from twelve independent experiments. (E) Quantification of (D). Values for Akt were normalized to the loading control and then to the parental line (A509T/WT). Values for the phosphorylation sites were normalized to the the loading control, to total Akt, and then to the parental line (A509T/WT). Graph represents the average \pm SEM of three independent experiments. * $p < 0.05$ (Student's t-test). (F) Immunoblot analysis of lysates from DLD1 parental or CRISPR-edited cells that were serum starved for 4 h and treated with vehicle or EGF (50 ng/mL) for 30 min. Blots probed with antibody against Akt or phospho-specific antibodies for the activation loop (p308), turn motif (p450), or hydrophobic motif (p473) sites.

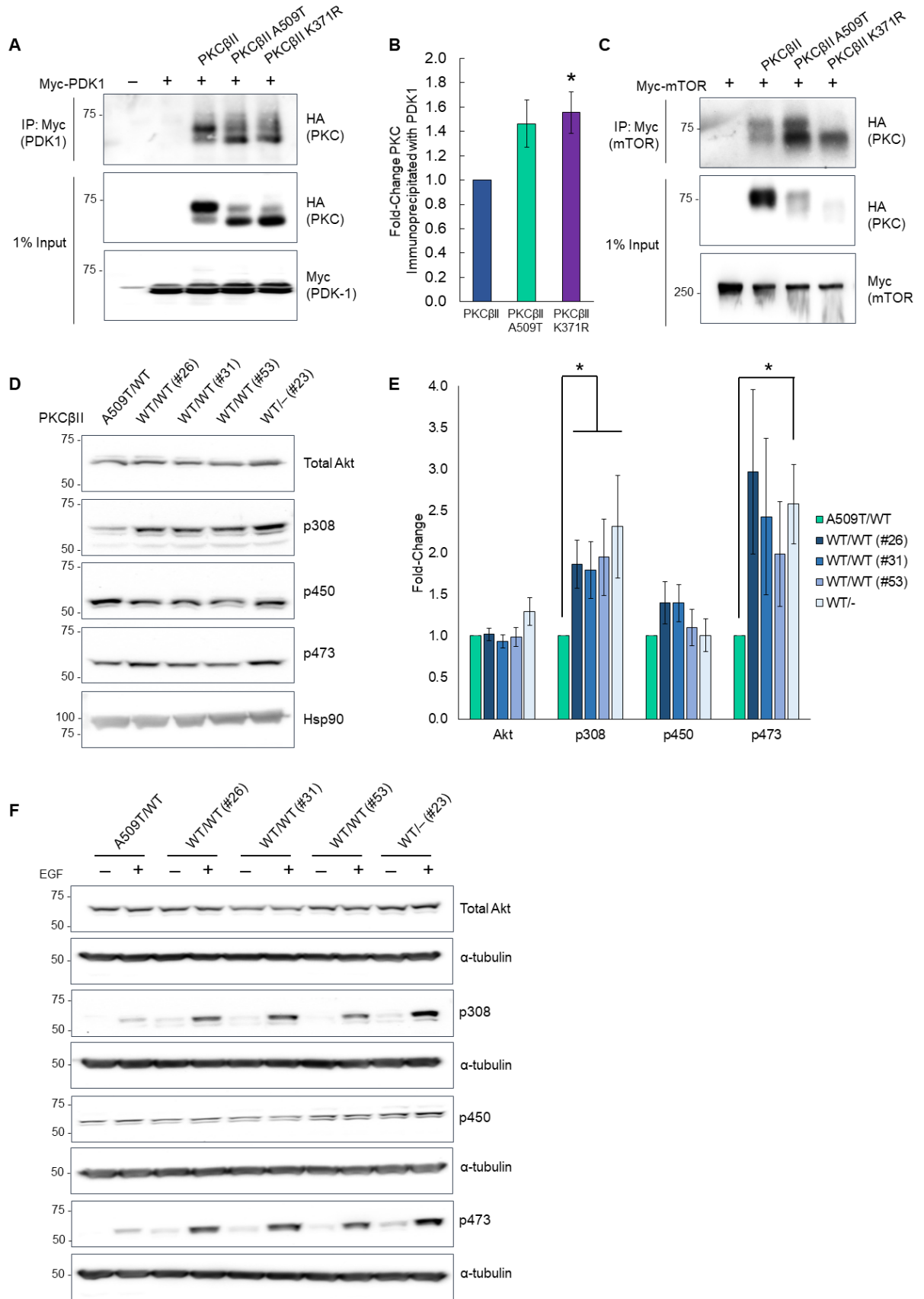


Figure 3.4: Cancer-associated PKC fusions are mislocalized upon stimulation. (A) and (B) Analysis of plasma membrane translocation in COS7 cells co-transfected with myristoylated-palmitoylated mCFP and YFP-tagged PKC α , TANC2-PKC α , or TANC2-PKC α N-Deletion (A) or mCFP and YFP-tagged PKC β II, GGA2-PKC β II, GGA2-PKC β II N-Deletion, and PKC β II Δ PS (B). Cells were treated with thapsigargin (5 μ M) and PDBu (200 nM). Graphs depict normalized FRET ratio changes (mean \pm SEM) from three independent experiments. (C) Images of cells from (A) depicting YFP fluorescence at baseline, post-thapsigargin treatment, and post-PDBu treatment. (D) Images of cells from (B) depicting YFP signal at baseline, post-thapsigargin treatment, and post-PDBu treatment. (E) and (F) Analysis of Golgi translocation in COS7 cells co-transfected with Golgi-targeted mCFP and YFP-tagged PKC α , TANC2-PKC α , TANC2-PKC α N-Deletion, or PKC α Δ PS (E) or mCFP and YFP-tagged PKC β II, GGA2-PKC β II, GGA2-PKC β II N-Deletion, and PKC β II Δ PS (F). Cells were treated with thapsigargin (5 μ M) and PDBu (200 nM). Graphs depict normalized YFP fluorescence at the Golgi (mean \pm SEM) from three independent experiments. Golgi region was demarcated by Golgi-targeted mCFP.

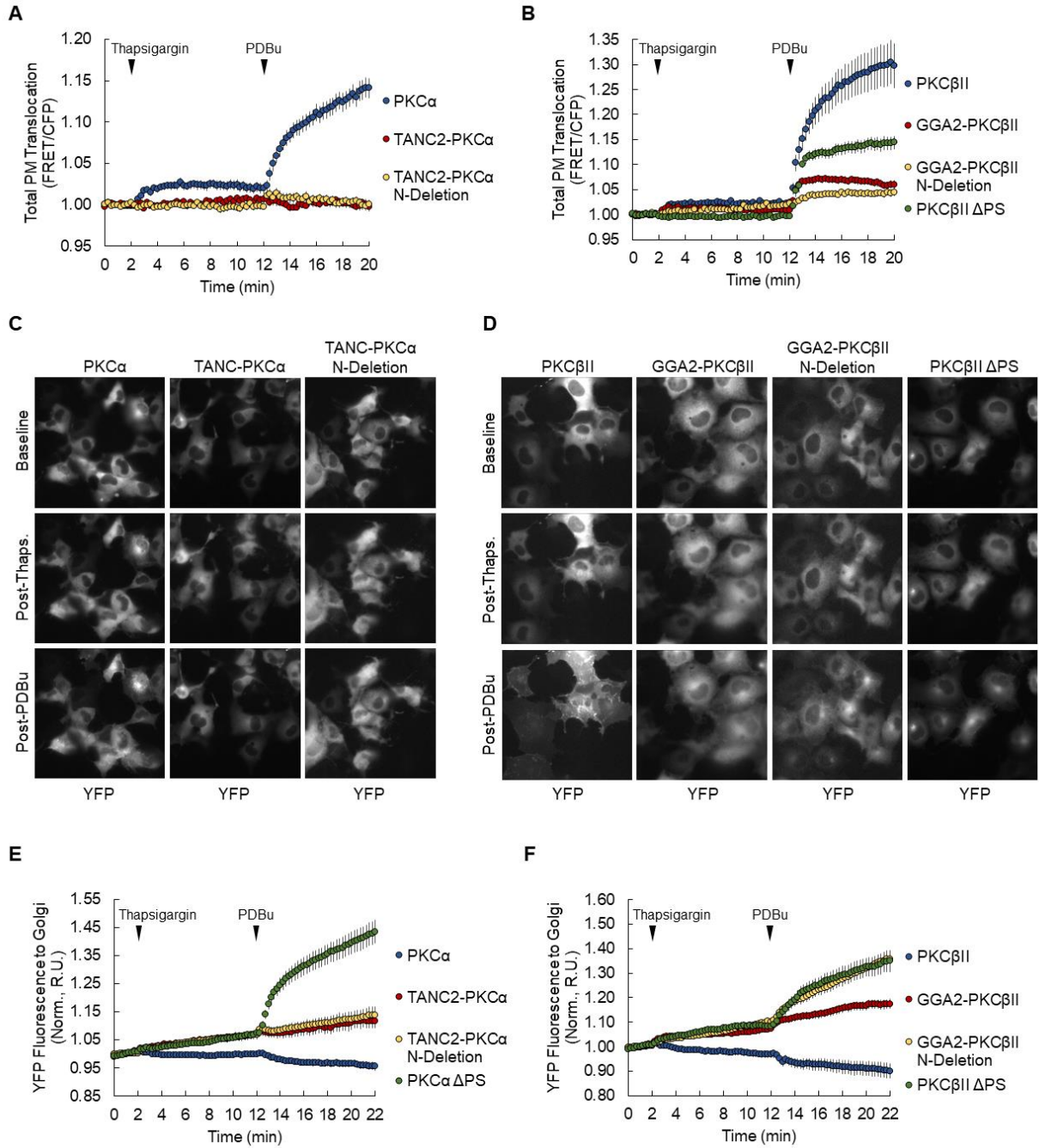
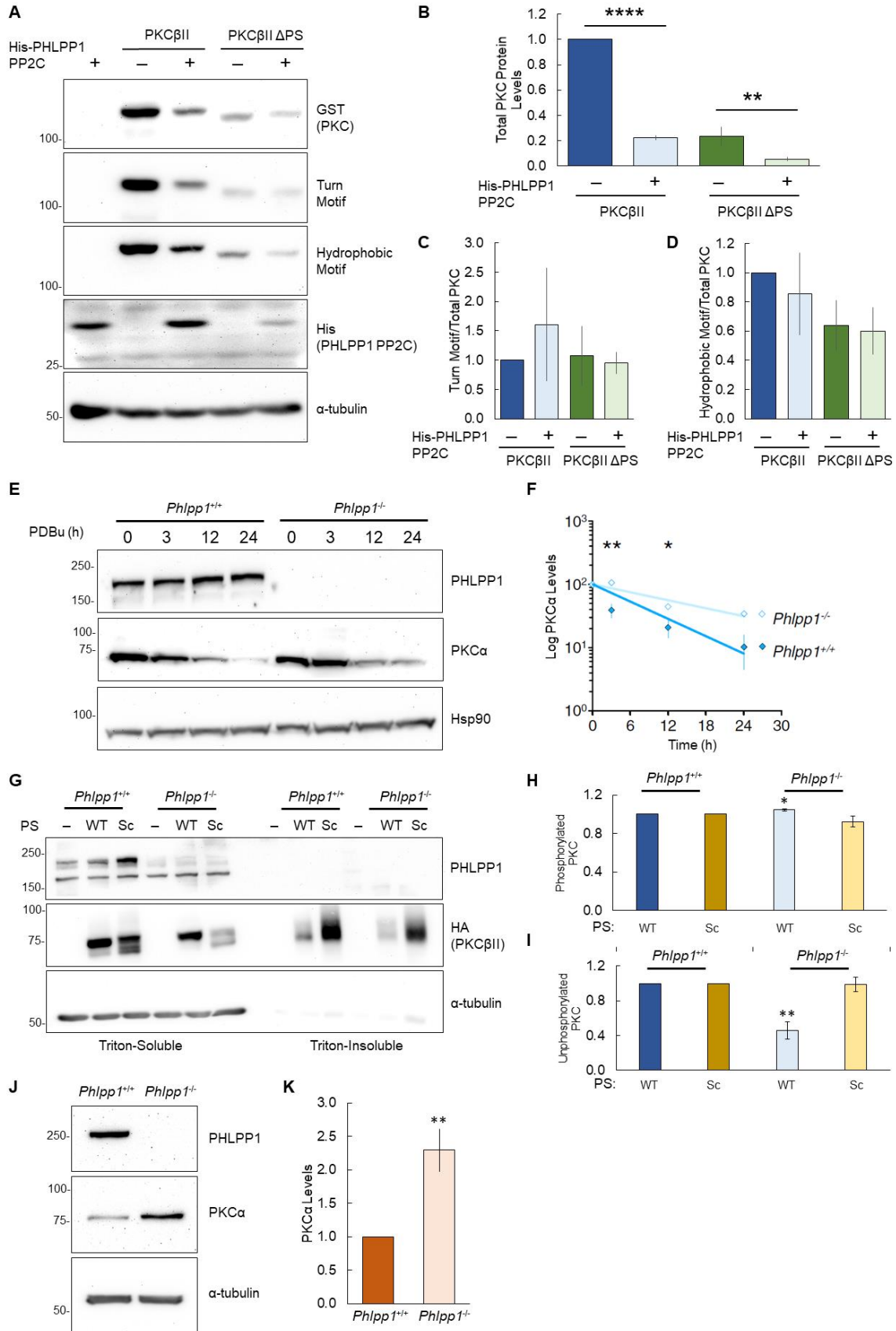


Figure 3.5: PHLPP negatively regulates steady-state levels of PKC. (A) Immunoblot analysis of lysates from Sf9 insect cells infected with baculovirus for the indicated GST-PKC constructs and His-tagged PHLPP1 PP2C (residues 1154-1422). Blots were probed with the indicated tag antibodies or phospho-specific antibodies. Data is representative from three independent experiments. (B), (C), and (D) Quantification of total PKC protein (B), turn motif phosphorylation (C), and hydrophobic motif phosphorylation (D) from (A). Total PKC protein was quantified by normalizing GST signal to the loading control and then to PKC β II alone. Phosphorylation was quantified by normalizing to the loading control, to total PKC, and then to PKC β II alone. Graphs represent the average \pm SEM of three independent experiments. **** $p < 0.0001$, *** $p < 0.001$ (Student's t-test). (E) Immunoblot analysis of lysates from *Phlpp1*^{+/+} or *Phlpp1*^{-/-} MEFs treated with PDBu (200 nM) for the indicated time points. Blots were probed with the indicated antibodies. Data is representative from three independent experiments. (F) Quantification of PKC α levels from (E), normalized to loading control and plotted as percentage of protein at time zero. Graph represents the average \pm SEM of three independent experiments. * $p < 0.05$, ** $p < 0.01$ (repeated-measures one-way ANOVA). (G) Immunoblot analysis of lysates from *Phlpp1*^{+/+} or *Phlpp1*^{-/-} MEFs transfected with HA-tagged PKC β II (WT) or scrambled pseudosubstrate mutant (Sc). Triton-insoluble lysates were run in equal proportion to triton-soluble lysates. Blots were probed with the indicated antibodies. Data is representative from three independent experiments. (H) and (I) Quantification of phosphorylated and unphosphorylated PKC from (G). Phosphorylated PKC was quantified by normalizing the upper band of PKC to total protein (H) whereas unphosphorylated PKC was normalized to the lower band (I). Graphs represent the average \pm SEM of three independent experiments. * $p < 0.05$, ** $p < 0.01$ (Student's t-test). (J) Immunoblot analysis of triton-soluble lysates from *Phlpp1*^{+/+} or *Phlpp1*^{-/-} MEFs. Blots were probed with the indicated antibodies. Data is representative from three independent experiments. (K) Quantification of PKC α levels from (J), normalized to the loading control. Graph represents the average \pm SEM of three independent experiments. ** $p < 0.01$ (Student's t-test).



Chapter 4

Conclusions

4.1 Conclusions

The paradigm for PKC as an oncogene was established following its identification as the receptor for tumor-promoting phorbol esters in the mid-1950s (13, 15, 100). Since PKC has been historically regarded as an oncogene, the majority of studies seeking to elucidate the role of PKC in various cancers have done so under the tenet that activation of PKC promotes tumorigenesis. However, the very cause underlying the dogma for PKC as an oncogene suggests that it is a tumor suppressor. Although phorbol esters indeed activate PKC, they also lock it in a conformation that is sensitive to dephosphorylation and consequently, degradation (95, 96). Treatment with phorbol esters thus results in PKC downregulation, and it is the long-term loss of PKC that contributes to tumor growth rather than its acute activation. In fact, treatment with phorbol esters was a commonly used technique to deplete the cell of PKC. Aside from phorbol ester-mediated downregulation of PKC, an analysis of PKC point mutations in cancer provided evidence contrary to an oncogenic role for PKC (11). Not only were the majority of the mutations inactivating but correction of one such mutation to wild-type inhibited anchorage-independent growth *in vitro* as well as tumor growth *in vivo*, thus establishing a bona fide role for at least one isozyme of PKC (PKC β II) as a tumor suppressor. While the bulk of the literature on PKC in cancer consider it to be an oncogene, PKC's tumor suppressive function may explain conflicting evidence wherein findings do not correspond with an oncogenic role. Still, further studies are required to dissect the extent of PKC's role as a tumor suppressor.

The work within this dissertation revealed diverse mechanisms by which PKC biology is altered in the context of cancer, specifically with regards to how PKC function

may be lost in cancer. In Chapter 2, PKC gene fusions identified in various cancers were characterized. Ultimately, these gene fusions were found to be loss-of-function rather than gain-of-function. In Chapter 3, regulation and, conversely, dysregulation of PKC was investigated through characterization of different PKC mutants in comparison to wild-type PKC. Varying aspects of PKC regulation were assessed to determine their impact on PKC function. The findings from these studies not only illustrate the specific functional consequence of a particular PKC mutation but increase understanding of the general mechanisms employed by cancer cells to lose PKC function and gain a survival advantage.

The work in Chapter 2 serves to characterize cancer-associated PKC gene fusions, identified in tumors through advances in RNA sequencing technology. While many cancer-associated point mutations have been characterized, these newly-identified fusions have been largely unstudied. Being the most frequently fused member of the AGC kinase superfamily, over 60 different PKC fusions were identified (114). These gene fusions occur in different isozymes of PKC and in a multitude of different cancers. The gene fusions are separated into two different types: 3' PKC fusions, whose resulting proteins retain the catalytic domain of PKC, and 5' PKC fusions, whose proteins retain the regulatory domain of PKC.

Three different catalytic domain fusions were selected for biochemical characterization, encoding the TANC2-PKC α , CTL1-PKC α , and GGA2-PKC β II proteins (115, 120). These fusion proteins were found to be unphosphorylated yet constitutively active, independent of agonist. PKC deleted in its pseudosubstrate mirrored the phenotype of the fusion proteins, suggesting that loss of pseudosubstrate can be

attributed to these effects on phosphorylation and activity. Without the pseudosubstrate, the fusion proteins adopt an open conformation, unable to autoinhibit as wild-type PKC. While this conformation permits activity in the absence of second messengers, it also renders it sensitive to degradation. Cycloheximide studies showed that the fusion proteins and pseudosubstrate-deleted mutants degraded at a much faster rate compared to their wild-type counterparts. Moreover, the TANC2-PKC α fusion protein was more appreciably ubiquitinated compared to wild-type PKC α . These findings suggest that catalytic domain fusions may not be able to accumulate in cells due to their marked instability. Utilizing CRISPR/Cas9-mediated gene editing to expression the *TANC2-PRKCA* gene fusion, this was proven true (129, 130). While the fusion was detected at the mRNA level, it was not detected at the protein level. Furthermore, expression of the *TANC2-PRKCA* fusion resulted in a decrease in basal cleaved caspase-3 levels, indicating decreased apoptosis. This was also observed in cells where PKC α was knocked out via gene editing. Thus, expression of the fusion essentially presents as a heterozygous knockout of PKC α , and one effect of this PKC loss is decreased apoptosis, lending a survival advantage to cancer cells.

In addition to catalytic domain fusions, the data in Chapter 2 also includes characterization of a regulatory domain fusion, PKC α -CDH8. Retaining the entire regulatory moiety, the PKC α -CDH8 fusion is able to engage with PKC's second messengers without resulting in catalysis. Consequently, the regulatory domain fusion suppressed the activity of wild-type PKC. Moreover, a major site of this fusion-mediated suppression was the Golgi. By competing with wild-type PKC for common titratable components, the regulatory fusion exerts a dominant-negative effect. Taken together,

both catalytic domain fusions and regulatory domain fusions are loss-of-function, supporting a tumor suppressive role for PKC.

Chapter 3 focuses on additional mechanisms in which PKC function may be perturbed in cancer. First, PKC β mutations in adult T-cell leukemia/lymphoma (ATLL) were biochemically characterized (143). These mutants showed similarities and important differences with PKC catalytic domain fusions. While both the catalytic domain fusions and ATLL mutants exhibited agonist-independent activity, the ATLL mutants retained their processing phosphorylations. However, the conformation that allowed retention of phosphates at the priming sites did not protect the enzymes from PDBu-induced downregulation. The mutants were more sensitive to dephosphorylation and degradation compared to wild-type protein, establishing the mutants as loss-of-function.

Next, the GGA2-PKC β II fusion protein appeared to be purified in complex with other proteins, both from mammalian cells and insect cells, so the effect of these unidentified proteins was examined in an *in vitro* kinase assay. A synergistic effect was observed when wild-type protein was mixed with the fusion protein, with greater apparent activity than expected from the sum of the activity of the two individual proteins. These unidentified proteins may therefore function to stabilize PKC.

Additionally, the dominant-negative effect of inactivating mutants of PKC was assessed, resulting in the identification of PDK1 and mTOR as two limiting components that may be sequestered such mutants. To look at the effect of the PKC β II A509T mutant endogenously, DLD1 cells harboring the mutation and CRISPR-edited cells in which the mutation was corrected were used (11). Dependent on PDK1 and mTOR for activity, Akt was examined as a target for the PKC mutant's dominant-negative effects. Indeed,

presence of the mutant suppressed phosphorylation of Akt, corroborating the ability of the PKC to compete with other substrates.

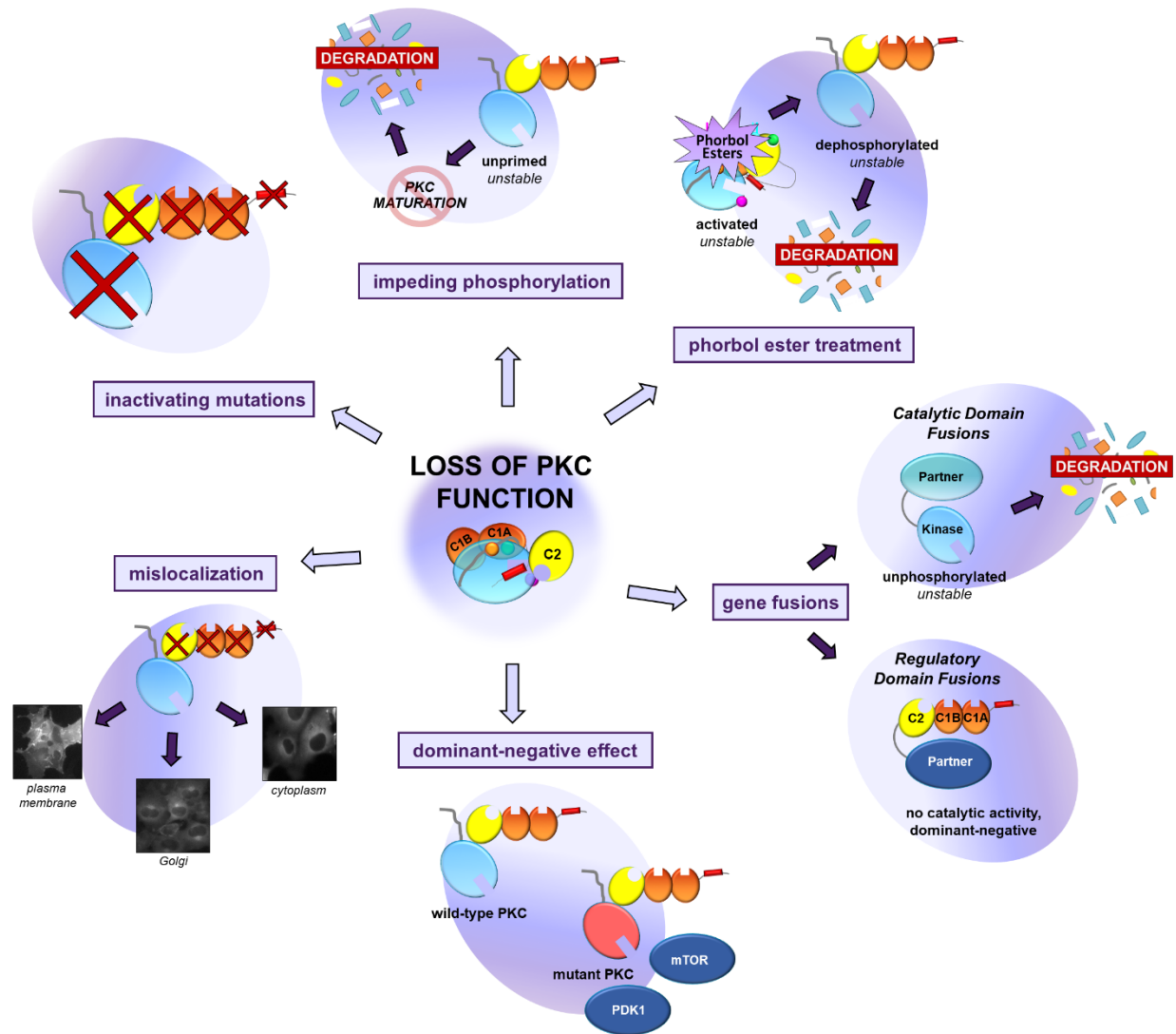
Chapter 3 also assessed the impact of loss of different components of the regulatory domain on agonist-induced translocation. Loss of the pseudosubstrate and the C1 domains altered translocation of PKC following stimulation. Compared to wild-type PKC that translocates to the plasma membrane, the TANC2-PKC α and N-Deletion proteins did not move from the cytosol. The GGA2-PKC β II and N-Deletion proteins translocated weakly to the plasma membrane and substantially more to the Golgi. The pseudosubstrate-deleted proteins translocated moderately to the plasma membrane and strongly to the Golgi. Mislocalization of PKC upon agonist stimulation could result in decreased phosphorylation of intended substrates and aberrant phosphorylation of others.

Lastly, Chapter 3 probed PHLPP-mediated regulation of PKC. Expression of the PHLPP1 PP2C domain in Sf9 cells caused dephosphorylation and degradation of wild-type PKC β II as well as PKC β II Δ PS. In *Phlpp1*^{-/-} MEFs, PKC α was more resistant to PDBu-induced downregulation. In addition, there is a greater proportion of phosphorylated:unphosphorylated species for wild-type PKC β II expressed in *Phlpp1*^{-/-} MEFs as opposed to *Phlpp1*^{+/+} MEFs. Finally, in the absence of PHLPP1, there was a 2-fold increase in steady-state levels of PKC α . PHLPP1 thus plays an important role in negatively regulating PKC by regulating its stability through dephosphorylation of its hydrophobic motif (118). Together, Chapter 3 highlights many more ways that PKC regulation is targeted in cancer to lose the function of this tumor suppressor.

The findings presented in this dissertation serve to elucidate some of the many avenues for suppression of PKC function in cancer, highlighting general themes in the approaches of cancer cells to remove this cellular brake to oncogenesis. While these data certainly add to the current knowledge of PKC's role as a tumor suppressor, they also invite more questions. These studies focused on conventional isozymes of PKC, so investigation of novel and atypical isozymes in cancer are necessary. Evidence in favor of an oncogenic or tumor suppressive role exists for all PKC isozymes, so consideration of cancer type and cell type is also essential (17). In addition to assessing whether mutations in other isozymes of PKC are inactivating, further studies are also required to determine the precise mechanisms by which PKC exerts its tumor suppressive properties. Different PKC isozymes have been associated with different roles in various biological processes, including proliferation, apoptosis, and migration (7, 15, 16). To add further complexity, contradicting roles for the same PKC isozyme for these processes are also evidenced in the literature. Nevertheless, while much is still to be learned, it is clear that appreciation of PKC's complexity and investigation of the kinase in defined physiological contexts are crucial to effectively understand what role PKC may play in a given cancer and consequently, how to target it therapeutically without potentially worsening patient outcome.

4.2 Figures

Figure 4.1: Mechanisms of PKC dysregulation in cancer. In this dissertation, we illustrate the multitude of ways by which PKC function is lost in cancer. Mutations in any of the functional domains of PKC can cause inactivation of the kinase by impairing catalysis, phosphorylation, or second messenger binding. Impeding PKC processing by phosphorylation renders it sensitive to degradation. Phorbol ester treatment locks PKC in an open conformation that is accessible to phosphatases, and the resulting dephosphorylated species is also sensitive to degradation. Gene fusions cause loss of PKC function in two ways. Catalytic domain fusions are unable to autoinhibit and adopt an open conformation that is sensitive to dephosphorylation and subsequent degradation. Regulatory domain fusions do not possess catalytic domains and may exert dominant-negative effects. These fusions and other inactivating mutants of PKC can act in a dominant-negative manner by sequestering common titratable components, such as PDK1 and mTOR. Finally, impairment of the PKC regulatory domains causes mislocalization of PKC, displacing it from its relevant subcellular compartment and relevant substrates.



References

1. Nakamura, S. I., and Yamamura, H. (2010) Yasutomi Nishizuka: Father of protein kinase C. *J. Biochem.* **148**, 125–130
2. Takai, Y., Kihimoto, A., Inoue, M., and Nishizuka, Y. (1977) Studies on a cyclic nucleotide-independent protein kinase and its proenzyme in mammalian tissues. I. Purification and characterization of an active enzyme from bovine cerebellum. *J. Biol. Chem.* **252**, 7603–7609
3. Takai, Y., Kishimoto, A., Kikkawa, U., Mori, T., and Nishizuka, Y. (1979) Unsaturated diacylglycerol as a possible messenger for the activation of calcium-activated, phospholipid-dependent protein kinase system. *Biochem. Biophys. Res. Commun.* **91**, 1218–1224
4. Kishimoto, A., Takai, Y., Mori, T., Kikkawa, U., and Nishizuka, Y. (1980) Activation of Calcium and Phospholipid-dependent Protein Kinase by Diacylglycerol, Its Possible Relation to Phosphatidylinositol Turnover. *J. Biol. Chem.* **255**, 2273–2276
5. Hokin, R.; Hokin, L. (1953) Enzyme secretion and into phospholipides. *J. Bio. Chem.* **203**, 967–977
6. Gallegos, L. L., Kunkel, M. T., and Newton, A. C. (2006) Targeting protein kinase C activity reporter to discrete intracellular regions reveals spatiotemporal differences in agonist-dependent signaling. *J. Biol. Chem.* **281**, 30947–30956
7. Dempsey, E. C., Newton, A. C., Mochly-rosen, D., Fields, A. P., Reyland, M. E., Insel, P. A., Messing, R. O., Edward, C., and Mochly-, D. (2000) EB2000 symposium report. *Cancer Cell*
8. Antal, C. E., and Newton, A. C. (2013) Spatiotemporal dynamics of phosphorylation in lipid second messenger signaling. *Mol. Cell. Proteomics.* **12**, 3498–3508
9. Newton, A. C. (2010) Protein kinase C: Poised to signal. *Am. J. Physiol. - Endocrinol. Metab.* 10.1152/ajpendo.00477.2009
10. Parker, P. J., and Murray-Rust, J. (2004) PKC at a glance. *J. Cell Sci.* **117**, 131–132
11. Antal, C. E., Hudson, A. M., Kang, E., Zanca, C., Wirth, C., Stephenson, N. L., Trotter, E. W., Gallegos, L. L., Miller, C. J., Furnari, F. B., Hunter, T., Brognard, J., and Newton, A. C. (2015) Cancer-associated protein kinase C mutations reveal kinase's role as tumor suppressor. *Cell.* **160**, 489–502
12. Antal, C. E., Violin, J. D., Kunkel, M. T., Skovsø, S., and Newton, A. C. (2014) Intramolecular conformational changes optimize protein kinase C signaling.

Chem. Biol. **21**, 459–469

13. Antal, C. E., and Newton, A. C. (2014) Tuning the signalling output of protein kinase C. *Biochem. Soc. Trans.* **42**, 1477–1483
14. Majumder, P. K., and Sellers, W. R. (2005) Akt-regulated pathways in prostate cancer. *Oncogene*. **24**, 7465–7474
15. Garg, R., Benedetti, L. G., Abera, M. B., Wang, H., Abba, M., and Kazanietz, M. G. (2014) Protein kinase C and cancer: What we know and what we do not. *Oncogene*. **33**, 5225–5237
16. Griner, E. M., and Kazanietz, M. G. (2007) Protein kinase C and other diacylglycerol effectors in cancer. *Nat. Rev. Cancer*. **7**, 281–294
17. Kang, J.-H. (2014) Protein Kinase C (PKC) Isozymes and Cancer. *New J. Sci.* **2014**, 1–36
18. Newton, A. C. (2001) Protein kinase C: Structural and spatial regulation by phosphorylation, cofactors, and macromolecular interactions. *Chem. Rev.* **101**, 2353–2364
19. Wu-Zhang, A. X., and Newton, A. C. (2013) Protein kinase C pharmacology: Refining the toolbox. *Biochem. J.* **452**, 195–209
20. Hansra, G., Garcia-Paramio, P., Prevostel, C., Whelan, R. D. H., Bornancin, F., and Parker, P. J. (1999) Multisite dephosphorylation and desensitization of conventional protein kinase C isoforms. *Biochem. J.* **342**, 337–344
21. Newton, A. C. (2010) Protein Kinase C in Cancer Signaling and Therapy. *Protein Kinase C Cancer Signal. Ther.* 10.1007/978-1-60761-543-9
22. Giorgione, J., Hysell, M., Harvey, D. F., and Newton, A. C. (2003) Contribution of the C1A and C1B domains to the membrane interaction of protein kinase C. *Biochemistry*. **42**, 11194–11202
23. Dries, D. R., Gallegos, L. L., and Newton, A. C. (2007) A single residue in the C1 domain sensitizes novel protein kinase C isoforms to cellular diacylglycerol production. *J. Biol. Chem.* **282**, 826–830
24. Stewart, M. D., and Igumenova, T. I. (2017) Toggling of Diacylglycerol Affinity Correlates with Conformational Plasticity in C1 Domains. *Biochemistry*. **56**, 2637–2640
25. Tobias, I. S., Kaulich, M., Kim, P. K., Simon, N., Jacinto, E., Dowdy, S. F., King, C. C., and Newton, A. C. (2016) Protein kinase C γ exhibits constitutive phosphorylation and phosphatidylinositol-3,4,5-triphosphate-independent regulation. *Biochem. J.* **473**, 509–523

26. House, C., and Kemp, B. E. (1990) PROTEIN KINASE C PSEUDOSUBSTRATE PROTOTYPE : S T R U C T U R E -. **2**, 187–190
27. Gould, C. M., Kannan, N., Taylor, S. S., and Newton, A. C. (2009) The chaperones Hsp90 and Cdc37 mediate the maturation and stabilization of protein kinase C through a conserved PXXP motif in the C-terminal tail. *J. Biol. Chem.* **284**, 4921–4935
28. Leonard, T. A., Róycki, B., Saidi, L. F., Hummer, G., and Hurley, J. H. (2011) Crystal structure and allosteric activation of protein kinase C β II. *Cell*. **144**, 55–66
29. Grodsky, N., Li, Y., Bouzida, D., Love, R., Jensen, J., Nodes, B., Nonomiya, J., and Grant, S. (2006) Structure of the catalytic domain of human protein kinase C β II complexed with a bisindolylmaleimide inhibitor. *Biochemistry*. **45**, 13970–13981
30. Messerschmidt, A., Macieira, S., Velarde, M., Bädeker, M., Benda, C., Jestel, A., Brandstetter, H., Neufeind, T., and Blaesche, M. (2005) Crystal structure of the catalytic domain of human atypical protein kinase C- ι reveals interaction mode of phosphorylation site in turn motif. *J. Mol. Biol.* **352**, 918–931
31. Xu, R. X., Pawelczyk, T., Xia, T. H., and Brown, S. C. (1997) NMR structure of a protein kinase C- γ phorbol-binding domain and study of protein-lipid micelle interactions. *Biochemistry*. **36**, 10709–10717
32. Zhang, G., Kazanietz, M. G., Blumberg, P. M., and Hurley, J. H. (1995) Crystal structure of the Cys2 activator-binding domain of protein kinase C δ in complex with phorbol ester. *Cell*. **81**, 917–924
33. Guerrero-Valero, M., Ferrer-Orta, C., Querol-Audí, J., Marin-Vicente, C., Fita, I., Gómez-Fernández, J. C., Verdaguer, N., and Corbalán-García, S. (2009) Structural and mechanistic insights into the association of PKC α -C2 domain to PtdIns(4,5)P 2. *Proc. Natl. Acad. Sci. U. S. A.* **106**, 6603–6607
34. Littler, D. R., Walker, J. R., She, Y. M., Finerty, P. J., Newman, E. M., and Dhe-Paganon, S. (2006) Structure of human protein kinase C η (PKC η) C2 domain and identification of phosphorylation sites. *Biochem. Biophys. Res. Commun.* **349**, 1182–1189
35. Ochoa, W. F., Garcia-Garcia, J., Fita, I., Corbalan-Garcia, S., Verdaguer, N., and Gomez-Fernandez, J. C. (2001) Structure of the C2 domain from novel protein kinase C ϵ . A membrane binding model for Ca²⁺-independent C2 domains. *J. Mol. Biol.* **311**, 837–849
36. Pappa, H., Murray-Rust, J., Dekker, L. V., Parker, P. J., and McDonald, N. Q. (1998) Crystal structure of the C2 domain from protein kinase C- δ . *Structure*. **6**, 885–894

37. Sutton, R. B., and Sprang, S. R. (1998) Structure of the protein kinase C β phospholipid-binding C2 domain complexed with Ca²⁺. *Structure*. **6**, 1395–1405
38. Verdaguer, N., Corbalan-garcia, S., Ochoa, W. F., Fita, I., and Go, J. C. (1999) Verdaguer-1999-Ca(2+) bridges the C2 membrane-. **18**, 6329–6338
39. Antal, C. E., Callender, J. A., Kornev, A. P., Taylor, S. S., and Newton, A. C. (2015) Intramolecular C2 Domain-Mediated Autoinhibition of Protein Kinase C β II. *Cell Rep*. **12**, 1252–1260
40. Sommese, R. F., Ritt, M., Swanson, C. J., and Sivaramakrishnan, S. (2017) The role of regulatory domains in maintaining autoinhibition in the multidomain kinase PKC α . *J. Biol. Chem*. **292**, 2873–2880
41. Yang, Y., Shu, C., Li, P., and Igumenova, T. I. (2018) Structural Basis of Protein Kinase C α Regulation by the C-Terminal Tail. *Biophys. J*. **114**, 1590–1603
42. Cheng, H. C., Qi, R. Z., Paudel, H., and Zhu, H. J. (2011) Regulation and function of protein kinases and phosphatases. *Enzyme Res*. **2011**, 7–10
43. Sonnenburg, E. D., Gao, T., and Newton, A. C. (2001) The Phosphoinositide-dependent Kinase, PDK-1, Phosphorylates Conventional Protein Kinase C Isozymes by a Mechanism That Is Independent of Phosphoinositide 3-Kinase. *J. Biol. Chem*. **276**, 45289–45297
44. Cenni, V., Döppler, H., Sonnenburg, E. D., Maraldi, N., Newton, A. C., and Toker, A. (2002) Regulation of novel protein kinase C ϵ by phosphorylation. *Biochem. J*. **363**, 537–545
45. Ikenoue, T., Inoki, K., Yang, Q., Zhou, X., and Guan, K. L. (2008) Essential function of TORC2 in PKC and Akt turn motif phosphorylation, maturation and signalling. *EMBO J*. **27**, 1919–1931
46. Behn-Krappa, A., and Newton, A. C. (1999) The hydrophobic phosphorylation motif of conventional protein kinase C is regulated by autophosphorylation. *Curr. Biol*. **9**, 728–737
47. Facchinetti, V., Ouyang, W., Wei, H., Soto, N., Lazorchak, A., Gould, C., Lowry, C., Newton, A. C., Mao, Y., Miao, R. Q., Sessa, W. C., Qin, J., Zhang, P., Su, B., and Jacinto, E. (2008) The mammalian target of rapamycin complex 2 controls folding and stability of Akt and protein kinase C. *EMBO J*. **27**, 1932–1943
48. Newton, A. C., and Johnson, J. E. (1998) Protein kinase C: A paradigm for regulation of protein function by two membrane-targeting modules. *Biochim. Biophys. Acta - Rev. Biomembr*. **1376**, 155–172
49. Tobias, I. S., and Newton, A. C. (2016) Protein scaffolds control localized protein kinase C ζ activity. *J. Biol. Chem*. **291**, 13809–13822

50. Tsai, L. C. L., Xie, L., Dore, K., Xie, L., Del Rio, J. C., King, C. C., Martinez-Ariza, G., Hulme, C., Malinow, R., Bourne, P. E., and Newton, A. C. (2015) Zeta inhibitory peptide disrupts electrostatic interactions that maintain atypical protein Kinase C in its active conformation on the scaffold p62. *J. Biol. Chem.* **290**, 21845–21856
51. Drummond, M. L., and Prehoda, K. E. (2016) Molecular control of atypical Protein Kinase C: tipping the balance between self-renewal and differentiation. *J. Mol. Biol.* **428**, 1455–1464
52. Kajimoto, T., Caliman, A. D., Tobias, I. S., Okada, T., Pilo, C. A., Van, A. A. N., Andrew McCammon, J., Nakamura, S. I., and Newton, A. C. (2019) Activation of atypical protein kinase C by sphingosine 1-phosphate revealed by an aPKC-specific activity reporter. *Sci. Signal.* 10.1126/scisignal.aat6662
53. Newton, A. C. (2003) Regulation of the ABC kinases by phosphorylation: Protein kinase C as a paradigm. *Biochem. J.* **370**, 361–371
54. Gao, T., Brognard, J., and Newton, A. C. (2008) The phosphatase PHLPP controls the cellular levels of protein kinase C. *J. Biol. Chem.* **283**, 6300–6311
55. Abrahamsen, H., O'Neill, A. K., Kannan, N., Kruse, N., Taylor, S. S., Jennings, P. A., and Newton, A. C. (2012) Peptidyl-prolyl isomerase Pin1 controls down-regulation of conventional protein kinase C isozymes. *J. Biol. Chem.* **287**, 13262–13278
56. Chen, D., Gould, C., Garza, R., Gao, T., Hampton, R. Y., and Newton, A. C. (2007) Amplitude control of protein kinase C by RINCK, a novel E3 ubiquitin ligase. *J. Biol. Chem.* **282**, 33776–33787
57. Santiskulvong, C., and Rozengurt, E. (2007) Protein kinase C α mediates feedback inhibition of EGF receptor transactivation induced by Gq-coupled receptor agonists. *Cell. Signal.* **19**, 1348–1357
58. Ouyang, X., Gulliford, T., and Epstein, R. J. (1998) The duration of phorbol-inducible ErbB2 tyrosine dephosphorylation parallels that of receptor endocytosis rather than threonine-686 phosphorylation: Implications for the physiological role of protein kinase C in growth factor receptor signalling. *Carcinogenesis.* **19**, 2013–2019
59. Marlene Hosey, M., Benovic, J. L., DebBurman, S. K., and Richardson, R. M. (1995) Multiple mechanisms involving protein phosphorylation are linked to desensitization of muscarinic receptors. *Life Sci.* **56**, 951–955
60. Namkung, Y., and Sibley, D. R. (2004) Protein kinase C mediates phosphorylation, desensitization, and trafficking of the D2 dopamine receptor. *J. Biol. Chem.* **279**, 49533–49541

61. Fujimoto, K., Ohta, K., Kangawa, K., Kikkawa, U., Ogino, S., and Fukui, H. (1999) Identification of protein kinase c phosphorylation sites involved in phorbol ester-induced desensitization of the histamine H1 receptor. *Mol. Pharmacol.* **55**, 735–742
62. Mayati, A., Moreau, A., Le Vée, M., Stieger, B., Denizot, C., Parmentier, Y., and Fardel, O. (2017) Protein kinases C-mediated regulations of drug transporter activity, localization and expression. *Int. J. Mol. Sci.* 10.3390/ijms18040764
63. Martelli, A. M., Evangelisti, C., Nyakern, M., and Manzoli, F. A. (2006) Nuclear protein kinase C. *Biochim. Biophys. Acta - Mol. Cell Biol. Lipids.* **1761**, 542–551
64. Abeyweera, T. P., Chen, X., and Rotenberg, S. A. (2009) Phosphorylation of α 6-tubulin by protein kinase C α activates motility of human breast cells. *J. Biol. Chem.* **284**, 17648–17656
65. Kang, J. H., Toita, R., Kim, C. W., and Katayama, Y. (2012) Protein kinase C (PKC) isozyme-specific substrates and their design. *Biotechnol. Adv.* **30**, 1662–1672
66. Ziegler, W. H., Tigges, U., Zieseniss, A., and Jockusch, B. M. (2002) A lipid-regulated docking site on vinculin for protein kinase C. *J. Biol. Chem.* **277**, 7396–7404
67. Farese, R. V, Sajan, M. P., Yang, H., Li, P., Mastorides, S., Jr, W. R. G., Nimal, S., Choi, C. S., Kim, S., Shulman, G. I., Kahn, C. R., Braun, U., and Leitges, M. (2007) PKC λ . **117**, 2289–2301
68. Bandyopadhyay, G., Sajan, M. P., Kanoh, Y., Standaert, M. L., Quon, M. J., Lea-Currie, R., Sen, A., and Farese, R. V. (2002) PKC- ζ mediates insulin effects on glucose transport in cultured preadipocyte-derived human adipocytes. *J. Clin. Endocrinol. Metab.* **87**, 716–723
69. Geraldès, P., and King, G. L. (2010) Emission security- Tempest Attacks. *Circ. Res.* **106**, 1319–1331
70. Noh, H., and King, G. L. (2007) The role of protein kinase C activation in diabetic nephropathy. *Kidney Int.* **72**, S49–S53
71. Li, L., Sawamura, T., and Renier, G. (2004) Glucose Enhances Human Macrophage LOX-1 Expression: Role for LOX-1 in Glucose-Induced Macrophage Foam Cell Formation. *Circ. Res.* **94**, 892–901
72. Osto, E., Kouroedov, A., Mocharla, P., Akhmedov, A., Besler, C., Rohrer, L., Von Eckardstein, A., Iliceto, S., Volpe, M., Lüscher, T. F., and Cosentino, F. (2008) Inhibition of protein kinase C β prevents foam cell formation by reducing scavenger receptor A expression in human macrophages. *Circulation.* **118**, 2174–2182

73. Ceolotto, G., Gallo, A., Miola, M., Sartori, M., Trevisan, R., Del Prato, S., Semplicini, A., and Avogaro, A. (2000) Protein kinase C activity is acutely regulated by plasma glucose concentration in human monocytes in vivo. *Diabetes*. **48**, 1316–1322
74. Singh, R. M., Cummings, E., Pantos, C., and Singh, J. (2017) Protein kinase C and cardiac dysfunction: a review. *Heart Fail. Rev.* **22**, 843–859
75. Hassouna, A., Matata, B. M., and Galiñanes, M. (2004) PKC- ϵ is upstream and PKC- α is downstream of mitoKATP channels in the signal transduction pathway of ischemic preconditioning of human myocardium. *Am. J. Physiol. - Cell Physiol.* **287**, 1418–1425
76. Murriel, C. L., and Mochly-Rosen, D. (2003) Opposing roles of δ and ϵ PKC in cardiac ischemia and reperfusion: Targeting the apoptotic machinery. *Arch. Biochem. Biophys.* **420**, 246–254
77. Inagaki, K., Chen, L., Ikeno, F., Lee, F. H., Imahashi, K. I., Bouley, D. M., Rezaee, M., Yock, P. G., Murphy, E., and Mochly-Rosen, D. (2003) Inhibition of δ -Protein Kinase C Protects Against Reperfusion Injury of the Ischemic Heart in Vivo. *Circulation*. **108**, 2304–2307
78. Dorn, G. W., Souroujon, M. C., Liron, T., Chen, C. H., Gray, M. O., Zhou, H. Z., Csukai, M., Wu, G., Lorenz, J. N., and Mochly-Rosen, D. (1999) Sustained in vivo cardiac protection by a rationally designed peptide that causes ϵ protein kinase C translocation. *Proc. Natl. Acad. Sci. U. S. A.* **96**, 12798–12803
79. Inagaki, K., Churchill, E., and Mochly-Rosen, D. (2006) Epsilon protein kinase C as a potential therapeutic target for the ischemic heart. *Cardiovasc. Res.* **70**, 222–230
80. Armstrong, J. S., and Whiteman, M. (2007) Measurement of Reactive Oxygen Species in Cells and Mitochondria. *Methods Cell Biol.* **80**, 355–377
81. Chen, C., Budas, G. R., Churchill, E. N., Disatnik, M., Thomas, D., and Mochly-rosen, D. (2009) An Activator of Mutant and Wildtype Aldehyde Dehydrogenase Reduces Ischemic Damage to the Heart. *Science (80-)*. **321**, 1493–1495
82. Baines, C. P., Song, C., Zheng, Y., Wang, G., Zhang, J., Wang, L., Guo, Y., Bolli, R., Cardwell, E. M., and Ping, P. (2013) NIH Public Access. **92**, 873–880
83. Ogbi, M., and Johnson, J. A. (2006) Protein kinase C ϵ interacts with cytochrome c oxidase subunit IV and enhances cytochrome c oxidase activity in neonatal cardiac myocyte preconditioning. *Biochem. J.* **393**, 191–199
84. Churchill, E. N., Ferreira, J. C., Brum, P. C., Szweda, L. I., and Mochly-Rosen, D. (2010) Ischaemic preconditioning improves proteasomal activity and increases the degradation of PKC during reperfusion. *Cardiovasc. Res.* **85**, 385–394

85. Alfonso, S. I., Callender, J. A., Hooli, B., Antal, C. E., Mullin, K., Sherman, M. A., Lesné, S. E., Leitges, M., Newton, A. C., Tanzi, R. E., and Malinow, R. (2016) Gain-of-function mutations in protein kinase C α (PKC α) may promote synaptic defects in Alzheimer's disease. *Sci. Signal.* **9**, 1–8
86. Callender, J. A., Yang, Y., Lordén, G., Stephenson, N. L., Jones, A. C., Brognard, J., and Newton, A. C. (2018) Protein kinase C α gain-of-function variant in Alzheimer's disease displays enhanced catalysis by a mechanism that evades down-regulation. *Proc. Natl. Acad. Sci. U. S. A.* **115**, E5497–E5505
87. Tagawa, K., Homma, H., Saito, A., Fujita, K., Chen, X., Imoto, S., Oka, T., Ito, H., Motoki, K., Yoshida, C., Hatsuta, H., Murayama, S., Iwatsubo, T., Miyano, S., and Okazawa, H. (2015) Comprehensive phosphoproteome analysis unravels the core signaling network that initiates the earliest synapse pathology in preclinical Alzheimer's disease brain. *Hum. Mol. Genet.* **24**, 540–558
88. Callender, J. A., and Newton, A. C. (2017) Conventional protein kinase C in the brain: 40 years later. *Neuronal Signal.* **1**, 1–10
89. Takahashi, H., Adachi, N., Shirafuji, T., Danno, S., Ueyama, T., Vendruscolo, M., Shuvaev, A. N., Sugimoto, T., Seki, T., Hamada, D., Irie, K., Hirai, H., Sakai, N., and Saito, N. (2015) Identification and characterization of PKC γ , a kinase associated with SCA14, as an amyloidogenic protein. *Hum. Mol. Genet.* **24**, 525–539
90. Verbeek, D. S., Goedhart, J., Bruinsma, L., Sinke, R. J., and Reits, E. A. (2008) PKC γ mutations in spinocerebellar ataxia type 14 affect C1 domain accessibility and kinase activity leading to aberrant MAPK signaling. *J. Cell Sci.* **121**, 2339–2349
91. Castagnag, M., Yoshimi, T., Kaibuchi, K., Sano, K., Kikkawa, U., and Nishizuka, Y. (1982) Direct Activation of Calcium-activated, Phospholipid-dependent Protein Kinase by Tumor-promoting Phorbol Esters. *J. Biol. Chem.* **257**, 7847–7851
92. Kikkawas, U., Takai, Y., Tanaka, Y., Miyake, R., and Nishizuka, Y. (1983) Protein Kinase C As a Possible Receptor Protein of Tumor-promoting Phorbol Esters. *J. Biol. Chem.* **258**, 11442–11445
93. Leach, K. L., James, M. L., and Blumberg, P. M. (1983) Characterization of a specific phorbol ester aporeceptor in mouse brain cytosol. *Proc. Natl. Acad. Sci. U. S. A.* **80**, 4208–4212
94. Zhang, L. L., Cao, F. F., Wang, Y., Meng, F. L., Zhang, Y., Zhong, D. S., and Zhou, Q. H. (2015) The protein kinase C (PKC) inhibitors combined with chemotherapy in the treatment of advanced non-small cell lung cancer: meta-analysis of randomized controlled trials. *Clin. Transl. Oncol.* **17**, 371–377
95. Szallasi, Z., Smith, C. B., Pettit, G. R., and Blumberg, P. M. (1994) Differential

- regulation of protein kinase C isozymes by bryostatin 1 and phorbol 12-myristate 13-acetate in NIH 3T3 fibroblasts. *J. Biol. Chem.* **269**, 2118–2124
96. Kraft, A. S., Anderson, W. B., Cooper, H. L., and Sando, J. J. (1982) Decrease in cytosolic calcium/phospholipid-dependent protein kinase activity following phorbol ester treatment of EL4 thymoma cells. *J. Biol. Chem.* **257**, 13193–13196
 97. Newton, A. C., and Brognard, J. (2017) Reversing the Paradigm: Protein Kinase C as a Tumor Suppressor. *Trends Pharmacol. Sci.* **38**, 438–447
 98. Prevostel, C., Alice, V., Joubert, D., and Parker, P. J. (2000) Protein kinase C α actively downregulates through caveolae-dependent traffic to an endosomal compartment. *J. Cell Sci.* **113**, 2575–2584
 99. Frey, M. R., Saxon, M. L., Zhao, X., Rollins, A., Evans, S. S., and Black, J. D. (1997) Protein kinase C isozyme-mediated cell cycle arrest involves induction of p21(waf1/cip1) and p27(kip1) and hypophosphorylation of the retinoblastoma protein in intestinal epithelial cells. *J. Biol. Chem.* **272**, 9424–9435
 100. Newton, A. C. (2018) Protein kinase C: perfectly balanced. *Crit. Rev. Biochem. Mol. Biol.* **53**, 208–230
 101. Dowling, C. M., Phelan, J., Callender, J. A., Cathcart, M. C., Mehigan, B., McCormick, P., Dalton, T., Coffey, J. C., Newton, A. C., O’Sullivan, J., and Kiely, P. A. (2016) Protein kinase C beta II suppresses colorectal cancer by regulating IGF-1 mediated cell survival. *Oncotarget.* **7**, 20919–20933
 102. Varga, A., Czifra, G., Tállai, B., Németh, T., Kovács, I., Kovács, L., and Bíró, T. (2004) Tumor grade-dependent alterations in the protein kinase C isoform pattern in urinary bladder carcinomas. *Eur. Urol.* **46**, 462–465
 103. Uhlen, M., Zhang, C., Lee, S., Sjöstedt, E., Fagerberg, L., Bidkhori, G., Benfeitas, R., Arif, M., Liu, Z., Edfors, F., Sanli, K., Von Feilitzen, K., Oksvold, P., Lundberg, E., Hober, S., Nilsson, P., Mattsson, J., Schwenk, J. M., Brunnström, H., Glimelius, B., Sjöblom, T., Edqvist, P. H., Djureinovic, D., Micke, P., Lindskog, C., Mardinoglu, A., and Ponten, F. (2017) A pathology atlas of the human cancer transcriptome. *Science (80-)*. 10.1126/science.aan2507
 104. Salzer, E., Santos-Valente, E., Klaver, S., Ban, S. A., Emminger, W., Prengemann, N. K., Garncarz, W., Müllauer, L., Kain, R., Boztug, H., Heitger, A., Arbeiter, K., Eitelberger, F., Seidel, M. G., Holter, W., Pollak, A., Pickl, W. F., Förster-Waldl, E., and Boztug, K. (2013) B-cell deficiency and severe autoimmunity caused by deficiency of protein kinase C δ . *Blood.* **121**, 3112–3116
 105. Belot, A., Kasher, P. R., Trotter, E. W., Foray, A. P., Debaud, A. L., Rice, G. I., Szykiewicz, M., Zobot, M. T., Rouvet, I., Bhaskar, S. S., Daly, S. B., Dickerson, J. E., Mayer, J., O’Sullivan, J., Juillard, L., Urquhart, J. E., Fawdar, S., Marusiak, A. A., Stephenson, N., Waszkowycz, B., Beresford, M. W., Biesecker, L. G.,

- Black, G. C. M., René, C., Eliaou, J. F., Fabien, N., Ranchin, B., Cochat, P., Gaffney, P. M., Rozenberg, F., Lebon, P., Malcus, C., Crow, Y. J., Brognard, J., and Bonnefoy, N. (2013) Protein kinase C δ deficiency causes mendelian systemic lupus erythematosus with B cell-defective apoptosis and hyperproliferation. *Arthritis Rheum.* **65**, 2161–2171
106. Kuehn, H. S., Niemela, J. E., Rangel-Santos, A., Zhang, M., Pittaluga, S., Stoddard, J. L., Hussey, A. A., Evbuomwan, M. O., Priel, D. A. L., Kuhns, D. B., Park, C. L., Fleisher, T. A., Uzel, G., and Oliveira, J. B. (2013) Loss-of-function of the protein kinase C δ (PKC δ) causes a B-cell lymphoproliferative syndrome in humans. *Blood.* **121**, 3117–3125
107. Parker, P. J., Justilien, V., Riou, P., Linch, M., and Fields, A. P. (2014) Atypical Protein Kinase C γ as a human oncogene and therapeutic target. *Biochem. Pharmacol.* **88**, 1–11
108. Beaugerie, L., Carrat, F., Nahon, S., Zeitoun, J. D., Sabaté, J. M., Peyrin-Biroulet, L., Colombel, J. F., Allez, M., Fléjou, J. F., Kirchgesner, J., Svrcek, M., Colombel, J. F., Cosnes, J., Gendre, J. P., Lémann, M., Hébuterne, X., Cortot, A., Bouhnik, Y., Laharie, D., Dupas, J. L., Flourié, B., Lerebours, E., Beaugerie, L., Peyrin-Biroulet, L., Allez, M., Messing, B., Cadiot, G., Marteau, P., Soulé, J. C., Gornet, J. M., Veyrac, M., Duclos, B., Beau, P., Bourreille, A., Baumer, P., Carbonnel, F., Heresbach, D., Metman, E. H., Florent, C., Blain, A., Faucheron, J. L., Bonaz, B., Roblin, X., Potier, P., Boehm, C., Kurtz, T., Lamouliatte, H., Nion-Larmurier, I., Delchier, J. C., Chaussade, S., Weiss, A. M., Cézard, J. P., Siproudhis, L., Nahon, S., Sondag, D., Jian, R., Souquet, J. C., Bord, P., Coffin, B., D'almagne, H., Delasalle, P., Fournier, R., Cavicchi, M., Souffran, M. H., Vandromme, L., Guedon, C., Seksik, P., Michiels, C., Renard, P., Rogier, P., Gouilloud, S., Rotenberg, A., Savoye, G., Thevenin, A., Mallet, L., Brazier, F., Jean, F., Justum, A. M., Latrive, J. P., Gerbal, J. L., Pierrugues, R., Chardonnal, G., Picon, L., Reix, N., D'aubigny, N. D., Uettwiller, H., Mallet, A. C., Palacci, A., Bensaude, R. J., Bonniaud, P., Empinet, O., Nisard, A., Rudelli, A., Tubiana, B., Capelle, P., Dabadie, A., Evard, D., Julien, P. E., Picon-Coste, M., Schneider, S., Goldfain, D., Bellanger, J., Blondelot, J. P., Lamy, P., Lemièrre, S., Mockly, J. F., Pellat, B., Gatineau-Sailliant, G., Nalet, B., Nancey, S., Kusielewicz, D., Loison, P., Popot, J. M., Merite, F., Roux, J. P., Afchain, P., Blanquart, A., Heyries, L., Reville, M., Viron, D., Zerbib, F., Claviere, C., Léostic, D., Poudroux, P., Moitry, A., Hagège, H., Hugot, J. P., Humeau, B., Sabate, J. M., Lederman, E., Lescut, D., Luneau, F., Mesnard, B., Smadja, L., Steinberg, M., Brun, M., Macaigne, G., Marchal, J. L., Ollivier, S., Ouvry, D., Perche, J. P., Rambaud, S., Benamouzig, R., Cazenave, J. L., Coffin, J. C., Blazquez, M., Lagneau, M., Person, B., Wittersheim, C., Napoleon, B., Cemachovic, I., Igllicki, F., Howaizi, M., Leprince, E., Leurent, B., Morin, T., Darsouni, R., Attar, A., Baron, P., Breton, A., Gillion, J. M., Guemene, J. M., Jouffre, C., Moreau, X., Claude, P., Quinton, A., Abitbol, V., Brichard, J. M., Desaint, B., Bouygues, M., Chatrenet, P., Salmeron, M., Silvie, J., Waldner, B., Emery, Y., Moraillon, A., Kunkel, D., Dubois, P., Faure, P., L'Hirondel, C., Labérenne, J. E., Moreau, P., Pereira, A., Plihon, G., Wolff, T., Ngo, Y.,

Boruchowicz, A., Jost, B., Gotlib, J. P., Danne, O., Raoux, P., Ramond-Bouhali, M. J., Baetz, A., Veyres, B., Chapoutot, C., Le Dréau, G., Filippi, J., Mudry, J., Kalt, P., Minault, S., Bounin, P. A., Andréani, T., Charneau, J., Reijasse, D., Bolze, J. L., Thauinat, J. L., Le Couteulx, C., Maurage, C., Bader, R., Codjovi, P., Migairou, J. L., Morali, A., Rey, P., Molard, B. R., Petit, R., Koch, S., Cassan, P., Deschamps, J. P., Caby, C. M., Meurisse, J. J., Prades, P., Boulant, J., Diacono, M., Monsch, J. M., Dupuy, J. F., Bellaiche, G., Guegan, M., Comte, J. M., Cayla, J. M., Le Tallec, F., Meurisse, F., Desurmont, P., Roget, L., Bouyssou, P., Le Gall, B., Bloch, F., Larvol, L., Jullien, M., Moreau, J., Rebouissoux, L., Decroix, B., Dib, N., Dieterling, P., Lenormand, F., Lagier, E., Fallourd, P., Charpin, S., Bertrand, H., Bommelaer, G., Battistelli, D., Delon, B., Dentant, L., Dorval, E., Dumortier, J., Gaye-Bareyt, E., Gerosa, Y., Guez, C., Mornet, M., Benfredj, P., Piperaud, R., Stremsoerfer, N., Verdier, E., Grinholtz, A., Barjonet, G., See, A., Arotçarena, R., Baudet, A., Broyer, J., Charachon, A., Blondon, H., Mouton, P., Claudez, H., Labat-Labourdette, J., Haëm, J., Estable, P., Levy, P., Rosenbaum, A., Balavoine, Y., Bianchi, A., Coutarel, P., Delaperriere, N., Dervichian, M., Marois, F., Seroka, J., Michaud, L., Leroy, O., Meyran, E., Poilroux, B., Tensaouti, A., Paupard, T., Agard, D., Beaulieu, S., Benfiguig, K., Capony, P., Cottereau, J., Desreumaux, P., Dramard, J. M., Duché, M., Mamou, P., Etienney, I., D'Abrigeon, G., Godeberge, B., Tucac, G., Puech, J., Roger, J., Lapalus, M. G., Bauret, P., Houcke, P., Pornin, B., Champigneulle, B., Cuissard, L., David, X. R., Lombard, F., Granveau, A., Hamon, J. F., Ink, O., Blondel, F., Namias, A., Pillon, D., Reignier, A., Tordjman, G., Christidis, C., Zirabe, S., Audebert, M., Bion, E., Bourgeaux, C., Poupardin, C., Deplaix, P., Fratini, G., Garnier, T., Desseaux, G., Magois, H., Lochum, S., Vergier, J. F., Texereau, P., Rat, C., Uzzan, F., Vidal, A., Vinante, N., Watrin, B., Wurtz-Huckert, C., Barre, B., Ferbus, D. C., Contou, J. F., Coupier, D., David, B., Gargot, D., Huc, D., Barraya, R., Faroux, R., Fourgeaud, J. L., Grimprel, H., Auroux, J., Rey, J. F., Arnoux, J. P., Lentini, F., Tardy, L., Mouterde, O., Spyckerelle, C., Vacherot, B., Weissman, A., Alpérine, M., Le Sidaner, A., Bonnet-Eymard, P. O., Colson, J. L., Pellet, D., Deltombe, B., Edouard, A., Maechel, H., Jaillet, J. C., Genes, J., Leveque, A. M., Lucidarme, D., Maignan, P., Gehrke, N. M., Sanchez, J., Tusseau, F., Casteur, A., Bottlaender, J., Constantini, D., Coton, T., Even, P., Druart, F., Riot, F., Gauchet, J. M., Hecquet, G., Henry, G., Hochain, P., Arpurt, J. P., Medini, A., Dartois-Hoguain, M., Moindrot, H., Emery, P., Periac, P., Prunier, A., Renkes, P., Tawil-Longreen, C., Vincent, E., Vitte, R. L., Loeb, C., Carwana, A., Barbereau, D., Bohon, P., Corrieri-Baizeau, C., Sahy, D., Derreveaux, P., David, D., Desbazeille, F., Fontenelle, P., Slama, J. L., Le Mercier, Y., Certin, M., Reig, J. J., Rosa, I., Helbert, T., Tounian, P., Turner, L., Perot, V., Aillet, L., Pauwels, A., Barré, P., Nury, B., Cazalbou, C., Devulder, F., Durget, A., Dubroca, J., Gaudy, D., Greff, M., Jacques, C., Lafarge, J., Kezachian, G., Le Gall, R., Pariente, A., Pinault, T., Bismuth, M., Boyer-Darrigrand, N., Bretagnolle, P., Carpentier, S., Cholet, F., Theodore, C., Combes, R., Combet, F., Delanoe, C., De Montigny, S., Soudan, D., Fourdan, O., Minier, G., Languépin, J., Roche, J., Ginies, J. L., Nouel, O., Petitgars, P., Robin, E., Hamm, R., Roques, J. F., Roussin-Bretagne, S., Sénéjoux, A., Muron, S., Bardoux, N., Berthelemy, P., Madonia, P., Carles, B., Reynier, C., Cuillerier, E., Dadamessi, I., Danis, J.,

Debenes, B., Dubuc-Rey, N., Lesur, G., Jouet, P., Lenaerts, C., Garret, M., Mineur, A., Chabry, B., Pigot, F., Rossi, V., Tennenbaum, R., Salloum, J., Slaoui, M. H., Mathieu, S., Papapietro, V., Viola, S., Bezet, A., Altman, C., Audan, A., Calabet, J., Masliah, C., Fayemendy, L., Duruy, M., Gauffeny, B., Helie, L., Imani, K., Janin-Manificat, R., Galmiche, J. P., Kerlirzin, A., Bedenne, L., Locher, C., Michaudel, G., Missonnier, G., Rinaldi-Dovio, M., Rouillon, J. M., Ecuier, S., Patenotte, A., Bronstein, J. A., Baty, V., Bougnol, M., Bourbon, P., Cerbelaud, P., Chavaillon, A., Boiffin, F., Dubern, B., De Laguerce, I. D., Greco, F., Bouhot, F., Godeberge, P., Grandmaison, B., Gros, P., Targues, G., Corallo, J., Boutin, J., Guilan, J., Barbieux, J. P., Lariviere, I. L., Le Genissel, H., Leroi, H., Bellaiche, M., Elie-Legrand, M. C., Dapoigny, M., Denoyel, P., Pienkowski, P., Pouche, P., Saurfelt, M. M., Thorel, J. M., Piche, T., Travers, B., Tuvignon, P., Zalcborg, M., Boulay, G., Zamora, C., Samama, J., Ricotie, E., De Fleury, P., Maille, F., Mougengel, J. L., Gonot, O., Menat, J. P., Kaassis, M., Lang, F., Abramowitz, L., Ganne, N., Pecriaux, O., Seyrig, J. A., Sobhani, I., Parmentier, T., Van Nieuwenhuysse, A., Weber, F. X., Glibert, A., Bineau, C., Canet, B., Collin, C., Cordet, F., Parlier, D. D., Carre, D., Peytier, A., Fein, F., Barouk, J., Dewannieux, J., Hartwig, J., Jouve, J. L., Laplane, B., Lascar, G., Legrand, C., Le Marchand, P., Liebaert, M. P., Terdiman-Pire, M., Abdelli, N., Neveu, D., De La Lande, P., De Saint Louvent, P., Pelatan, C., Petit, A., Richecoeur, M., Texier, F., Cazals, J. B., Tissot, B., Mourrut, C., Doubremelle, M., Foltz, M., Gautier-Jubé, F., Martin, J., Khouri, E., Lons, T., Carlier-Bandu, M., Monnin, J. L., Roche, H., Willemin, B., Houard, X., Fatisse, A., Algard, M., Arab, K., Borel, I., Lagarrigue, C., Chryssostalis, A., Boutroux, D., Dupuychaffray, J. P., Khaddari, S., Mion, F., Puy-Montbrun, T., Girardet, J. P., Gury, B., Landau, A., Le Bihan, M., Nieuviarts, S., Ollivry, J., Le Bourgeois, P., Piquet, M. A., Escartin, M. P., Systchenko, R., Venezia, F., Wantiez, M., Lesage, X., Zrihen, E., Aygalenq, P., Dieumegard, B., Savarieau, B., Bulois, P., Cattan, S., Diez, J. L., Fauchot, O., Durous, E., Gazut, V., Guilleminet, C., Bories, J. M., Le Floch, I. J., Vove, J. P., Lelouch, S., Lévy, P., Lhopital, F., Marcato, N., Mozer-Bernardeau, M., Nousbaum, J. B., Cattan, P., Plane, A., Raymond, J. M., Roseau, G., Rozental, G., Boustière, C., Bonny, C., Cordier-Collet, M., Courat, L., Croguennec, B., Tardy, K. D., Labarriere, D., Geagea, E., Gottrand, F., Gelsi, E., Thieffin, G., Wohlschies, E., Miguët, M., Ponsot, P., Suzanne, J., Teste, Y., Dupont Gossart, A. C., Baroni, J. L., Benchaa, B., Blanc, G., Maroy, B., Bonjean, P., Brézault, C., Bridoux-Henno, L., Chayette, C., Auby, D., Fiorucci, R., Galindo, G., Hubert, G., Bonneau, G., Marinier, E., Pouteau, M., Alamdari, A., Delbende, B., Chamouard, P., D'Abravanel, P., Dall'Osto, H., Hervé, S., Lefebvre, J., Levoir, D., Lillo, P., Rouch, M., Mathonnet, M., De Lustrac, M., Ramond, F. J., Roupret, B., and Soupison, A. (2018) High Risk of Anal and Rectal Cancer in Patients With Anal and/or Perianal Crohn's Disease. *Clin. Gastroenterol. Hepatol.* **16**, 892-899.e2

109. Nakanishi, Y., Reina-Campos, M., Nakanishi, N., Llado, V., Elmen, L., Peterson, S., Campos, A., De, S. K., Leitges, M., Ikeuchi, H., Pellecchia, M., Blumberg, R. S., Diaz-Meco, M. T., and Moscat, J. (2016) Control of Paneth Cell Fate, Intestinal Inflammation, and Tumorigenesis by PKC λ /i. *Cell Rep.* **16**, 3297–3310

110. Vandana Sachdev, MD*, Roberto F. Machado, MD†, Yukitaka Shizukuda, MD, PHD*, Yesoda N. Rao, MD*, Stanislav Sidenko*, Inez Ernst, RN, RDCS*, Marilyn St. Peter, RDCS*, Wynona A. Coles, RRT†, Douglas R. Rosing, MD*, William C. Blackwelder, PHD‡, Oswaldo Cast, M. (2011) 基因的改变 NIH Public Access. *Bone*. **23**, 1–7
111. Lambros, M. B. K., Wilkerson, P. M., Natrajan, R., Patani, N., Pawar, V., Vatcheva, R., Mansour, M., Laschet, M., Oelze, B., Orr, N., Muller, S., and Reis-Filho, J. S. (2011) High-throughput detection of fusion genes in cancer using the Sequenom MassARRAY platform. *Lab. Investig.* **91**, 1491–1501
112. Mitelman, F., Johansson, B., and Mertens, F. (2007) The impact of translocations and gene fusions on cancer causation. *Nat. Rev. Cancer*. **7**, 233–245
113. Mertens, F., Johansson, B., Fioretos, T., and Mitelman, F. (2015) The emerging complexity of gene fusions in cancer. *Nat. Rev. Cancer*. **15**, 371–381
114. Yoshihara, K., Wang, Q., Torres-Garcia, W., Zheng, S., Vegesna, R., Kim, H., and Verhaak, R. G. W. (2015) The landscape and therapeutic relevance of cancer-associated transcript fusions. *Oncogene*. **34**, 4845–4854
115. Stransky, N., Cerami, E., Schalm, S., Kim, J. L., and Lengauer, C. (2014) The landscape of kinase fusions in cancer. *Nat. Commun.* **5**, 1–10
116. Hantschel, O. (2012) Structure, Regulation, Signaling, and Targeting of Abl Kinases in Cancer. *Genes and Cancer*. **3**, 436–446
117. Seo, J. S., Ju, Y. S., Lee, W. C., Shin, J. Y., Lee, J. K., Bleazard, T., Lee, J., Jung, Y. J., Kim, J. O., Shin, J. Y., Yu, S. B., Kim, J., Lee, E. R., Kang, C. H., Park, I. K., Rhee, H., Lee, S. H., Kim, J. Il, Kang, J. H., and Kim, Y. T. (2012) The transcriptional landscape and mutational profile of lung adenocarcinoma. *Genome Res*. **22**, 2109–2119
118. Baffi, T. R., Van, A. A. N., Zhao, W., Mills, G. B., and Newton, A. C. (2019) Protein Kinase C Quality Control by Phosphatase PHLPP1 Unveils Loss-of-Function Mechanism in Cancer. *Mol. Cell*. **74**, 378-392.e5
119. Lee, M., Lee, K., Yu, N., Jang, I., Choi, I., Kim, P., EunJang, Y., Kim, B., Kim, S., Lee, B., Kang, J., and Lee, S. (2017) ChimerDB 3.0: An enhanced database for fusion genes from cancer transcriptome and literature data mining. *Nucleic Acids Res*. **45**, D784–D789
120. Bridge, J. A., Liu, X. Q., Sumegi, J., Nelson, M., Reyes, C., Bruch, L. A., Rosenblum, M., Puccioni, M. J., Bowdino, B. S., and McComb, R. D. (2013) Identification of a novel, recurrent SLC44A1-PRKCA fusion in papillary glioneuronal tumor. *Brain Pathol*. **23**, 121–128
121. Pages, M., Lacroix, L., Tauziede-Espariat, A., Castel, D., Daudigeos-Dubus, E.,

- Ridola, V., Gilles, S., Fina, F., Andreiuolo, F., Polivka, M., Lechapt-Zalcman, E., Puget, S., Boddaert, N., Liu, X. Q., Bridge, J. A., Grill, J., Chretien, F., and Varlet, P. (2015) Papillary glioneuronal tumors: histological and molecular characteristics and diagnostic value of SLC44A1-PRKCA fusion. *Acta Neuropathol. Commun.* **3**, 85
122. Nagaishi, M., Nobusawa, S., Matsumura, N., Kono, F., Ishiuchi, S., Abe, T., Ebato, M., Wang, Y., Hyodo, A., Yokoo, H., and Nakazato, Y. (2016) SLC44A1-PRKCA fusion in papillary and rosette-forming glioneuronal tumors. *J. Clin. Neurosci.* **23**, 73–75
123. Gasparini, A., Tosatto, S. C. E., Murgia, A., and Leonardi, E. (2017) Dynamic scaffolds for neuronal signaling: In silico analysis of the TANC protein family. *Sci. Rep.* **7**, 1–14
124. Han, S., Nam, J., Li, Y., Kim, S., Cho, S. H., Cho, Y. S., Choi, S. Y., Choi, J., Han, K., Kim, Y., Na, M., Kim, H., Bae, Y. C., Choi, S. Y., and Kim, E. (2010) Regulation of dendritic spines, spatial memory, and embryonic development by the TANC family of PSD-95-interacting proteins. *J. Neurosci.* **30**, 15102–15112
125. Hedtke, V., and Bakovic, M. (2019) Choline transport for phospholipid synthesis: An emerging role of choline transporter-like protein 1. *Exp. Biol. Med.* **244**, 655–662
126. Von Einem, B., Wahler, A., Schips, T., Serrano-Pozo, A., Proepper, C., Boeckers, T. M., Rueck, A., Wirth, T., Hyman, B. T., Danzer, K. M., Thal, D. R., and Von Arnim, C. A. F. (2015) The golgi-localized γ -ear-containing ARF-binding (GGA) proteins alter amyloid- β precursor protein (APP) processing through interaction of their GAE domain with the beta-site APP cleaving enzyme 1 (BACE1). *PLoS One.* **10**, 1–22
127. Keranen, L. M., Dutil, E. M., and Newton, A. C. (1995) Protein kinase C is regulated in vivo by three functionally distinct phosphorylations. *Curr. Biol.* **5**, 1394–1403
128. Violin, J. D., Zhang, J., Tsien, R. Y., and Newton, A. C. (2003) A genetically encoded fluorescent reporter reveals oscillatory phosphorylation by protein kinase C. *J. Cell Biol.* **161**, 899–909
129. Kaulich, M., Lee, Y. J., Lönn, P., Springer, A. D., Meade, B. R., and Dowdy, S. F. (2015) Efficient CRISPR-rAAV engineering of endogenous genes to study protein function by allele-specific RNAi. *Nucleic Acids Res.* **43**, e45
130. Kaulich, M., and Dowdy, S. F. (2015) Combining CRISPR/Cas9 and rAAV Templates for Efficient Gene Editing. *Nucleic Acid Ther.* **25**, 287–296
131. Murata, S., Minami, Y., Minami, M., Chiba, T., and Tanaka, K. (2001) CHIP is a chaperone-dependent E3 ligase that ubiquitylates unfolded protein. *EMBO Rep.*

2, 1133–1138

132. Memi, F., Killen, A. C., Barber, M., Parnavelas, J. G., and Andrews, W. D. (2019) Cadherin 8 regulates proliferation of cortical interneuron progenitors. *Brain Struct. Funct.* **224**, 277–292
133. Johnson, J. E., Giorgione, J., and Newton, A. C. (2000) The C1 and C2 domains of protein kinase C are independent membrane targeting modules, with specificity for phosphatidylserine conferred by the C1 domain. *Biochemistry.* **39**, 11360–11369
134. Tanaka, Y., Gavrielides, M. V., Mitsuuchi, Y., Fujii, T., and Kazanietz, M. G. (2003) Protein Kinase C Promotes Apoptosis in LNCaP Prostate Cancer Cells through Activation of p38 MAPK and Inhibition of the Akt Survival Pathway. *J. Biol. Chem.* **278**, 33753–33762
135. Okuda, H., Adachi, M., Miyazawa, M., Hinoda, Y., and Imai, K. (1999) Protein kinase C α promotes apoptotic cell death in gastric cancer cells depending upon loss of anchorage. *Oncogene.* **18**, 5604–5609
136. Shimizu, T., Cao, C. X., Shao, R. G., and Pommier, Y. (1998) Lamin B phosphorylation by protein kinase C α and proteolysis during apoptosis in human leukemia HL60 cells. *J. Biol. Chem.* **273**, 8669–8674
137. Stransky, N., and Kim, J. L. (2020) PRKC FUSIONS - United States Patent Application Publication
138. Płaszczycza, A., Nilsson, J., Magnusson, L., Brosjö, O., Larsson, O., Vult Von Steyern, F., Domanski, H. A., Lilljebjörn, H., Fioretos, T., Tayebwa, J., Mandahl, N., Nord, K. H., and Mertens, F. (2014) Fusions involving protein kinase C and membrane-associated proteins in benign fibrous histiocytoma. *Int. J. Biochem. Cell Biol.* **53**, 475–481
139. Panagopoulos, I., Gorunova, L., Bjerkehagen, B., Lobmaier, I., and Heim, S. (2015) LAMTOR1-PRKCD and NUMA1-SFMBT1 fusion genes identified by RNA sequencing in aneurysmal benign fibrous histiocytoma with t(3;11)(p21;q13). *Cancer Genet.* **208**, 545–551
140. Walther, C., Hofvander, J., Nilsson, J., Magnusson, L., Domanski, H. A., Gisselsson, D., Tayebwa, J., Doyle, L. A., Fletcher, C. D. M., and Mertens, F. (2015) Gene fusion detection in formalin-fixed paraffin-embedded benign fibrous histiocytomas using fluorescence in situ hybridization and RNA sequencing. *Lab. Investig.* **95**, 1071–1076
141. Dutil, E. M., Toker, A., and Newton, A. C. (1998) Regulation of conventional protein kinase C isozymes by phosphoinositide-dependent kinase 1 (PDK-1). *Curr. Biol.* **8**, 1366–1375

142. Newton, A. C. (2010) Protein Kinase C in Cancer Signaling and Therapy. *Protein Kinase C Cancer Signal. Ther.* 10.1007/978-1-60761-543-9
143. Kataoka, K., Nagata, Y., Kitanaka, A., Shiraishi, Y., Shimamura, T., Yasunaga, J. I., Totoki, Y., Chiba, K., Sato-Otsubo, A., Nagae, G., Ishii, R., Muto, S., Kotani, S., Watatani, Y., Takeda, J., Sanada, M., Tanaka, H., Suzuki, H., Sato, Y., Shiozawa, Y., Yoshizato, T., Yoshida, K., Makishima, H., Iwanaga, M., Ma, G., Nosaka, K., Hishizawa, M., Itonaga, H., Imaizumi, Y., Munakata, W., Ogasawara, H., Sato, T., Sasai, K., Muramoto, K., Penova, M., Kawaguchi, T., Nakamura, H., Hama, N., Shide, K., Kubuki, Y., Hidaka, T., Kameda, T., Nakamaki, T., Ishiyama, K., Miyawaki, S., Yoon, S. S., Tobinai, K., Miyazaki, Y., Takaori-Kondo, A., Matsuda, F., Takeuchi, K., Nureki, O., Aburatani, H., Watanabe, T., Shibata, T., Matsuoka, M., Miyano, S., Shimoda, K., and Ogawa, S. (2015) Integrated molecular analysis of adult T cell leukemia/lymphoma. *Nat. Genet.* **47**, 1304–1315
144. Hein, M. Y., Hubner, N. C., Poser, I., Cox, J., Nagaraj, N., Toyoda, Y., Gak, I. A., Weisswange, I., Mansfeld, J., Buchholz, F., Hyman, A. A., and Mann, M. (2015) A Human Interactome in Three Quantitative Dimensions Organized by Stoichiometries and Abundances. *Cell.* **163**, 712–723